K-factors

- Often we work at LO by necessity (LO parton shower Monte Carlos), but would like to know the impact of NLO corrections
- K-factors (NLO/LO) can be a useful short-hand for this information
- But caveat emptor; the value of the K-factor depends on a number of things
  - PDFs used at LO and NLO
  - scale(s) at which the cross sections are evaluated
- And often the NLO corrections result in a shape change, so that one K-factor is not sufficient to modify the LO cross sections

K-factor table from CHS paper

K-factors for LHC slightly less K-factors at Tevatron

K-factors with NLO PDFs at LO are more often closer to unity

Process	Typical scales μ_0	Typical scales μ_1	Tevatron K-factor $\mathcal{K}(\mu_0)$	Tevatron K-factor $\mathcal{K}(\mu_1)$	Tevatron K-factor $\mathcal{K}'(\mu_0)$	LHC K-factor $\mathcal{K}(\mu_0)$	LHC K-factor $\mathcal{K}(\mu_1)$	LHC K-factor $\mathcal{K}'(\mu_0)$
W	m_W	$2m_W$	1.33	1.31	1.21	1.15	1.05	1.15
W+1jet	m_W	$p_T^{\rm jet}$	1.42	1.20	1.43	1.21	1.32	1.42
W+2jets	m_W	$p_T^{\rm jet}$	1.16	0.91	1.29	0.89	0.88	1.10
WW+jet	m_W	$2m_W$	1.19	1.37	1.26	1.33	1.40	1.42
$t\bar{t}$	m_t	$2m_t$	1.08	1.31	1.24	1.40	1.59	1.19
$t\bar{t}$+1jet	m_t	$2m_t$	1.13	1.43	1.37	0.97	1.29	1.10
$b\bar{b}$	m_b	$2m_b$	1.20	1.21	2.10	0.98	0.84	2.51
Higgs	m_H	$p_T^{\rm jet}$	2.33	–	2.33	1.72	–	2.32
Higgs via VBF	m_H	$p_T^{\rm jet}$	1.07	0.97	1.07	1.23	1.34	0.85
Higgs+1jet	m_H	$p_T^{\rm jet}$	2.02	–	2.13	1.47	–	1.90
Higgs+2jets	m_H	$p_T^{\rm jet}$	–	–	–	1.15	–	–

Table 3: K-factors for various processes at the LHC calculated using a selection of input parameters. Have to fix this table. In all cases, the CTEQ6M PDF set is used at NLO. $\mathcal{K}$ uses the CTEQ6L1 set at leading order, whilst $\mathcal{K}'$ uses the same set, CTEQ6M, as at NLO and $\mathcal{K}''$ uses the modified LO (2-loop) PDF set. For Higgs+1,2jets, a jet cut of 40 GeV/c and $|\eta| < 4.5$ has been applied. A cut of $p_T^{\rm jet} > 20\ GeV/c$ has been applied for the $t\bar{t}$+jet process, and a cut of $p_T^{\rm jet} > 50\ GeV/c$ for WW+jet. In the W(Higgs)+2jets process the jets are separated by $\Delta R > 0.52$, whilst the VBF calculations are performed for a Higgs boson of mass 120 GeV. In each case the value of the K-factor is compared at two often-used scale choices, where the scale indicated is used for both renormalization and factorization scales.

Shapes of distributions may be different at NLO than at LO, but sometimes it is still useful to define a K-factor.

Note the value of the K-factor depends critically on its definition.

Go back to K-factor table

- Some rules-of-thumb
- NLO corrections are larger for processes in which there is a great deal of color annihilation
  - gg->Higgs
  - gg->γγ
  - *K*(gg->tT) > *K*(qQ -> tT)
  - these gg initial states want to radiate like crazy (see Sudakovs)
- NLO corrections decrease as more final-state legs are added
  - *K*(gg->Higgs + 2 jets) < *K*(gg->Higgs + 1 jet) < *K*(gg->Higgs)
  - unless can access new initial state gluon channel
- Can we generalize for uncalculated HO processes?
- What about effect of jet vetoes on K-factors? Signal processes compared to background.

	Typical scales		Tevatron K-factor			LHC K-factor		
Process	μ_0	μ_1	$\mathcal{K}(\mu_0)$	$\mathcal{K}(\mu_1)$	$\mathcal{K}'(\mu_0)$	$\mathcal{K}(\mu_0)$	$\mathcal{K}(\mu_1)$	$\mathcal{K}'(\mu_0)$
W	m_W	$2m_W$	1.33	1.31	1.21	1.15	1.05	1.15
W+1jet	m_W	$p_T^{\rm jet}$	1.42	1.20	1.43	1.21	1.32	1.42
W+2jets	m_W	$p_T^{\rm jet}$	1.16	0.91	1.29	0.89	0.88	1.10
WW+jet	m_W	$2m_W$	1.19	1.37	1.26	1.33	1.40	1.42
$t\bar{t}$	m_t	$2m_t$	1.08	1.31	1.24	1.40	1.59	1.48
$t\bar{t}$+1jet	m_t	$2m_t$	1.13	1.43	1.37	0.97	1.29	1.10
$b\bar{b}$	m_b	$2m_b$	1.20	1.21	2.10	0.98	0.84	2.51
Higgs	m_H	$p_T^{\rm jet}$	2.33	–	2.33	1.72	–	2.32
Higgs via VBF	m_H	$p_T^{\rm jet}$	1.07	0.97	1.07	1.23	1.34	1.09
Higgs+1jet	m_H	$p_T^{\rm jet}$	2.02	–	2.13	1.47	–	1.90
Higgs+2jets	m_H	$p_T^{\rm jet}$	–	–	–	1.15	–	–

Table 2: K-factors for various processes at the Tevatron and the LHC calculated using a selection of input parameters. In all cases, the CTEQ6M PDF set is used at NLO. $\mathcal{K}$ uses the CTEQ6L1 set at leading order, whilst $\mathcal{K}'$ uses the same set, CTEQ6M, as at NLO. For most of the processes listed, jets satisfy the requirements $p_T > 15$ GeV/c and $|\eta| < 2.5$ (5.0) at the Tevatron (LHC). For Higgs+1,2jets, a jet cut of 40 GeV/c and $|\eta| < 4.5$ has been applied. A cut of $p_T^{\rm jet} > 20\ GeV/c$ has been applied for the $t\bar{t}$+jet process, and a cut of $p_T^{\rm jet} > 50\ GeV/c$ for WW+jet. In the W(Higgs)+2jets process the jets are separated by $\Delta R > 0.52$, whilst the VBF calculations are performed for a Higgs boson of mass 120 GeV. In each case the value of the K-factor is compared at two often-used scale choices, where the scale indicated is used for both renormalization and factorization scales.

Casimir for biggest color representation final state can be in

Simplistic rule

$C_{i1} + C_{i2} - C_{f,max}$

L. Dixon

Casimir color factors for initial state

Shape dependence of a K-factor

- Inclusive jet production probes very wide x,Q^2 range along with varying mixture of gg,gq,and qq subprocesses
- PDF uncertainties are significant at high p_T
- Over limited range of p_T and y, can approximate effect of NLO corrections by K-factor but not in general
  - in particular note that for forward rapidities, K-factor <<1
  - LO predictions will be large overestimates
  - this is true for both the Tevatron and for the LHC

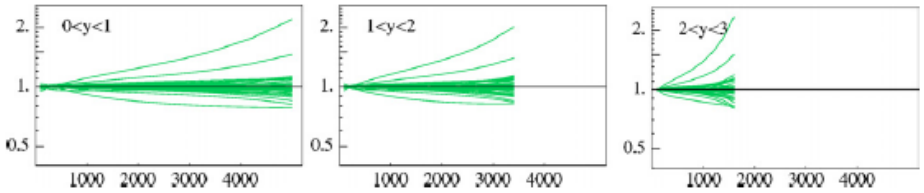

Figure 105. The ratios of the jet cross section predictions for the LHC using the CTEQ6.1 error pdfs to the prediction using the central pdf. The extremes are produced by eigenvector 15.

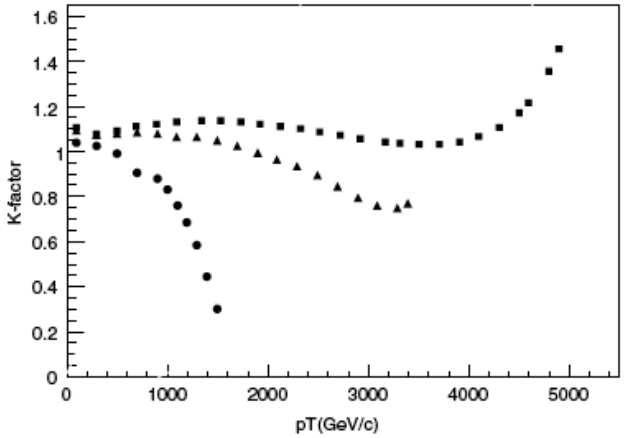

Figure 106. The ratios of the NLO to LO jet cross section predictions for the LHC using the CTEQ6.1 pdfs for the three different rapidity regions (0–1 (squares), 1–2 (triangles), 2–3 (circles)).

Aside: Why K-factors < 1 for inclusive jet prodution?

- Go back to slides we encountered before
- Write cross section indicating explicit scale-dependent terms
- First term (lowest order) in Eq. 3 leads to monotonically decreasing behavior as scale increases (the LO piece)
- Second term is negative for $\mu<p_T$, positive for $\mu>p_T$
- Third term is negative for factorization scale $M < p_T$
- Fourth term has same dependence as lowest order term
- Thus, lines one and four give contributions which decrease monotonically with increasing scale while lines two and three start out negative, reach zero when the scales are equal to p_T, and are positive for larger scales
- At NLO, result is a roughly parabolic behavior

Consider a large transverse momentum process such as the single jet inclusive cross section involving only massless partons. Furthermore, in order to simplify the notation, suppose that the transverse momentum is sufficiently large that only the quark distributions need be considered. In the following, a sum over quark flavors is implied. Schematically, one can write the lowest order cross section as

$$E\frac{d^3\sigma}{dp^3} \equiv \sigma = a^2(\mu)\,\hat{\sigma}_B \otimes q(M) \otimes q(M) \tag{1}$$

where $a(\mu) = \alpha_s(\mu)/2\pi$ and the lowest order parton-parton scattering cross section is denoted by $\hat{\sigma}_B$. The renormalization and factorization scales are denoted by μ *and* M, respectively. In addition, various overall factors have been absorbed into the definition of $\hat{\sigma}_B$. The symbol $\otimes$ denotes a convolution defined as

$$f \otimes g = \int_x^1 \frac{dy}{y}\, f(\frac{x}{y})\, g(y). \tag{2}$$

When one calculates the $\mathcal{O}(\alpha_s^3)$ contributions to the inclusive cross section, the result can be written as

$$\begin{aligned}
(1) \quad \sigma &= a^2(\mu)\,\hat{\sigma}_B \otimes q(M) \otimes q(M) \\
(2) \quad &+ 2a^3(\mu)\, b \ln(\mu/p_T)\hat{\sigma}_B \otimes q(M) \otimes q(M) \\
(3) \quad &+ 2a^3(\mu)\, \ln(p_T/M) P_{qq} \otimes \hat{\sigma}_B \otimes q(M) \otimes q(M) \\
(4) \quad &+ a^3(\mu)\, K \otimes q(M) \otimes q(M).
\end{aligned} \tag{3}$$

In writing Eq. (3), specific logarithms associated with the running coupling and the scale dependence of the parton distributions have been explicitly displayed; the remaining higher order corrections have been collected in the function K in the last line of Eq. (3). The μ

Aside: Why K-factors < 1 for inclusive jet prodution?

- It's the decomposition into the form shown here that allows the scale uncertainties to be calculated on-the-fly in the Blackhat/Sherpa ntuples

Consider a large transverse momentum process such as the single jet inclusive cross section involving only massless partons. Furthermore, in order to simplify the notation, suppose that the transverse momentum is sufficiently large that only the quark distributions need be considered. In the following, a sum over quark flavors is implied. Schematically, one can write the lowest order cross section as

$$E\frac{d^3\sigma}{dp^3} \equiv \sigma = a^2(\mu)\,\hat{\sigma}_B \otimes q(M) \otimes q(M) \tag{1}$$

where $a(\mu) = \alpha_s(\mu)/2\pi$ and the lowest order parton-parton scattering cross section is denoted by $\hat{\sigma}_B$. The renormalization and factorization scales are denoted by μ *and* M, respectively. In addition, various overall factors have been absorbed into the definition of $\hat{\sigma}_B$. The symbol $\otimes$ denotes a convolution defined as

$$f \otimes g = \int_x^1 \frac{dy}{y}\, f(\frac{x}{y})\, g(y). \tag{2}$$

When one calculates the $\mathcal{O}(\alpha_s^3)$ contributions to the inclusive cross section, the result can be written as

$$\begin{aligned}
(1) \qquad \sigma &= a^2(\mu)\,\hat{\sigma}_B \otimes q(M) \otimes q(M) \\
(2) \qquad &+ 2a^3(\mu)\, b \ln(\mu/p_T)\hat{\sigma}_B \otimes q(M) \otimes q(M) \\
(3) \qquad &+ 2a^3(\mu)\, \ln(p_T/M) P_{qq} \otimes \hat{\sigma}_B \otimes q(M) \otimes q(M) \\
(4) \qquad &+ a^3(\mu)\, K \otimes q(M) \otimes q(M).
\end{aligned} \tag{3}$$

In writing Eq. (3), specific logarithms associated with the running coupling and the scale dependence of the parton distributions have been explicitly displayed; the remaining higher order corrections have been collected in the function K in the last line of Eq. (3). The μ

Why K-factor for inclusive jets < 1?

- First term (lowest order) in (3) leads to monotonically decreasing behavior as scale increases
- Second term is negative for $\mu<p_T$, positive for $\mu>p_T$
- Third term is negative for factorization scale $M < p_T$
- Fourth term has same dependence as lowest order term
- Thus, lines one and four give contributions which decrease monotonically with increasing scale while lines two and three start out negative, reach zero when the scales are equal to p_T, and are positive for larger scales
- NLO parabola moves out towards higher scales for forward region
- Scale of $E_T/2$ results in a K-factor of ~1 for low E_T, <<1 for high E_T for forward rapidities at Tevatron, and at the LHC

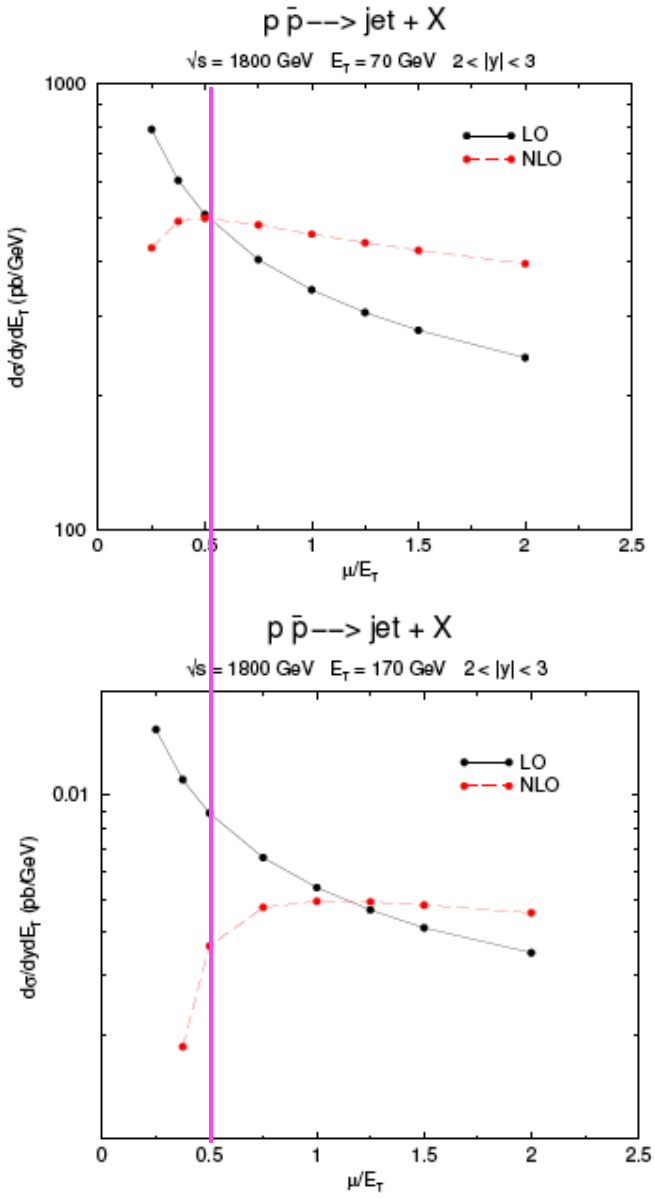

Look at K-factors for W + n jets production at LHC

The K-factors for W + jets (p_T>30 GeV/c) fall near a straight line, as do the K-factors for the Tevatron. By definition, the K-factors for Higgs + jets fall on a straight line.

Using a scale of m_W; one of choices used at Tevatron.

Why does it have this behavior?

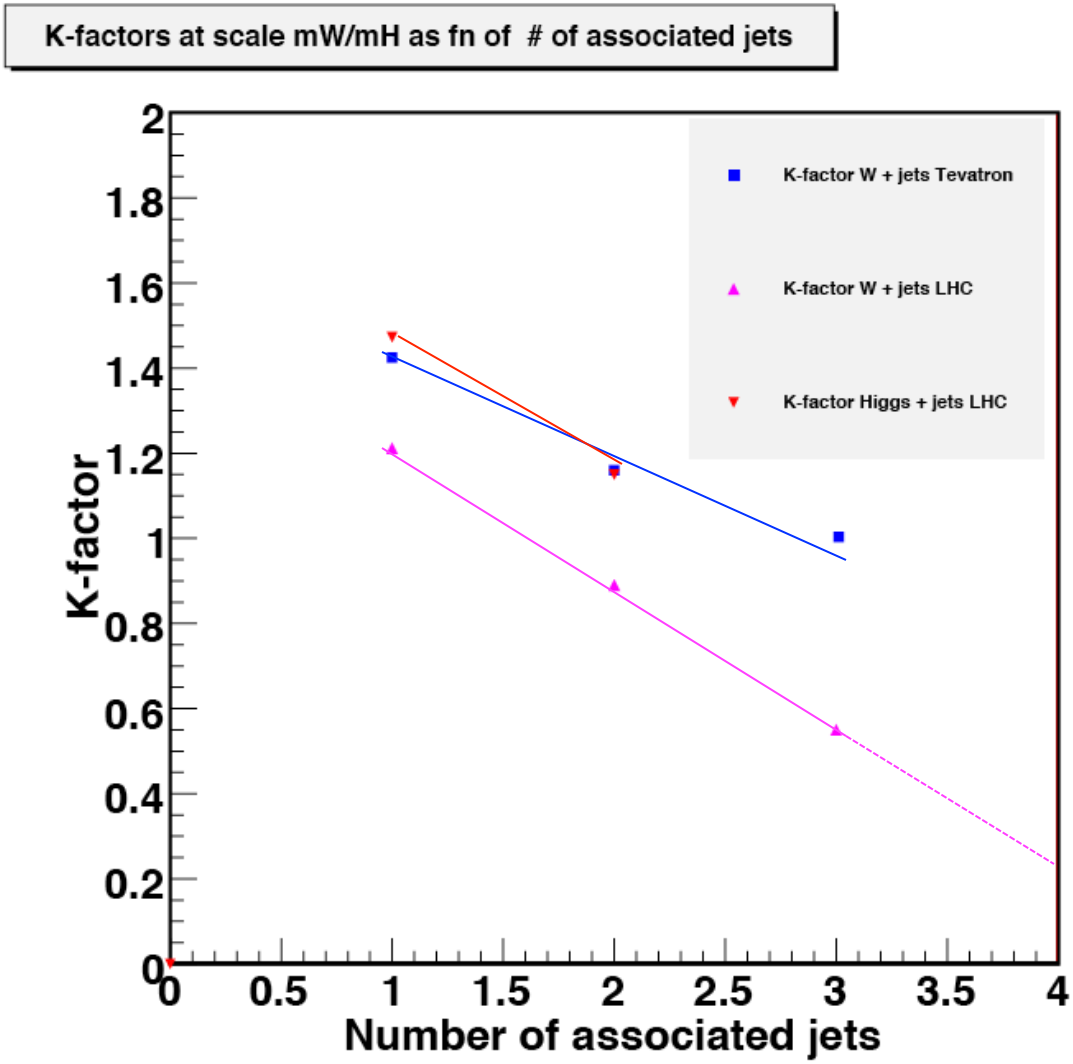

To understand this further, we have to discuss jet algorithms

Jet algorithms at LO

- At (fixed) LO, 1 parton = 1 jet
  - why not more than 1? I have to put a ΔR cut on the separation between two partons; otherwise, there's a collinear divergence. LO parton shower programs effectively put in such a cutoff
  - Remember the collinear singularity

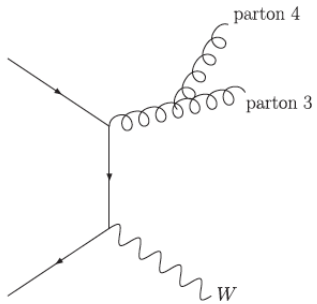

$$\log\left(\frac{1}{\Delta R_{34}}\right)$$

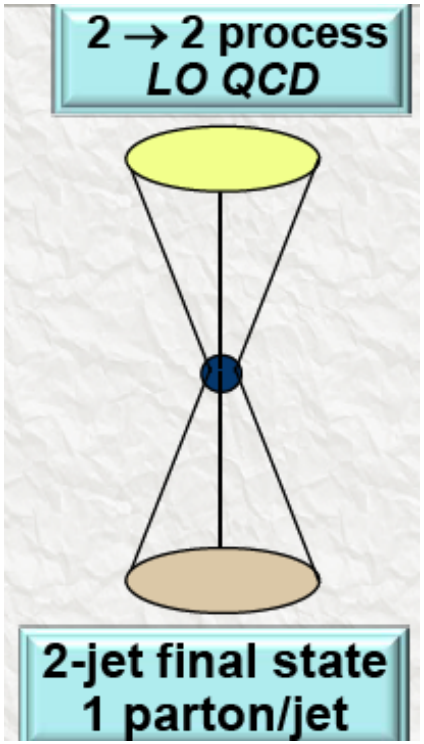

- But at NLO, I have to deal with more than 1 parton in a jet, and so now I have to talk about how to cluster those partons
  - i.e. jet algorithms

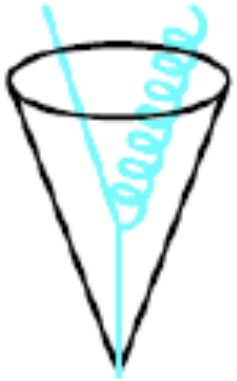

Jet algorithms at NLO

- At NLO, there can be two partons in a jet, life becomes more interesting and we have to start talking about jet algorithms to define jets
  - the addition of the real and virtual terms at NLO cancels the divergence.

- A jet algorithm is based on some measure of localization of the expected collinear spray of particles
- Start with an inclusive list of particles/partons/calorimeter towers/topoclusters
- End with lists of same for each jet
- …and a list of particles… not in any jet; for example, remnants of the initial hadrons
- Two broad classes of jet algorithms
  - cluster according to proximity in space: cone algorithms
  - cluster according to proximity in momenta: k_T algorithms

What do I want out of a jet algorithm?

- It should be fully specified, including defining in detail any pre-clustering, merging and splitting issues
- It should be simple to implement in an experimental analysis, and should be independent of the structure of the detector
- It should be boost-invariant
- It should be simple to implement in a theoretical calculation
  - it should be defined at any order in perturbation theory
  - it should yield a finite cross section at any order in perturbation theory
  - it should yield a cross section that is relatively insensitive to hadronization effects

- It should be IR safe, i.e. adding a soft gluon should not change the results of the jet clustering

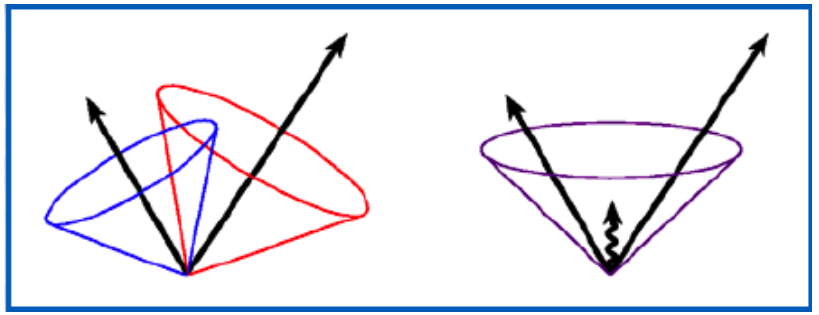

- It should be collinear safe, i.e. splitting one parton into two collinear partons should not change the results of the jet clustering

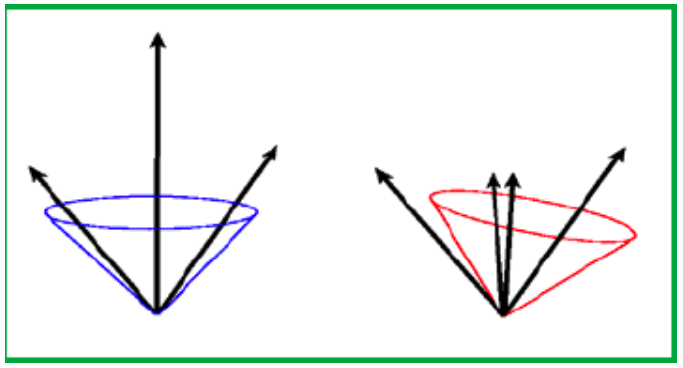

Jet algorithms

- The algorithm should behave in a similar manner (as much as possible) at the parton, particle and detector levels. Note that differences between levels can unavoidably creep in.

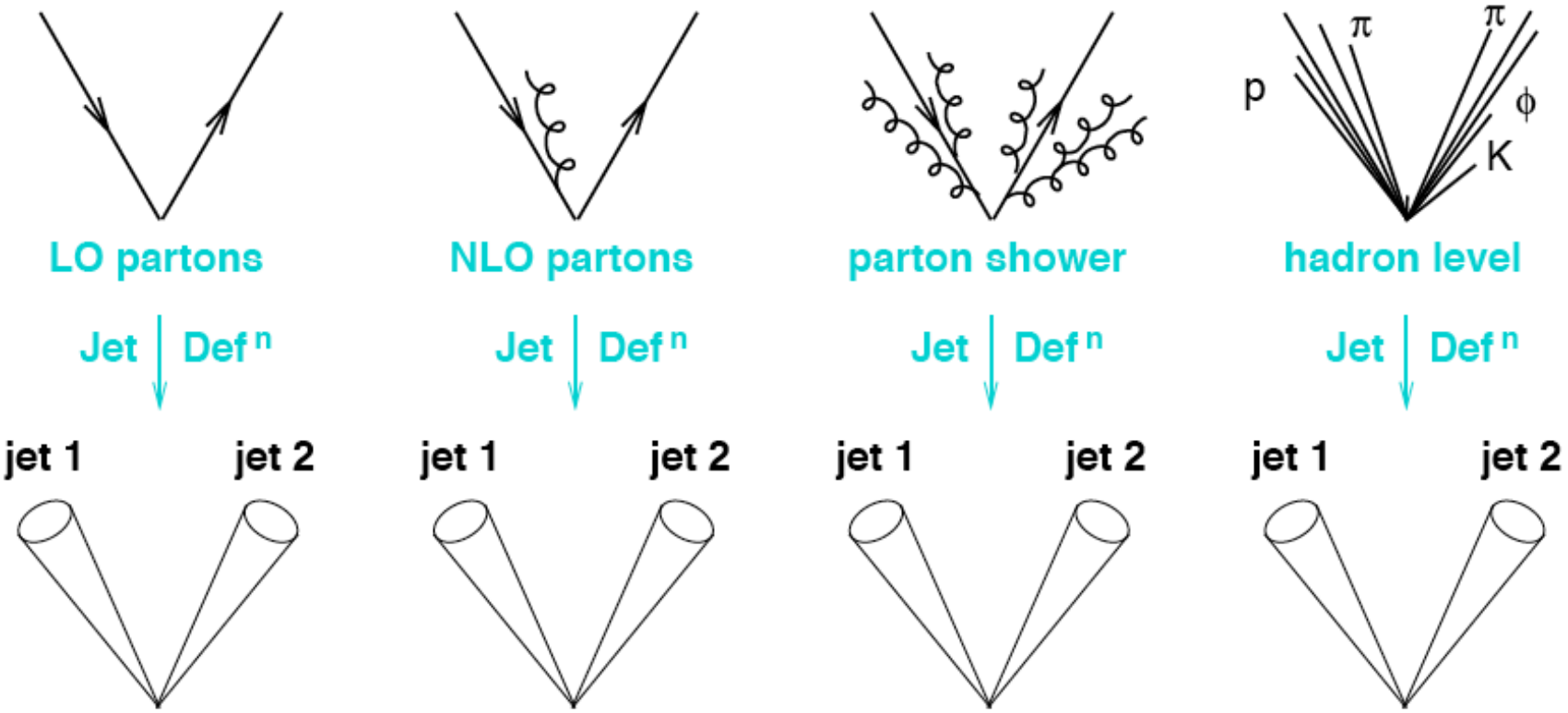

Projection to jets should be resilient to QCD effects

Some kinematic definitions

Rapidity (y) and Pseudo-rapidity (η)

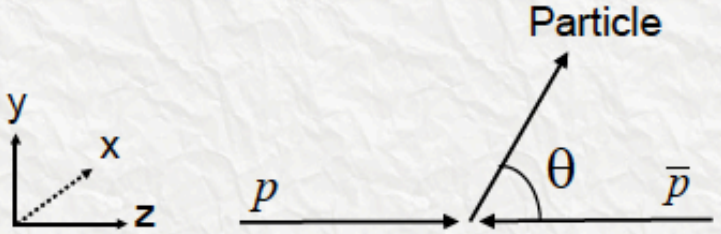

$$y \equiv \frac{1}{2}\ln\frac{E+p_z}{E-p_z} = \frac{1}{2}\ln\frac{1+\beta\cos\theta}{1-\beta\cos\theta}$$

$$\beta\cos\theta = \tanh y \quad \text{where} \quad \beta = p/E$$

In the limit $\beta \to 1$ (or $m << p_T$) then

$$\eta \equiv y\big|_{m=0} = \frac{1}{2}\ln\frac{1+\cos\theta}{1-\cos\theta} = -\ln\tan\frac{\theta}{2}$$

LAB System ≠ parton-parton CM system

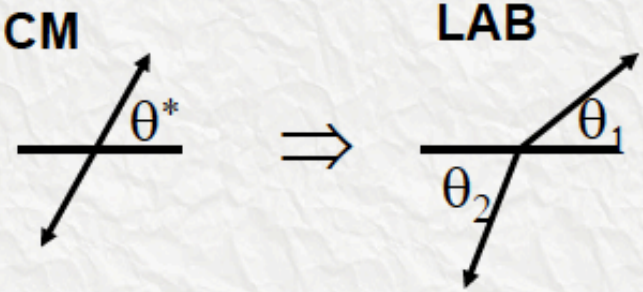

Δη and p_T are invariant under longitudinal boosts

Some kinematic definitions

To satisfy listed requirements for jet algorithms, use p_T,y and ϕ to characterize jets

Transverse Energy/Momentum

$$E_T^2 \equiv p_x^2 + p_y^2 + m^2 = p_T^2 + m^2 = E^2 - p_z^2$$

$$p_z = E \tanh y$$
$$E = E_T \cosh y$$
$$p_z = E_T \sinh y$$

$$p_T \equiv p \sin\theta \xrightarrow[m \to 0]{} E_T$$

Invariant Mass

$$M_{12}^2 \equiv (p_1^\mu + p_2^\mu)(p_{1\mu} + p_{2\mu})$$
$$= m_1^2 + m_2^2 + 2(E_1 E_2 - \boldsymbol{p}_1 \cdot \boldsymbol{p}_2)$$
$$\xrightarrow[m_1, m_2 \to 0]{} 2E_{T1}E_{T2}(\cosh\Delta\eta - \cos\Delta\phi)$$

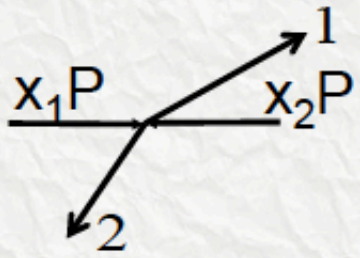

Partonic Momentum Fractions

$$x_1 = \left(e^{\eta_1} + e^{\eta_2}\right) E_T / \sqrt{s}$$
$$x_2 = \left(e^{-\eta_1} + e^{-\eta_2}\right) E_T / \sqrt{s}$$

$$x_T \equiv 2E_T / \sqrt{s} = x_{1,2}(\eta_{1,2} = 0)$$

Parton CM $(\text{energy})^2 \rightarrow \hat{s} = x_a x_b s$

$$0 < x_1, x_2 < 1$$
$$x_T^2 < x_1 x_2 < 1$$

(Legacy) cone algorithms

- The cone algorithm was most often used at the Tevatron
  - perhaps most intuitive
  - draw a cone of radius R in $\eta-\phi$ space $R_{\text{cone}} = \sqrt{(\Delta\eta)^2 + (\Delta\phi)^2}$
- But where to start the cone?
  - use 'seeds' (towers, particles, partons…) of energy ~1 GeV to save computing time

streetlight approach

  - combine seed towers with other towers within a radius R of the seed tower
  - re-calculate jet centroid using new list of towers… inside cone
  - lather, rinse, iterate until a stable solution is found

typically use R~0.7 for inclusive measurements; R~0.4 for *complex* measurements, such as t-tbar

- But you may end up with overlapping jet cones (starting from different jet seeds)
- So need to come up with a provision for splitting/merging
  - merge 2 jets if overlap energy is > f*p_T (smaller jet)
  - f=0.50-0.75

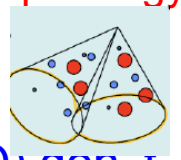

- Note: partons (at NLO) don't know nothing about splitting/ merging
  - experience says f=0.75 is best

Midpoint cone algorithm

- But this type of cone algorithm is not infra-red safe, since the two partons in the figure on the right will/will not be clustered into a single jet depending on whether or not a soft gluon is present at the midpoint
  - also (in Run 1 at the Tevatron) used E_T and η, rather than p_T and y
- Fundamental difference between data and fixed order pert QCD
  - data has "seeds" everywhere
- So the Midpoint algorithm was devised
  - seeds were placed at the midpoints between nearby protojets
  - used in Run 2 at the Tevatron

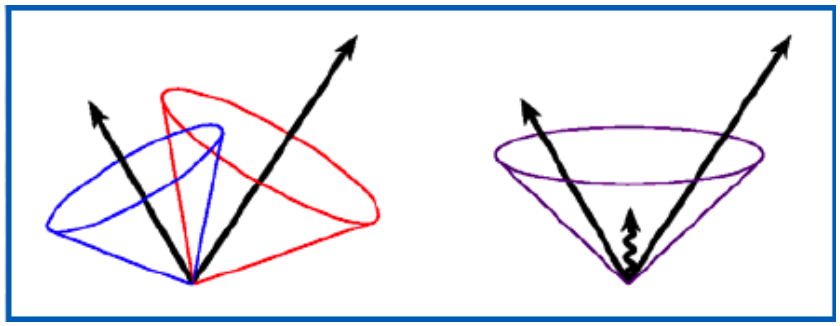

- this works for 2->3 final states (NLO inclusive), but not for 2->4 (NNLO inclusive) where I may cluster 3 partons in 1 jet

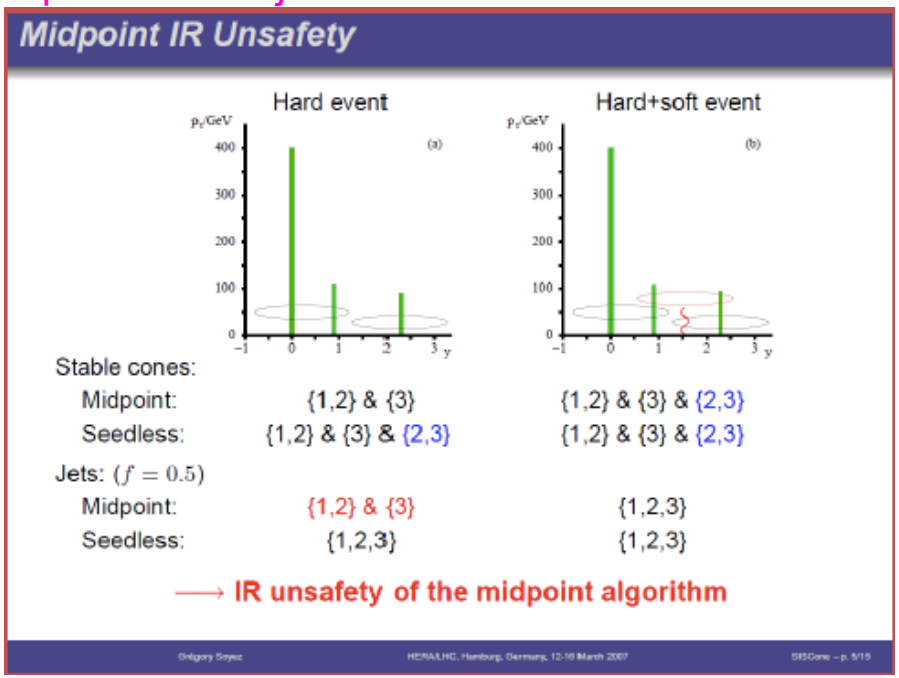

Seedless cone algorithm

- Put seeds everywhere
- Can be time-consuming
- Enter the SISCone algorithm
  - Seedless Infrared Safe Cone jet algorithm
  - G. Salam, G. Soyez, arXiv: 0704.0292
- …uses a geometric approach to find all distinct cones
- …with a speed similar to that of the Midpoint algorithm
- Still have the split/merge issue
- …and the issue of *dark towers*
- Differences with the midpoint algorithm typically of the order of 1 percent or so in practice
  - see later discussion, however

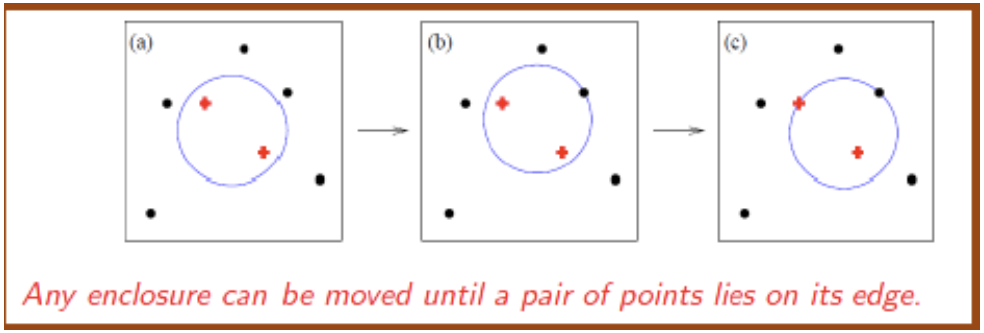

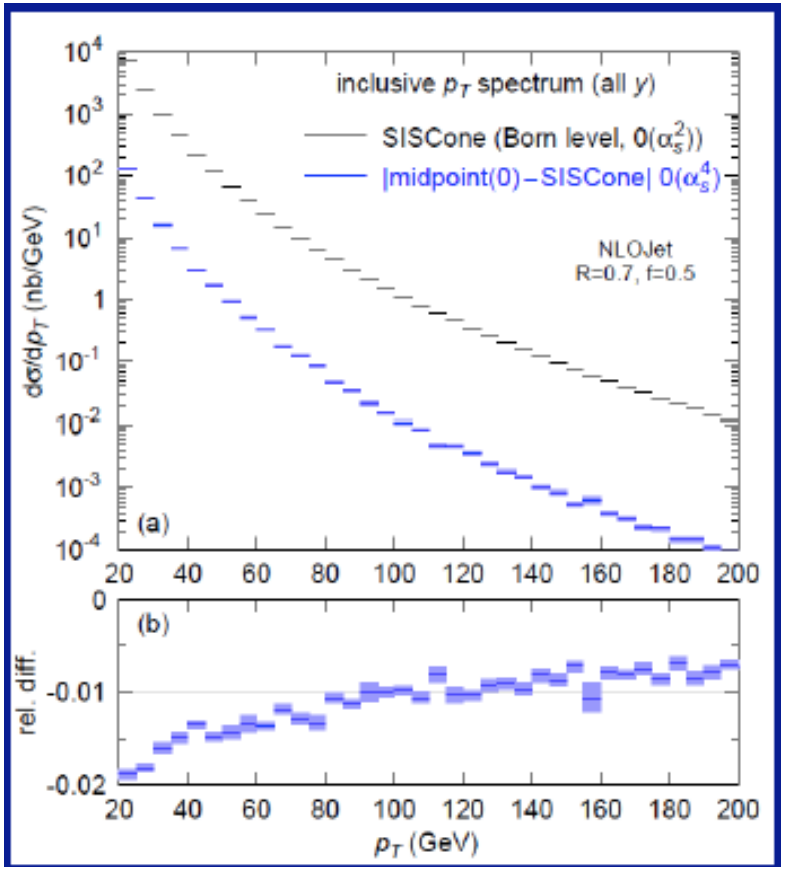

The k_T family of jet algorithms

- p=1
  - the regular k_T jet algorithm
- p=0
  - Cambridge-Aachen algorithm
- p=-1
  - anti-k_T jet algorithm
  - Cacciari, Salam, Soyez ' 08
  - also P-A Delsart ' 07 (reverse k_T)
  - soft particles will first cluster with hard particles before clustering among themselves
  - no split/merge
  - leads mostly to constant area hard jets

$$d_{ij} = \min\left(p_{T,i}^{2p}, p_{T,j}^{2p}\right)\frac{\Delta R_{ij}^2}{D^2}$$

$$d_{ii} = p_{T,i}^{2p}$$

- #1 algorithm for ATLAS, CMS
- Actually, seems to be the only algorithm used

k_T (recombination) algorithms

- Cluster particles nearby in momentum space first
- The k_T algorithm is IR and collinear safe
- No overlapping of jets
- No biases from seed towers
- The kT algorithm is sensitive to soft particles and the area can depend on pileup

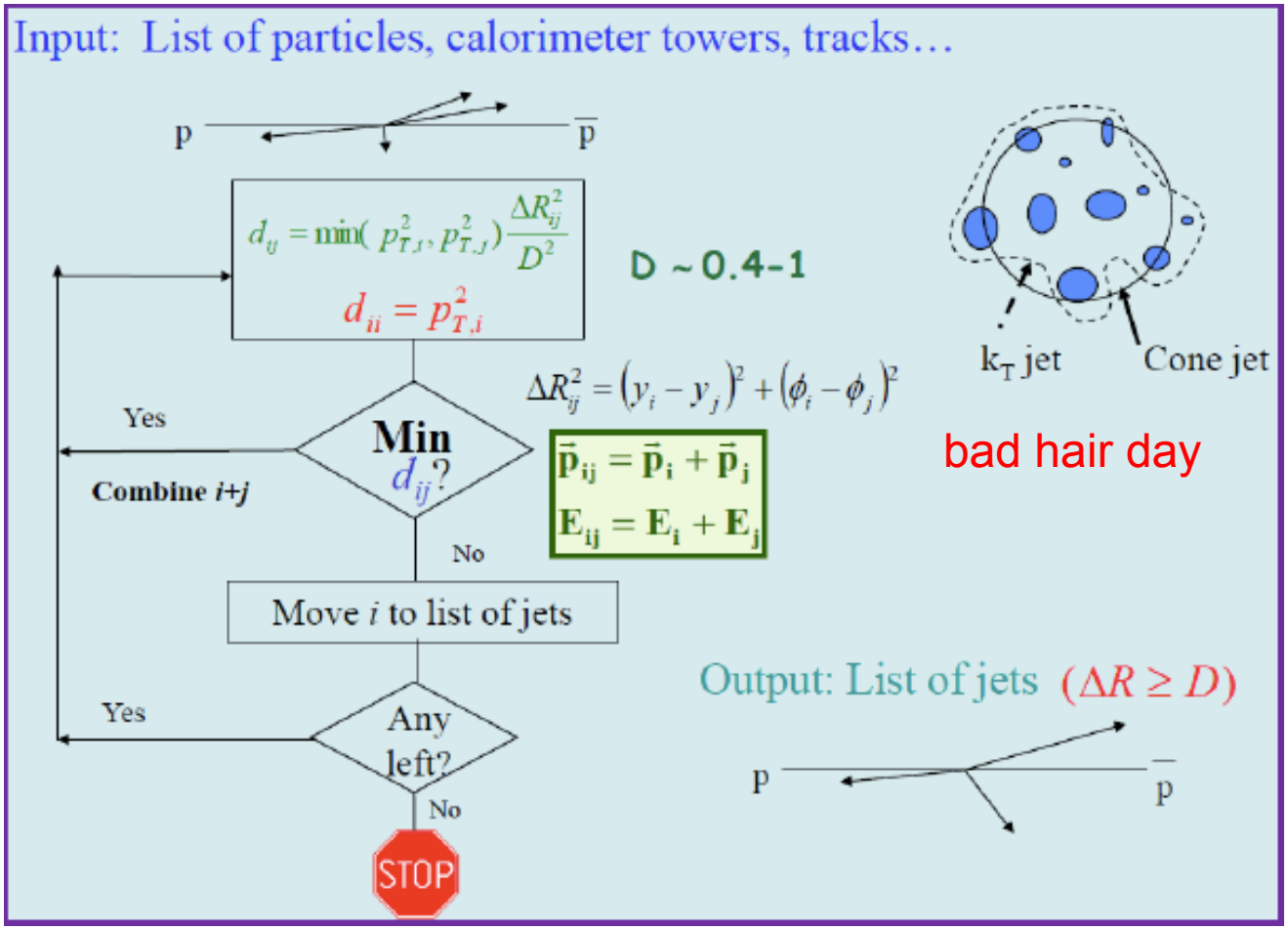

The antikT algorithm seems to have no major problems.

Jet algorithms at LO/NLO

- Remember at LO, 1 parton = 1 jet
- By choosing a jet algorithm with size parameter D, we are requiring any two partons to be > D apart
- The matrix elements have $1/\Delta R$ poles, so larger D means smaller cross sections
  - it's because of the poles that we have to make a ΔR cut
- At NLO, there can be two (or more) partons in a jet and jets for the first time can have some structure
  - we don't need a ΔR cut, since the virtual corrections cancel the collinear singularity from the gluon emission
  - **but there are residual (Sudakov) logs that can become important if D is too small**
- Increasing the size parameter D increases the phase space for including an extra gluon in the jet, and thus increases the cross section at NLO (in most cases)

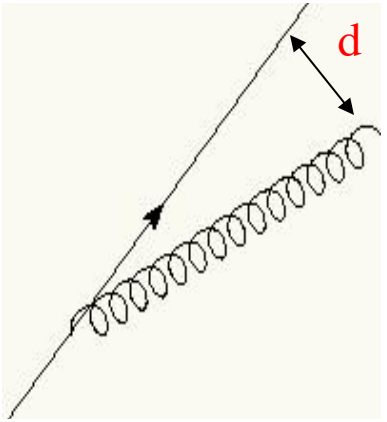

$z=p_{T2}/p_{T1}$

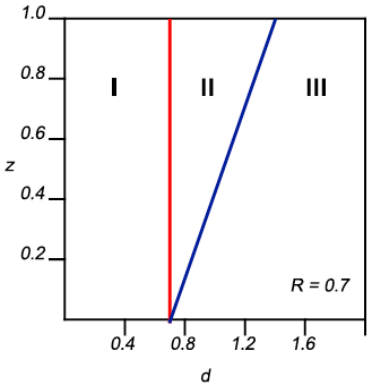

Figure 22. The parameter space (d,Z) for which two partons will be merged into a single jet.

For $D=R_{cone}$, Region I = k_T jets, Region II (nominally) = cone jets; I say nominally because in data not all of Region II is included for cone jets

Jets at NLO continued

- Construct what is called a Snowmass potential (see jet review paper)

shown in Figure 50, where the towers unclustered into any jet are shaded black. A simple way of understanding these dark towers begins by defining a "Snowmass potential" in terms of the 2-dimensional vector $\overrightarrow{r} = (y, \phi)$ via

$$V(\overrightarrow{r}) = -\frac{1}{2}\sum_j p_{T,j}\left(R^2_{cone} - (\overrightarrow{r_j} - \overrightarrow{r})^2\right)\Theta\left(R^2_{cone} - (\overrightarrow{r_j} - \overrightarrow{r})^2\right) . \quad (39)$$

The flow is then driven by the "force" $\overrightarrow{F}(\overrightarrow{r}) = -\overrightarrow{\nabla} V(\overrightarrow{r})$ which is thus given by,

$$\begin{aligned}\overrightarrow{F}(\overrightarrow{r}) &= \sum_j p_{T,j}(\overrightarrow{r_j} - \overrightarrow{r})\,\Theta\left(R^2_{cone} - (\overrightarrow{r_j} - \overrightarrow{r})^2\right) \\ &= \left(\overrightarrow{\overline{r}}_{C(\overrightarrow{r})} - \overrightarrow{r}\right)\sum_{j\subset C(r)} p_{T,j}, \end{aligned} \quad (40)$$

where $\overrightarrow{\overline{r}}_{C(\overrightarrow{r})} = \left(\overline{y}_{C(\overrightarrow{r})}, \overline{\phi}_{C(\overrightarrow{r})}\right)$ and the sum runs over $j \subset C(\overrightarrow{r})$ such that $\sqrt{(y_j - y)^2 + (\phi_j - \phi)^2} \leq R_{cone}$. As desired, this force pushes the cone to the stable cone position.

- The minima of the potential function indicates the positions of the stable cone solutions
  - the derivative of the potential function is the force that shows the direction of flow of the iterated cone
- The midpoint solution contains both partons

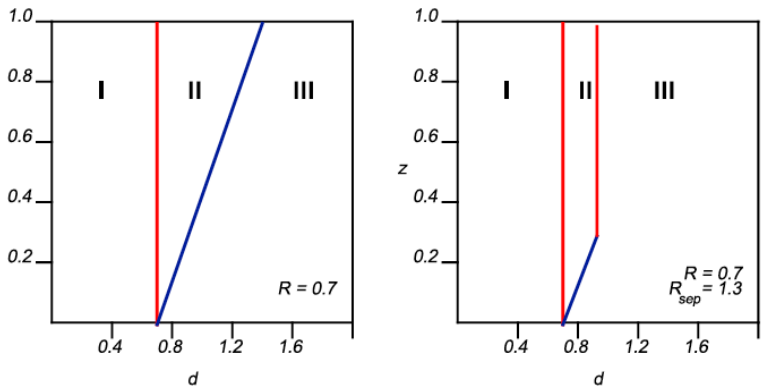

Figure 22. The parameter space (d,Z) for which two partons will be merged into a single jet.

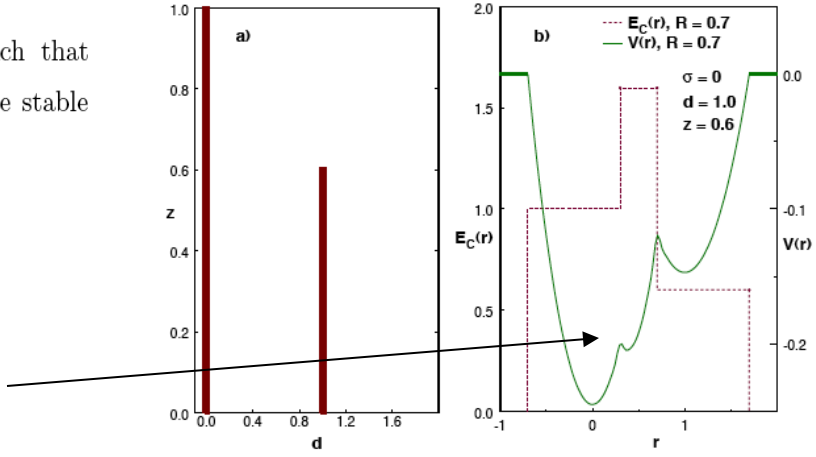

Figure 51. A schematic depiction of a specific parton configuration and the results of applying the midpoint cone jet clustering algorithm. The potential discussed in the text and the resulting energy in the jet are plotted.

Is the K-factor (at m_W) at the LHC surprising?

The problem is not the NLO cross section; that is well-behaved.
The problem is that the LO cross section sits 'too-high'. The reason (one of them) for this is that we are 'too-close' to the collinear pole (R=0.4) leading to an enhancement of the LO cross section (double-enhancement if the gluon is soft (~20 GeV/c)). Note that at LO, the cross section increases with decreasing R; at NLO it decreases. The collinear dependence gets stronger as n_{jet} increases.
The K-factors for W + 3 jets would be more *normal* (>1) if a larger cone size and/or a larger jet p_T cutoff were used. But that's a LO problem; the best approach is to use the appropriate jet sizes/jet p_T's for the analysis and understand the best scales to use at LO (matrix element + parton shower) to approximate the NLO calculation (as well as comparing directly to the NLO calculation).

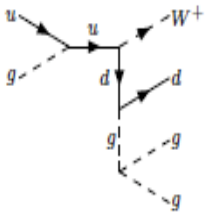

LHC total cross section

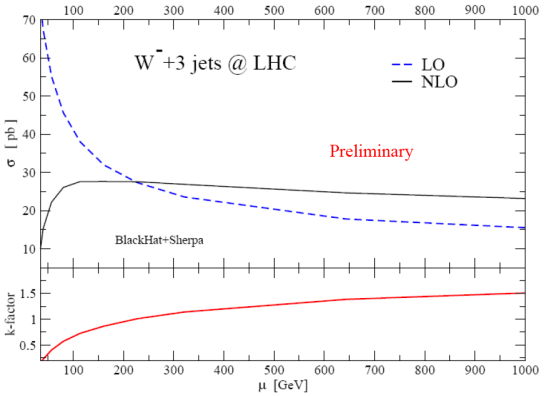

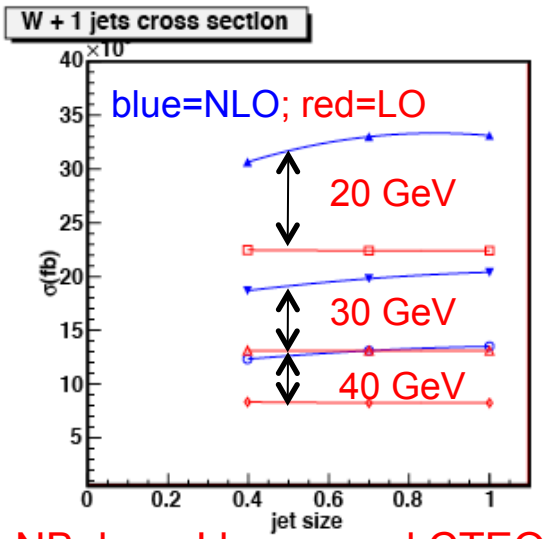

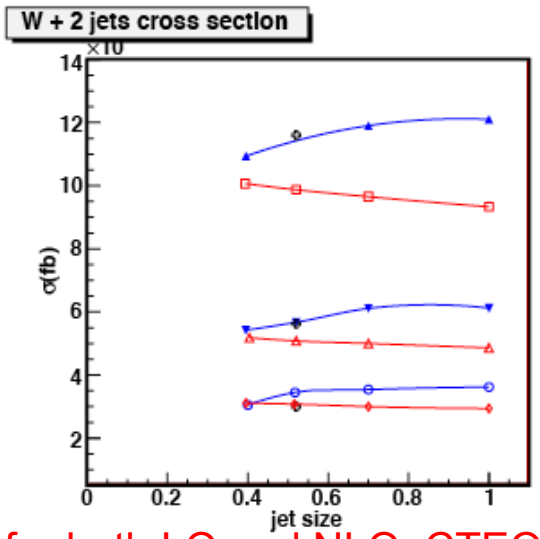

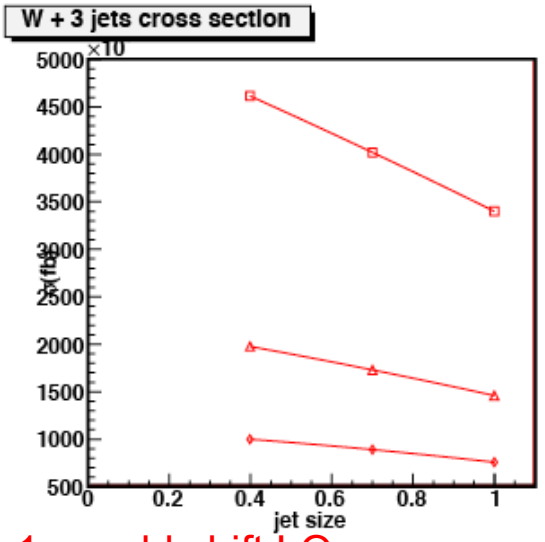

For 3 jets, the LO collinear singularity effects are even more pronounced.

NB: here I have used CTEQ6.6 for both LO and NLO; CTEQ6L1 would shift LO curves up

Cross sections and jets

- Compare the behavior of the jet cross sections at LO and NLO
- At LO
  - SISCone and antikT result in very different cross sections
  - there is a very large jet size dependence
- At NLO
  - SISCone and antikT have very similar cross sections that are mainly independent on jet size
- In data
  - ditto
- Lesson
  - don't trust fixed LO cross section predictions for multi-parton final states
  - MLM scheme/Sherpa dont have this problem; they aren't fixed order

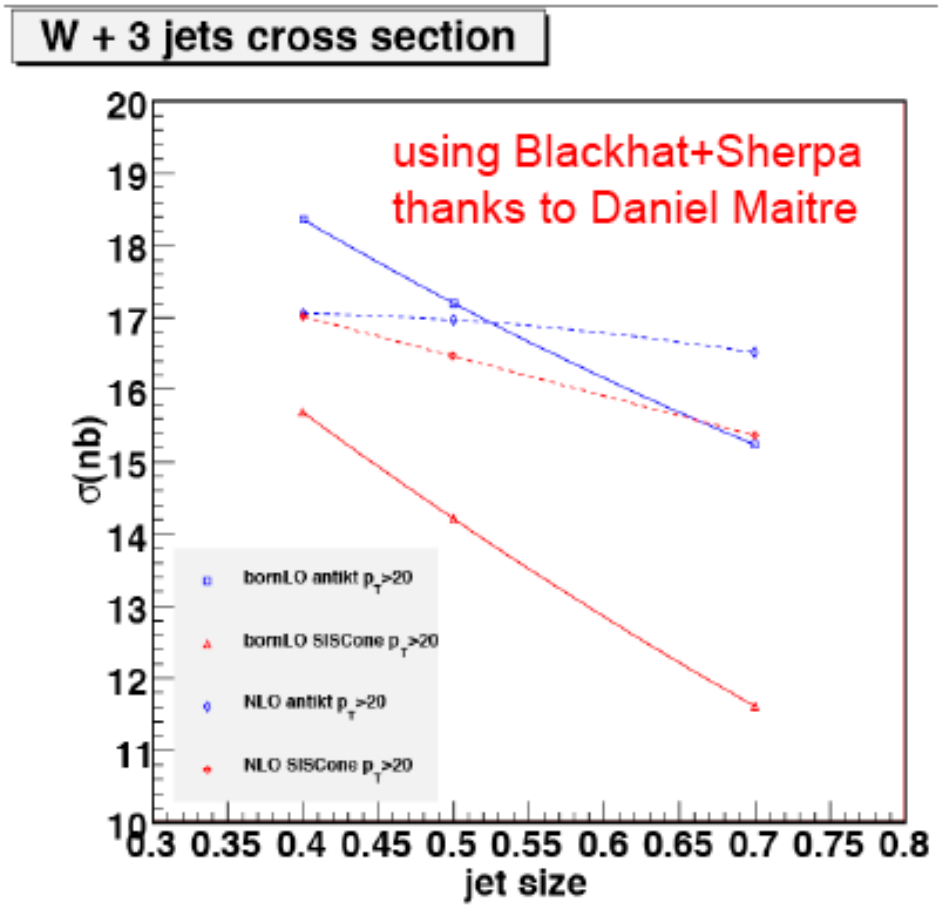

note NLO~LO because a scale of H_T has been used

Why does mlm matching/CKKW help stabilize the cross section?

- mlm
  - generate parton-level configurations for a given hard parton multiplicity N_{part}, with partons constrained by $p_T > p_{Tmin}$, $\Delta R_{jj} > R_{min}$
  - perform the parton showering
  - process the showered event with a cone jet algorithm defined by p_T^{jet} and R_{jet}
  - match partons and jet
    - for each hard parton, select the jet with min $\Delta R_{j\text{-parton}}$
    - if $\Delta R_{j\text{-parton}} < R_{jet}$, the parton is matched
    - a jet can only be matched to a single parton
    - if all partons are matched, keep the event; otherwise throw it away
    - for exclusive, require $N_{jets} = N_{part}$

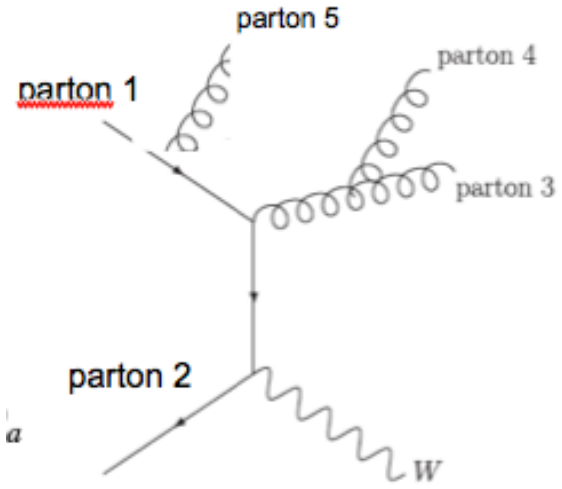

$$d\sigma = \sigma_0(W + 1\ \text{jet})\left[1 + \alpha_S(c_{12}L^2 + c_{11}L + c_{10}) + \alpha_S{}^2(c_{24}L^4 + c_{23}L^3 + c_{22}L^2 + c_{21}L + c_{20}) + \cdots\right]$$

- if partons 1 and 5 and/or partons 3 and 4 become collinear, then large logs and larger parton level cross section
- however, the requirement that $N_{jets} = N_{part}$ tends to equalize the cross sections regardless of R_{min} cut (for given R_{jet})

Is this the end of the complications?

- We'll see later that additional complications are introduced by the fact that we don't measure partons in our jets in ATLAS, but energy that is distributed over a wide area of the detector by parton showering, hadronization and showering

W + jets at the Tevatron

- At the Tevatron, m_W is a reasonable scale (in terms of K-factor~1)

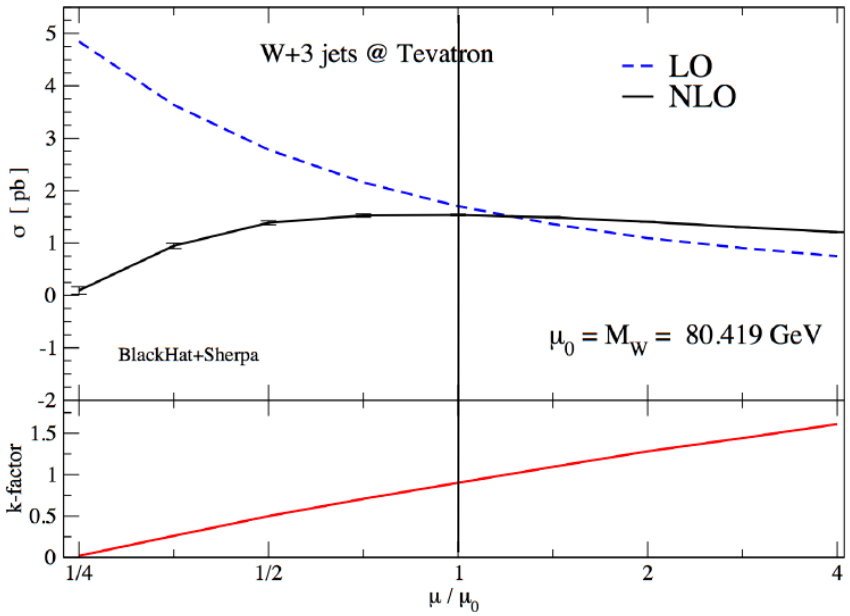

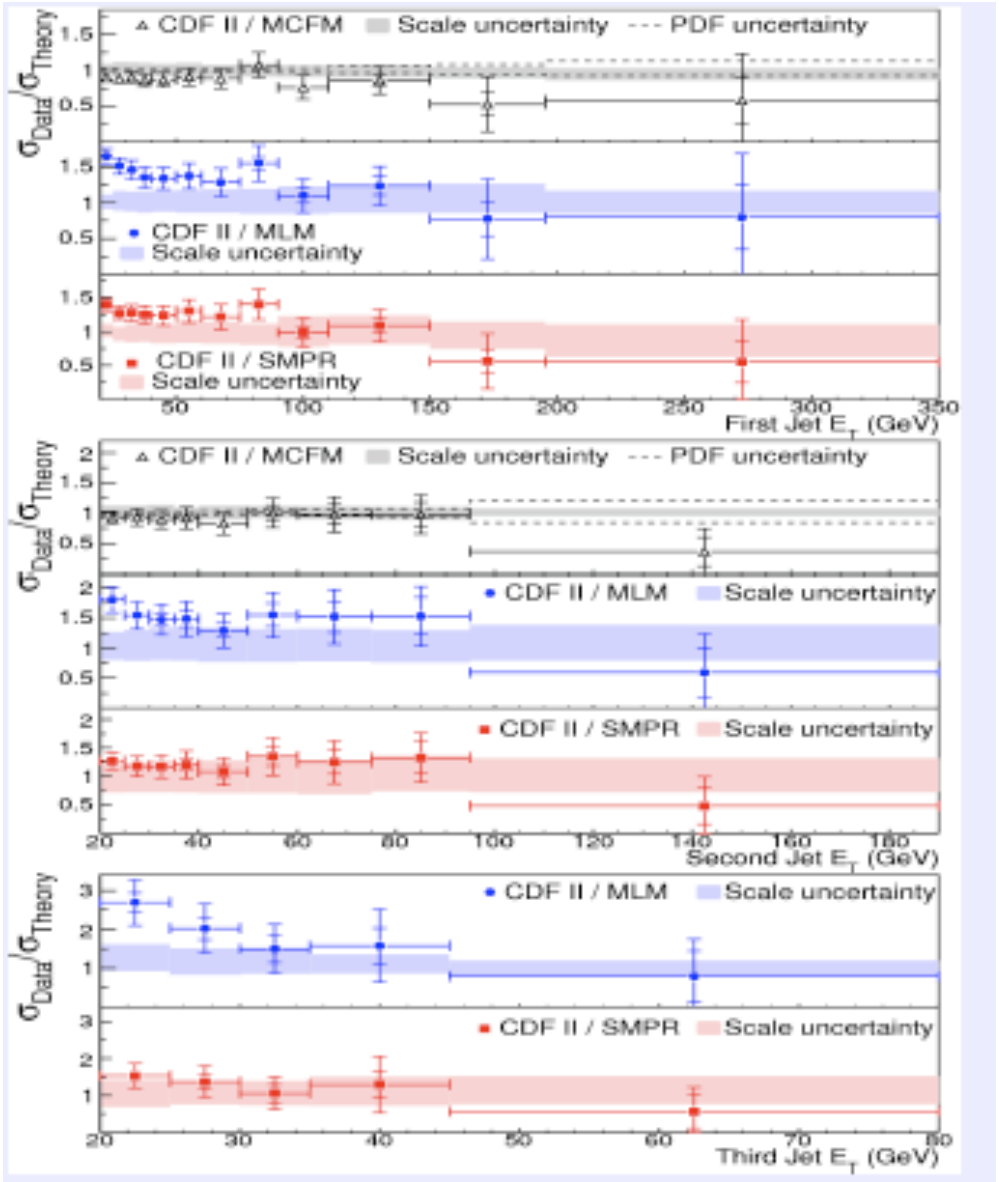

W + 3 jets at the LHC

A scale choice of m_W would be in a region where LO >> NLO. In addition, such a scale choice (or related scale choice), leads to sizeable shape differences in the kinematic distributions. The Blackhat people found that a scale choice of $H_T/2$ worked best to get a constant K-factor for all distributions that they looked at. This has also been found for a number of other processes, like tttt.

LHC total cross section

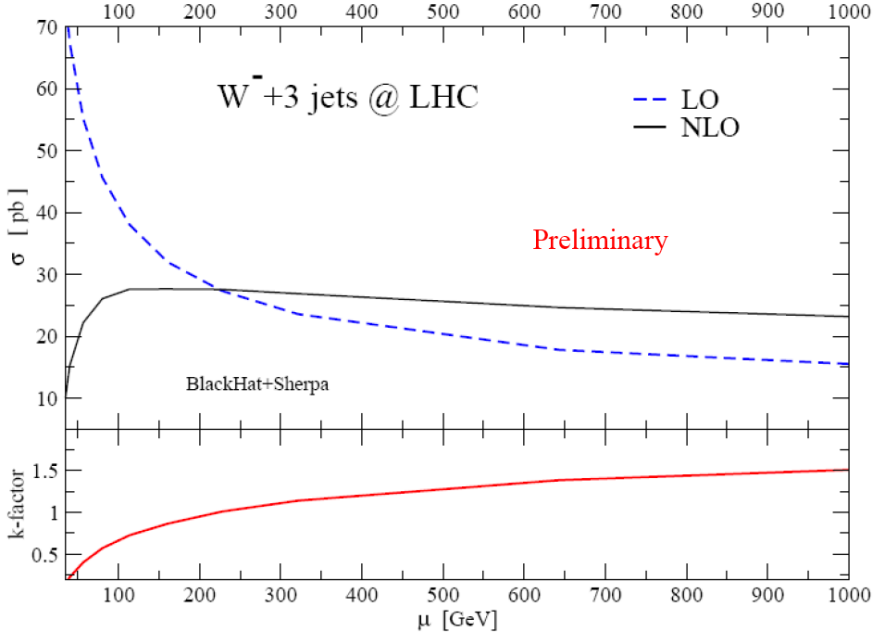

$H_T = \sum_j E_{T,j}^{\text{jet}} + E_T^e + \not{E}_T$ distribution

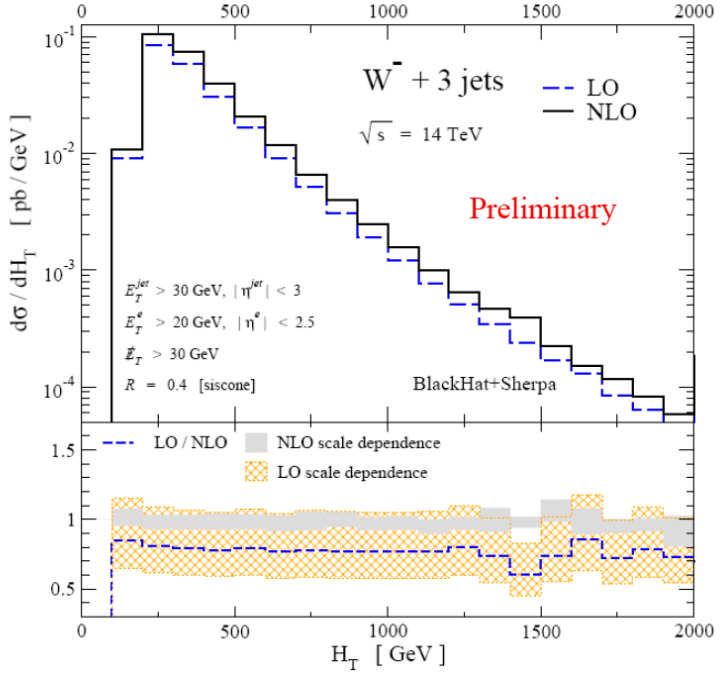

mu = H_T

Scales at LO and NLO

- Using a CKKW-like scale at LO leads to better agreement (with NLO) for shapes of kinematic distributions

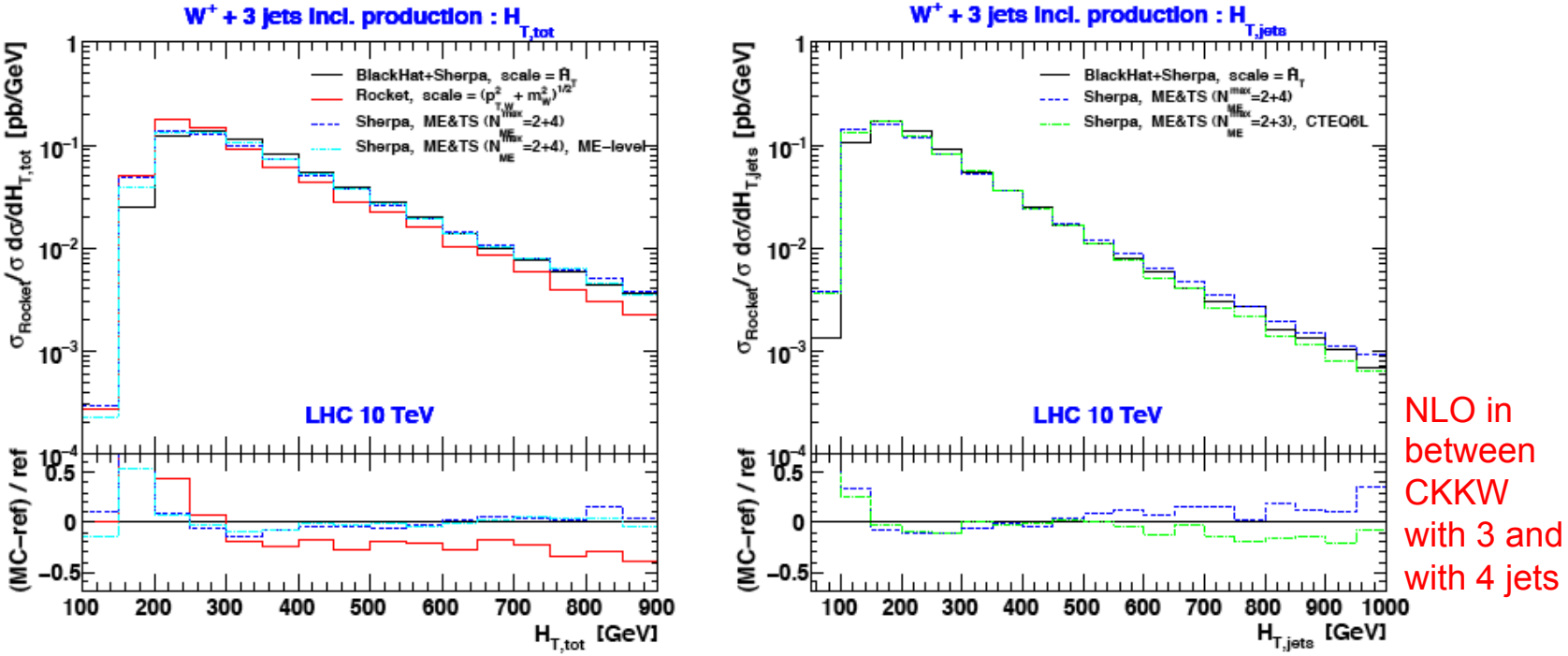

NLO in between CKKW with 3 and with 4 jets

Fig. 19: H_T and $H_{T,\text{jets}}$ distributions in inclusive W^+ + 3 jet production at the LHC. NLO predictions obtained from BLACKHAT+SHERPA (black line) and ROCKET (red line) are compared to LO results from SHERPA using the ME&TS merging. All curves have been rescaled to the ROCKET NLO cross section of Table 5; the BLACKHAT+SHERPA prediction is used as the reference; cuts and parameters are detailed in Section 12.2

See review of W + 3 jets in Les Houches 2009 NLM proceedings

also 0910.3671 Melnikov, Zanderighi

Choosing jet size

- Experimentally
  - in complex final states, such as W + n jets, it is useful to have jet sizes smaller so as to be able to resolve the n jet structure
  - this can also reduce the impact of pileup/ underlying event
- Theoretically
  - hadronization effects become larger as R decreases
  - for small R, the ln R perturbative terms referred to previously can become noticeable
  - this restriction in the gluon phase space can affect the scale dependence, i.e. the scale uncertainty for an n-jet final state can depend on the jet size,

Another motivation for the use of multiple jet algorithms/parameters in LHC analyses.

Another perspective

- There are fluctuations in radiation, hadronization and in UE subtraction
- Perturbative radiation
  - quark
  $$\Delta p_T \approx \frac{\alpha_s C_A}{\pi} p_T \ln R$$
  - gluon
  $$\Delta p_T \approx \frac{\alpha_s C_F}{\pi} p_T \ln R$$
- Hadronization
  - quark
  $$\Delta p_T \approx \frac{C_F}{R} \bullet 0.4 \text{ GeV}$$
  - gluon
  $$\Delta p_T \approx \frac{C_A}{R} \bullet 0.4 \text{ GeV}$$
- Underlying event
  $$\Delta p_T \approx \frac{R^2}{2} \bullet 2.5 - 15 \text{ GeV}$$

	Dependence of jet $\langle \delta p_t \rangle$ on			
	'partonic' p_t	colour factor	R	$\sqrt{s}$
perturbative radiation	$\sim \alpha_s(p_t)\, p_t$	C_i	$\ln R + \mathcal{O}(1)$	–
hadronization	–	C_i	$-1/R + \mathcal{O}(R)$	–
underlying event	–	–	$R^2 + \mathcal{O}(R^4)$	s^ω

Table 1: Summary of the main physical effects that contribute to the relation between the transverse momentum of a jet and that of a parton, together with their dependence on the properties of the parton, the jet radius R and collider centre of mass energy. Cases labelled "–" do not have any dependence on the corresponding variable in a leading approximation, but may develop anomalous-dimension type dependences at higher orders.

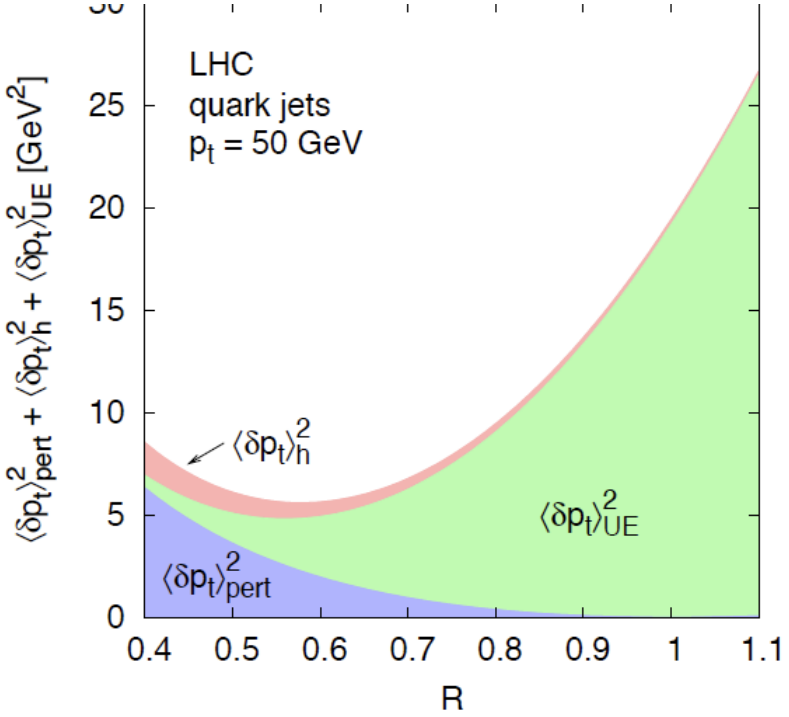

crude analytical estimates

cf. Dasgupta, Magnea & GPS '07

This doesn't take interplay between virtual and real gluons into account.

Jet sizes and scale uncertainties: the Goldilocks theorm

- Take inclusive jet production at the LHC for transverse momenta of the order of 50 GeV
- Look at the theory uncertainty due to scale dependence as a function of jet size
- It appears to be a minimum for cone sizes of the order of 0.7
  - i.e. if you use a cone size of 0.4, there are residual un-cancelled virtual effects
  - if you use a cone size of 1.0, you are adding too much tree level information with its intrinsically larger scale uncertainty
- This effect becomes smaller for jet p_T values on the order of 100 GeV/c
  - how does it translate for multi-parton final states?

Jet vetos and scale dependence: WWjet

- Often, we cut on the presence of an extra jet
- This can have the impact of improving the signal to background ratio
  - …and it may appear that the scale dependence is improved
- However, in the cases I know about, the scale dependence was *anomalous* at NLO without the jet veto, indicating the presence of uncancelled logs
- The apparent improvement in scale dependence may be illusory

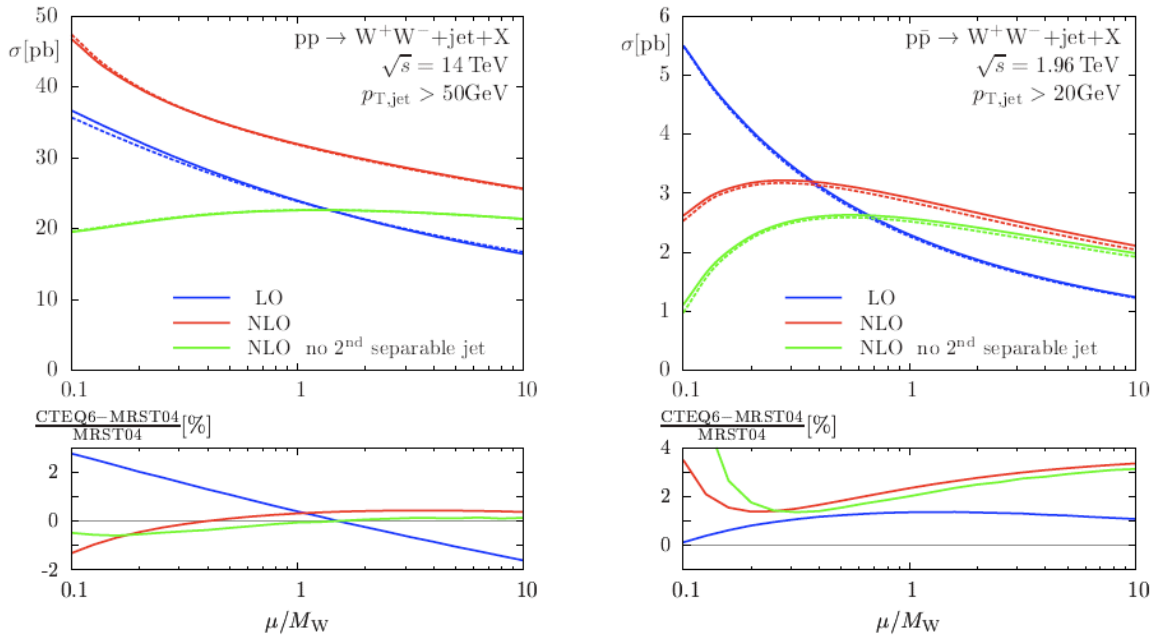

Figure 11: Comparison of WW+jet production cross sections in the LHC setup with $p_{T,jet} > 50\,\text{GeV}$ and for Tevatron with $p_{T,jet} > 20\,\text{GeV}$: The straight lines show the results calculated with the five-flavour PDFs of CTEQ6, the dashed lines those calculated with the four-flavour PDFs of MRST2004F4. Contributions from external bottom (anti-)quarks are omitted, as described in Section 2.2.

Consider tTbB

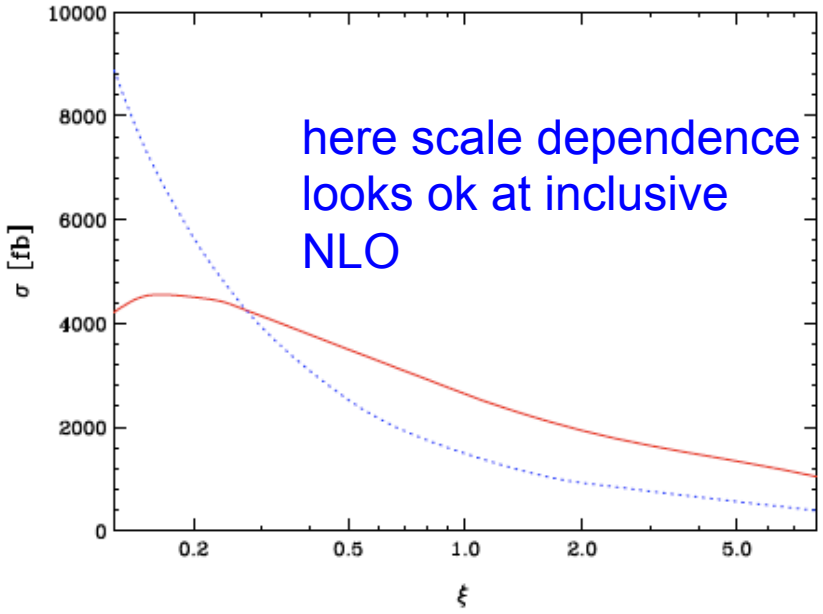

Perturbative instability for small $p_{\mathrm{jet,veto}}$

- veto $\Rightarrow$ negative contribution $-\alpha_s^5 \ln^2(Q_0/p_{\mathrm{jet,veto}})$
- IR log dramatically enhances NLO uncertainty
- $p_{\mathrm{jet,veto}} < 40\,\mathrm{GeV} \Rightarrow$ NLO-band enters $K < 0$ range
  NLO prediction completely unrealiable!

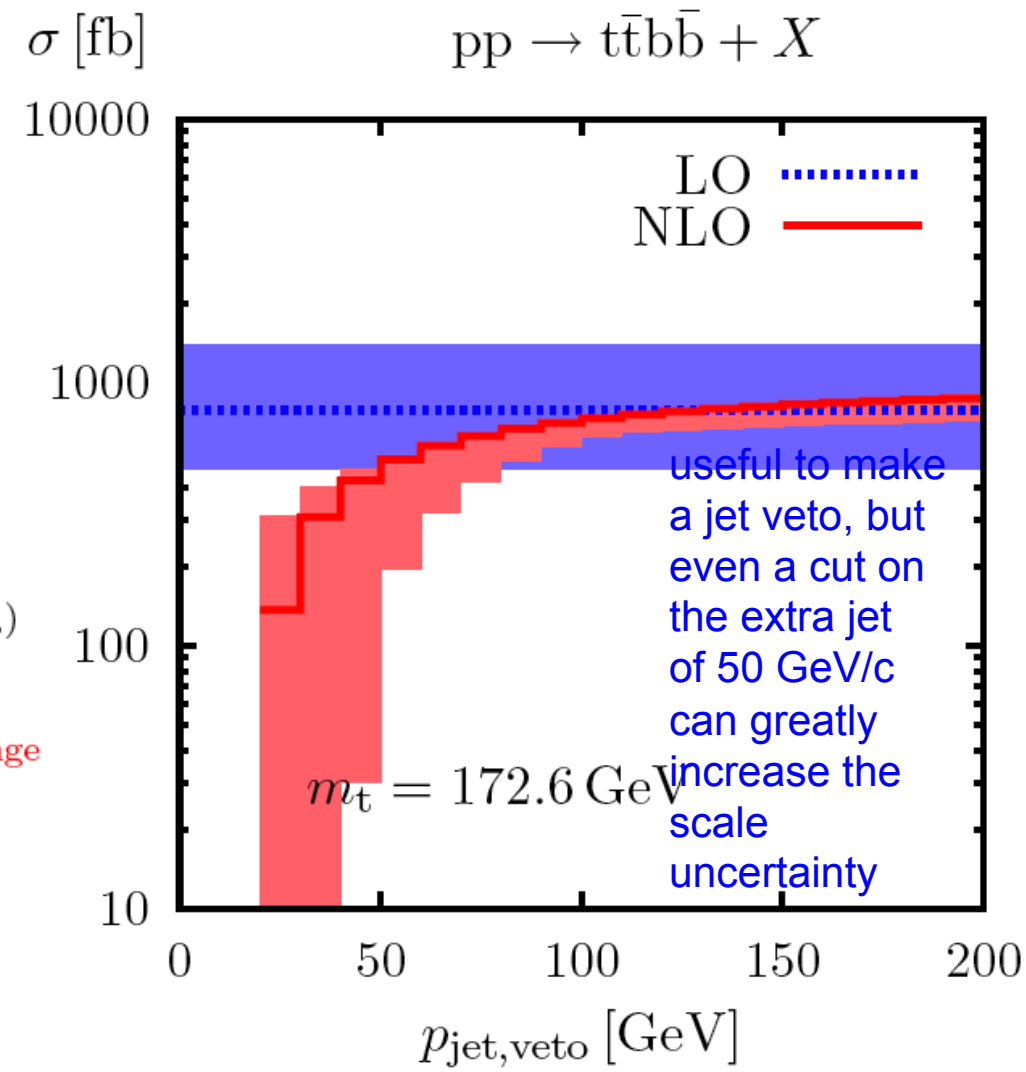

Uncertainties in the face of jet vetos/bins

- For Higgs searches (with decays into WW*), important to divide sample into separate jet bins
  - backgrounds are different
- If I calculate the scale uncertainties naively, I get the following

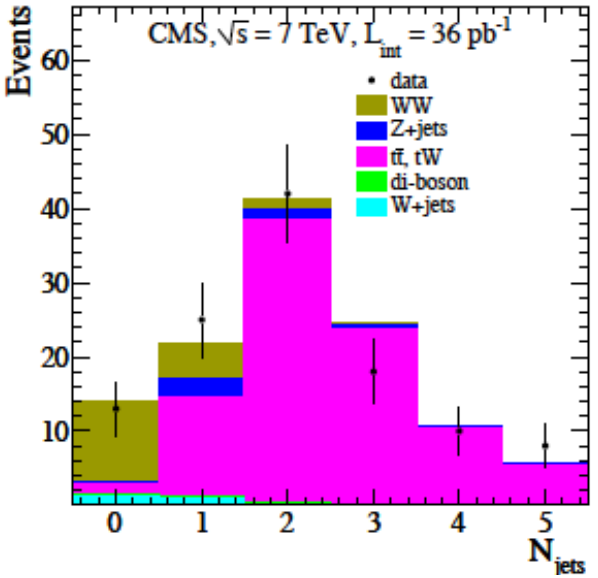

- Common scale variation for jet bins, e.g. for the Tevatron

$$\frac{\Delta\sigma}{\sigma} = \underbrace{66.5\% \times \binom{+5\%}{-9\%}}_{0\text{ jets}} + \underbrace{28.6\% \times \binom{+24\%}{-22\%}}_{1\text{ jet}} + \underbrace{4.9\% \times \binom{+78\%}{-41\%}}_{\geq 2\text{ jets}} = \binom{+14\%}{-14\%}$$

- *Smaller* uncertainty in 0-jet bin than in inclusive cross section

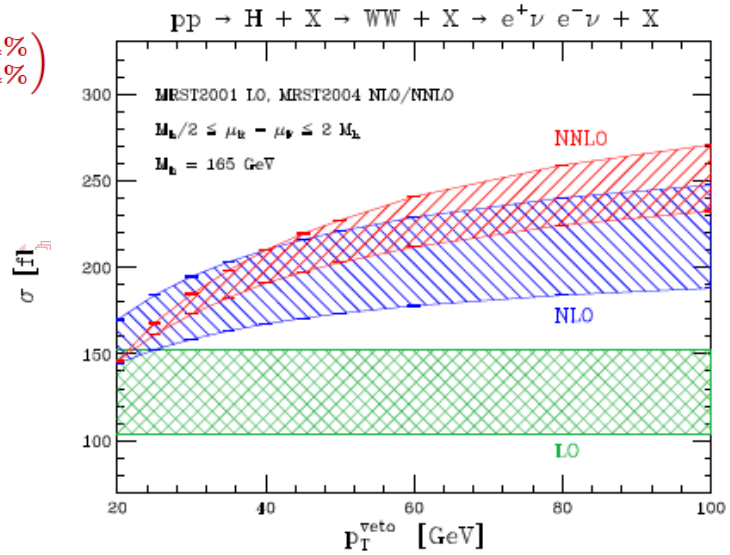

Perturbative Structure of Jet Cross Sections

$$\sigma_{\text{total}} = \underbrace{\int_0^{p_T^{\text{cut}}} \mathrm{d}p_T \frac{\mathrm{d}\sigma}{\mathrm{d}p_T}}_{\sigma_0(p_T^{\text{cut}})} + \underbrace{\int_{p_T^{\text{cut}}}^{\infty} \mathrm{d}p_T \frac{\mathrm{d}\sigma}{\mathrm{d}p_T}}_{\sigma_{\geq 1}(p_T^{\text{cut}})}$$

$$\sigma_{\text{total}} = 1 + \alpha_s + \alpha_s^2 + \cdots$$

$$\sigma_{\geq 1}(p_T^{\text{cut}}) = \alpha_s(L^2 + L) + \alpha_s^2(L^4 + L^3 + L^2 + L) + \cdots$$

$$\begin{aligned}\sigma_0(p_T^{\text{cut}}) &= \sigma_{\text{total}} - \sigma_{\geq 1}(p_T^{\text{cut}}) \\ &= \left[1 + \alpha_s + \alpha_s^2 + \cdots\right] - \left[\alpha_s(L^2 + L) + \alpha_s^2(L^4 + \cdots) + \cdots\right]\end{aligned}$$

- Perturbative series in σ_{total} and $\sigma_{\geq 1}(p_T^{\text{cut}})$ have different structures and are unrelated
- Apparent small uncertainties in $\sigma_0(p_T^{\text{cut}})$ arise from cancellation between two series with large corrections

…should treat perturbation series for $\sigma_{>=0\text{jets}}$, $\sigma_{>=1\text{ jet}}$, $\sigma_{>=2\text{ jets}}$ as independent with uncorrelated systematic errors (i.e, add in quadrature)

Realistic Fixed-Order Scale Uncertainties

Using naive scale variation for σ_0

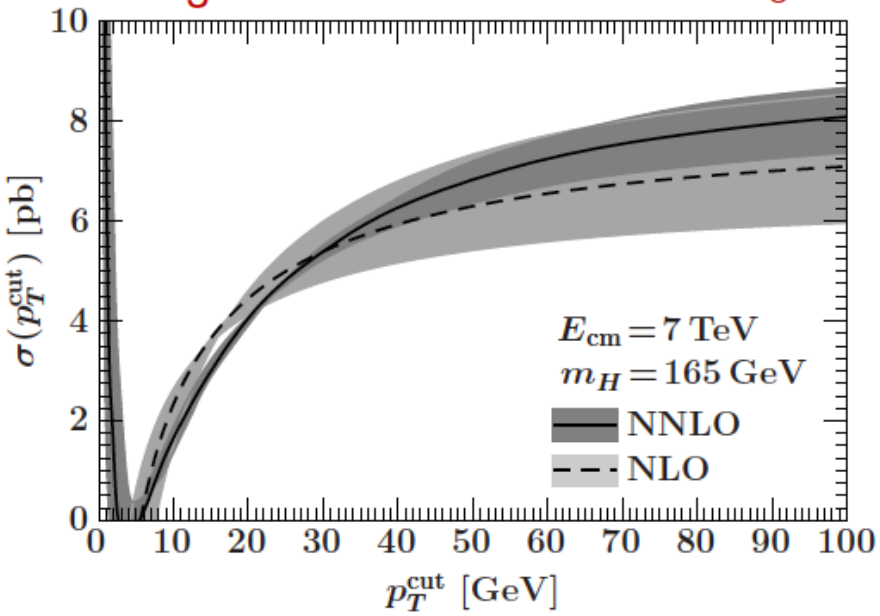

Using above procedure for σ_0

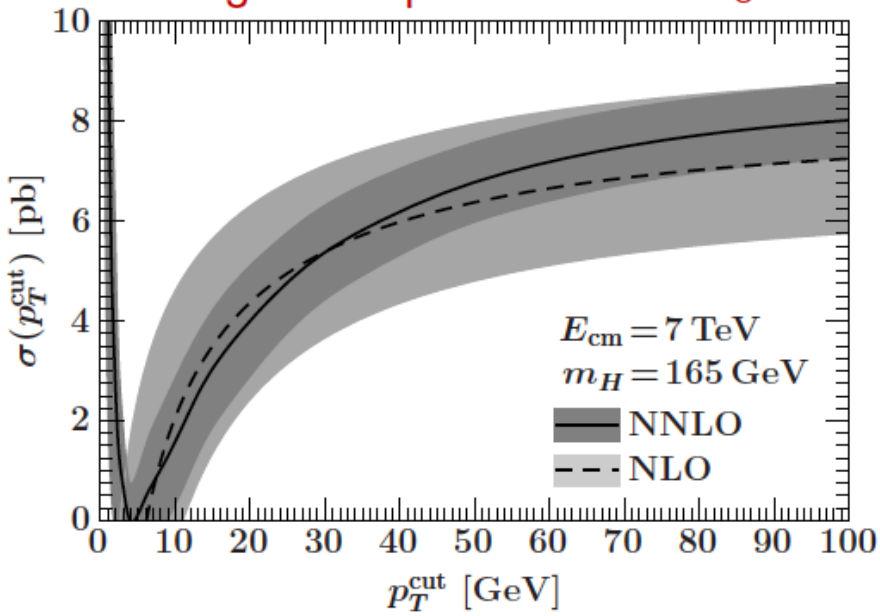

- Uncertainties reproduce naive scale variation at large cut values
- Larger uncertainties at small cut values $\rightarrow$ take into account presence of large logarithmic corrections

e.g. at LHC with $p_T^{\rm cut} = 30\,{\rm GeV}$

method	$\frac{\Delta\sigma_{\rm total}}{\sigma_{\rm total}}$	$\frac{\Delta\sigma_0}{\sigma_0}$	$\frac{\Delta\sigma_1}{\sigma_1}$	$\frac{\Delta\sigma_{\geq 2}}{\sigma_{\geq 2}}$
naive	10%	5%	14%	45%
new	10%	17%	29%	45%

Jet algorithms and scale uncertainty

•Look at results for SISCone/antikT; antikT cross sections larger than SISCone, smaller scale dependence?

Multi-jet systematics: jet-algorithms Z+n jets.

CDF: Phys. Rev. Lett. 100, 102001 (2008)
[BlackHat: 0912.4927, 1004.1659]
See also talk by J. Huston

σ in [fb]

# of jets	LO parton SISCone	NLO parton SISCone	LO parton anti-k_T	NLO parton anti-k_T	Non-pert correction
1	$4635(2)^{+928}_{-715}$	$6080(12)^{+354}_{-402}$	$4635(2)^{+928}_{-715}$	$5783(12)^{+257}_{-334}$	~1.1
2	$429.8(0.3)^{+171.7}_{-111.4}$	$564(2)^{+59}_{-70}$	$481.2(0.4)^{+191}_{-124}$	$567(2)^{+31}_{-57}$	~1.2
3	$24.6(0.03)^{+14.5}_{-8.2}$	$35.9(0.9)^{+7.8}_{-7.2}$	$37.88(0.04)^{+22.2}_{-12.6}$	$44.9(0.3)^{+4.7}_{-7.1}$	~1.4

Z + 3 jets: scale dependence

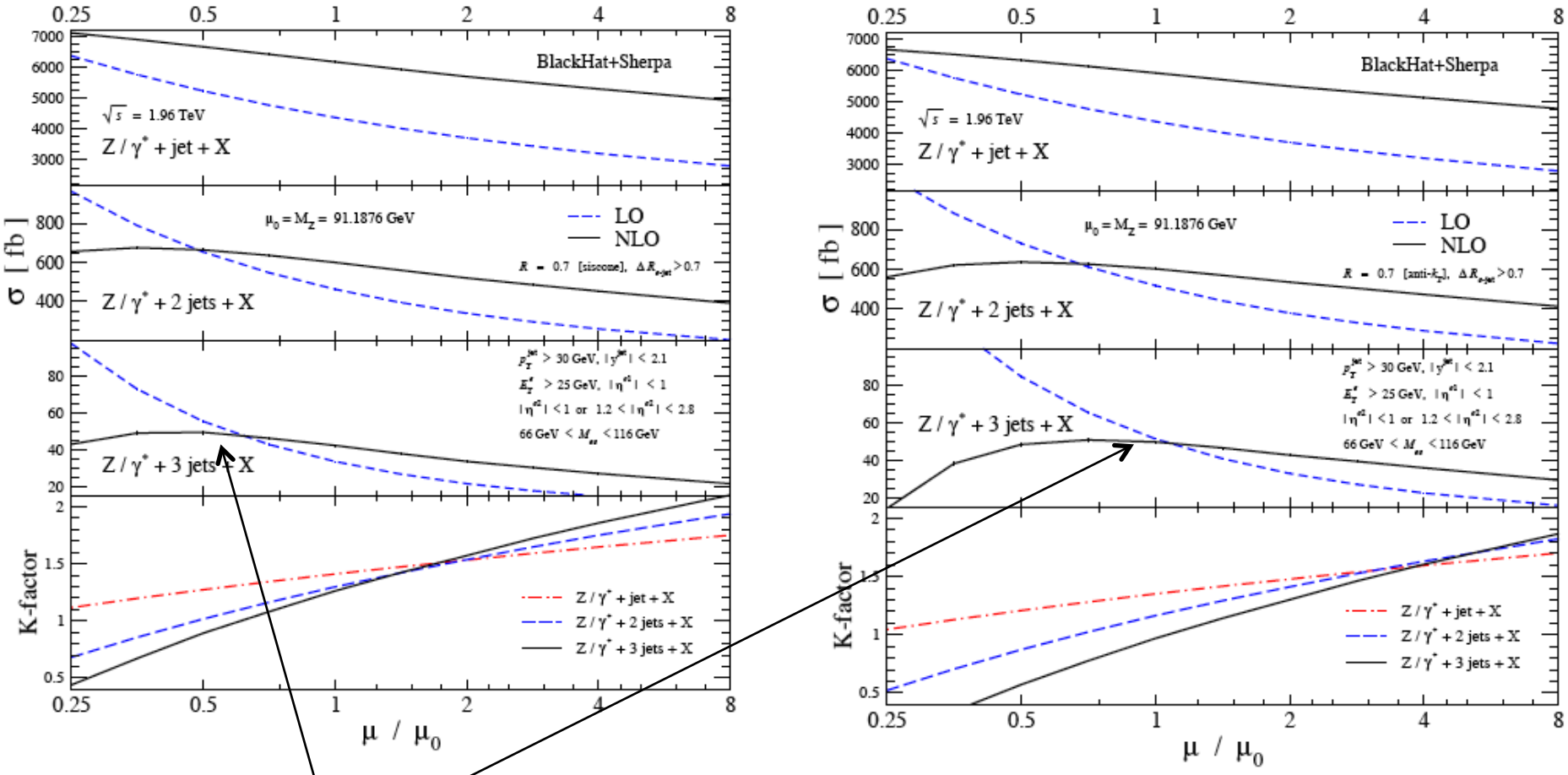

Note that peak cross sections are actually quite close; the cross sections just peak at different scales.

1004.1659

All-orders approaches

- Rather than systematically calculating to higher and higher orders in the perturbative expansion, can also use a number of all-orders approaches
- In resummation, dominant contributions from each order in perturbation theory are singled out and resummed by use of an evolution equation
- Near boundaries of phase space, fixed order calculations break down due to large logarithmic corrections, and these contributions can become important. Resummation takes them into account.

- Consider W production
  - one large logarithm associated with production of vector boson close to threshold
  - takes form of

$$\frac{\alpha_s^n \log^{2n-1}(1-z)}{1-z}$$

  - where

$$z = \frac{Q^2}{\hat{s}} - 1$$

  - other large logarithm is associated with recoil of vector boson at very small p_T
  - logarithms appear as $\alpha_s^n \log^{2n-1}(Q^2/p_T^2)$

In both cases there is a restriction of phase space for gluon emission and thus the logs become large and are crucial for an accurate prediction

All-orders approaches

- Remember the expression we had after adding gluons on to the W + 1 jet process
  - each gluon added yields an additional factor of α_s and two new logarithms

$$d\sigma = \sigma_0(W + 1 \text{ jet})\left[1 + \alpha_S(c_{12}L^2 + c_{11}L + c_{10}) + \alpha_S{}^2(c_{24}L^4 + c_{23}L^3 + c_{22}L^2 + c_{21}L + c_{20}) + \cdots\right]$$

- q_T resummation is resumming the effects of logs of $Q^2/p_T{}^2$

- note that q_T resummation does not change the size of the cross section; it just modifies the p_T distribution of the W

- These are the leading logs (LL) (highest power of log for each power of α_s)
- These are the next-to-leading logs (NLL) (next highest power of log…)
  - …and so on
- We know the structure of the LL's, NLL's, NNLL's
- But we don't know the c_{ij} factors until we do the finite order calculation
- LO gives us the LL
- NLO gives us the NLL
  - …and so on
- The accuracy of the resummation improves with the addition for further higher order information
- A resummation program like ResBos has NNLL accuracy

All-orders approaches

- Remember the expression we had after adding gluons on to the W + 1 jet process
  - each gluon added yields an additional factor of α_s and two new logarithms

$$d\sigma = \sigma_0(W+1\text{ jet})\left[1+\alpha_S(c_{12}L^2+c_{11}L+c_{10}) + \alpha_S{}^2(c_{24}L^4+c_{23}L^3+c_{22}L^2+c_{21}L+c_{20})+\cdots\right]$$

- q_T resummation is resumming the effects of logs of $Q^2/p_T{}^2$

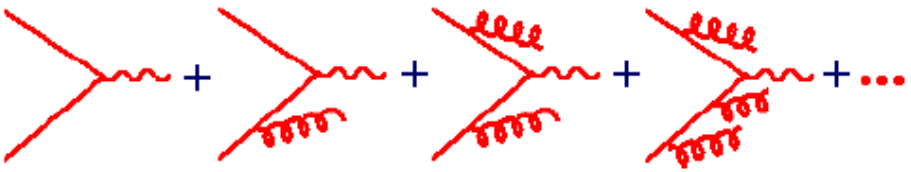

- note that q_T resummation does not change the size of the cross section; it just modifies the p_T distribution of the W

- Expression for W boson transverse momentum in which leading logarithms have been resummed to all orders is given by

$$\frac{d\sigma}{dp_T^2} = \sigma\frac{d}{dp_T^2}\exp\left(-\frac{\alpha_S C_F}{2\pi}\log^2 M_W^2/p_T^2\right)$$

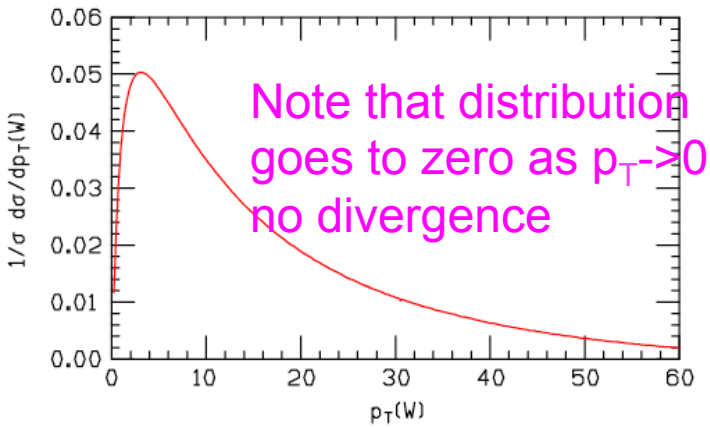

Figure 20. The resummed (leading log) *W* boson transverse momentum distribution.

You could get the same predictions by using PDFs in which the transverse momentum (k_T) has not been integrated out

W/Z p_T distributions at the Tevatron and LHC

- Expect p_T distributions will be shifted (slightly) upwards due to larger phase space for gluon emission
- BFKL logs may become important and have a noticeable effect on the W/Z p_T distributions
- One of early benchmarks; range of importance for BFKL physics
  - no sign so far at 7 TeV

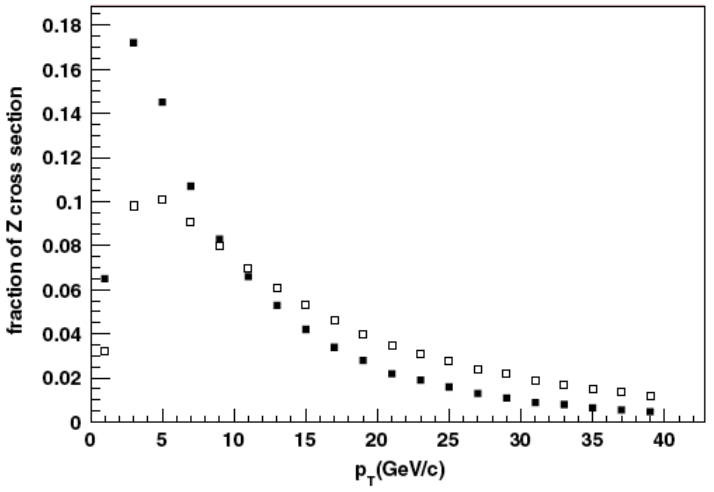

Figure 89. Predictions for the transverse momentum distributions for Z production at the Tevatron (solid squares) and LHC (open squares).

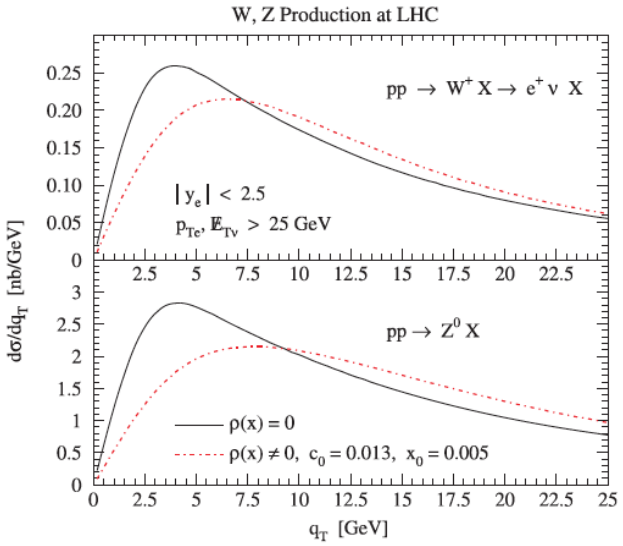

Figure 90. The predictions for the transverse momentum distributions for W and Z production with and without the p_T-broadening effects.

Parton showers

- A different, but related approach for re-summing logarithms, is provided by parton showering
- By the use of the parton showering process, a few partons produced in a hard interaction at a high-energy scale can be related to partons at an energy scale close to Λ_{QCD}.
- At this lower energy scale, a universal non-perturbative model can then be used to provide the transition to hadrons
- Parton showering allows for evolution, using DGLAP formalism, of parton fragmentation function

Parton Cascade

…plus similar for initial state

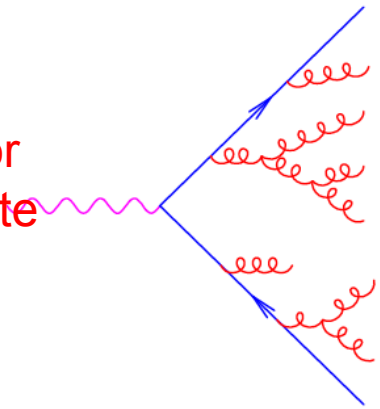

- Due to successive branching, parton cascade or shower develops. Each outgoing line is source of new cascade, until all outgoing lines have stopped branching. At this stage, which depends on cutoff scale t_0, outgoing partons have to be converted into hadrons via a hadronization model.

- Successive values of an evolution variable t, a momentum fraction z and an azimuthal angle ϕ are generated, along with the flavors of the partons emitted during the parton shower

Parton shower evolution

- On average, emitted gluons have decreasing angles with respect to parent parton directions
  - angular ordering, an aspect of color coherence
- The evolution variable *t* can be the virtuality of the parent parton [old Pythia and old Sherpa], $E^2(1-\cos\theta)$ where E is the energy of the parent parton and and θ is the opening angle between the two partons [Herwig], or the square of the transverse momentum between the two partons [new Pythia]

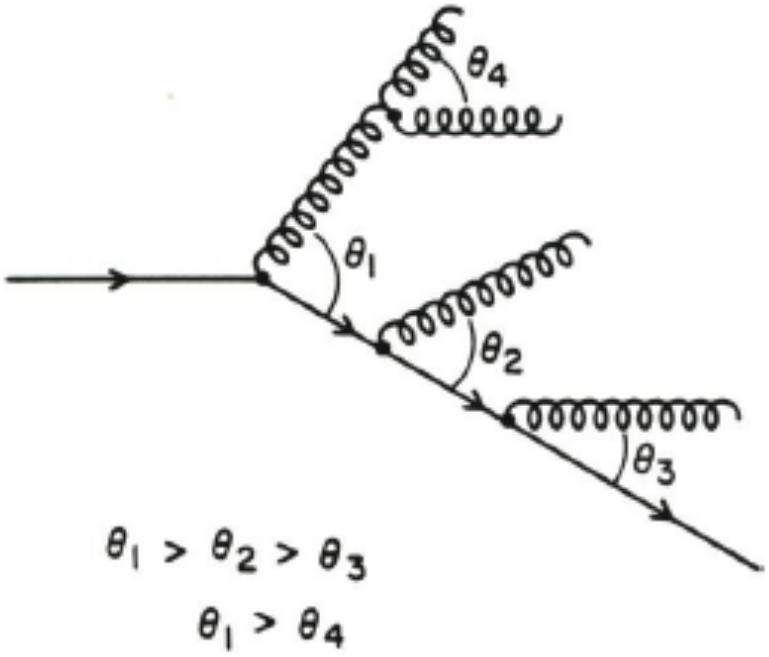

Sudakov form factors

- Sudakov form factors form the basis for both resummation and parton showering
- We can write an expression for the Sudakov form factor of an initial state parton in the form below, where *t* is the hard scale, t_0 is the cutoff scale and *P(z)* is the splitting function

$$\Delta(t) \equiv \exp\left[-\int_{t_0}^{t} \frac{dt'}{t'} \int \frac{dz}{z} \frac{\alpha_S}{2\pi} P(z) \frac{f(x/z,t)}{f(x,t)}\right]$$

- Similar form for the final state but without the pdf weighting
- Sudakov form factor resums all effects of soft and collinear gluon emission (so again the double logs), but does not include non-singular regions that are due to large energy, wide angle gluon emission
- Gives the probability **not** to radiate a gluon greater than some energy
- We can draw explicit (approximate) curves for the Sudakov form factors

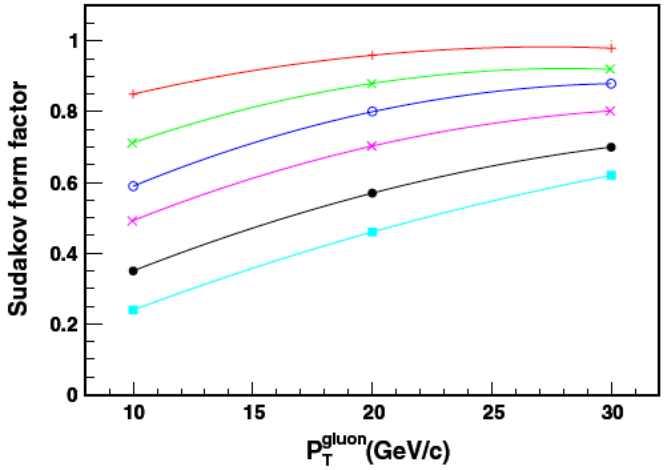

Figure 21. The Sudakov form factors for initial-state gluons at a hard scale of 100 GeV as a function of the transverse momentum of the emitted gluon. The form factors are for (top to bottom) parton x values of 0.3, 0.1, 0.03, 0.01, 0.001 and 0.0001.

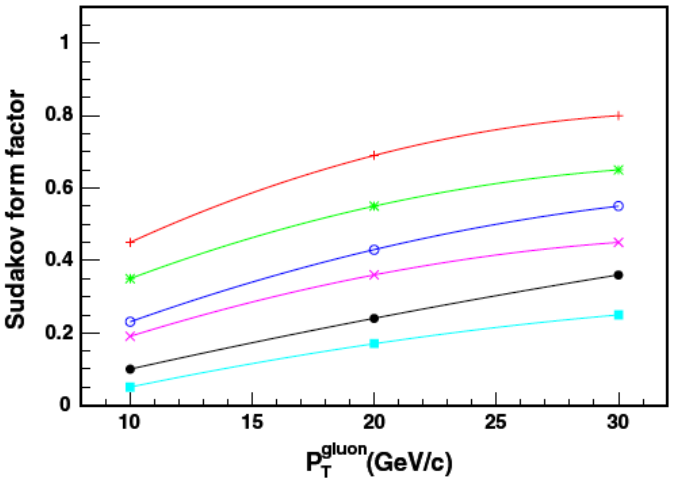

Figure 22. The Sudakov form factors for initial-state gluons at a hard scale of 500 GeV as a function of the transverse momentum of the emitted gluon. The form factors are for (top to bottom) parton x values of 0.3, 0.1, 0.03, 0.01, 0.001 and 0.0001.

Sudakov form factors

- The Sudakov form factor decreases (the probability of radiating increases) as the p_T of the radiated gluon decreases, as the hardness of the interaction increases, or as the x value of the incoming parton decreases (more phase space for gluon radiation)
- NB: some additional kinematic factors (related to available energy for gluon emission) not indicated

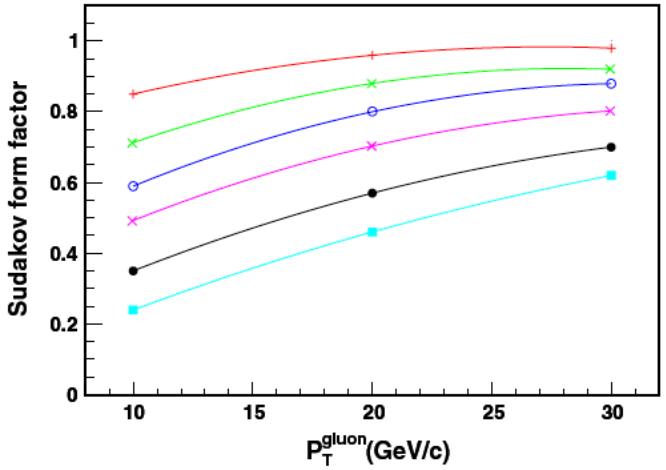

Figure 21. The Sudakov form factors for initial-state gluons at a hard scale of 100 GeV as a function of the transverse momentum of the emitted gluon. The form factors are for (top to bottom) parton x values of 0.3, 0.1, 0.03, 0.01, 0.001 and 0.0001.

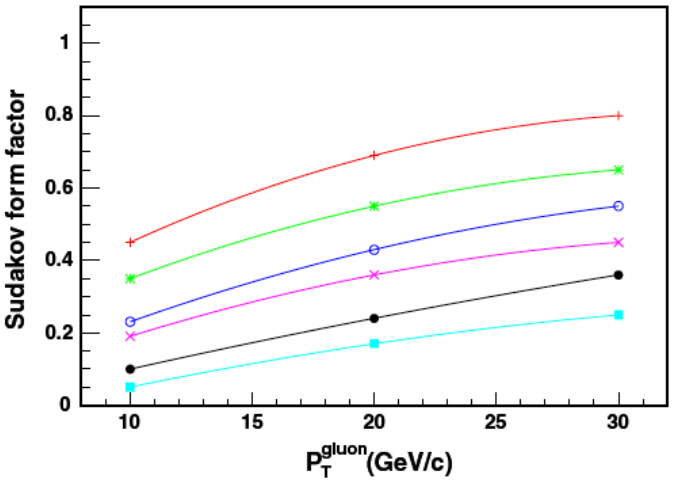

Figure 22. The Sudakov form factors for initial-state gluons at a hard scale of 500 GeV as a function of the transverse momentum of the emitted gluon. The form factors are for (top to bottom) parton x values of 0.3, 0.1, 0.03, 0.01, 0.001 and 0.0001.

Sudakov form factors: quarks and gluons

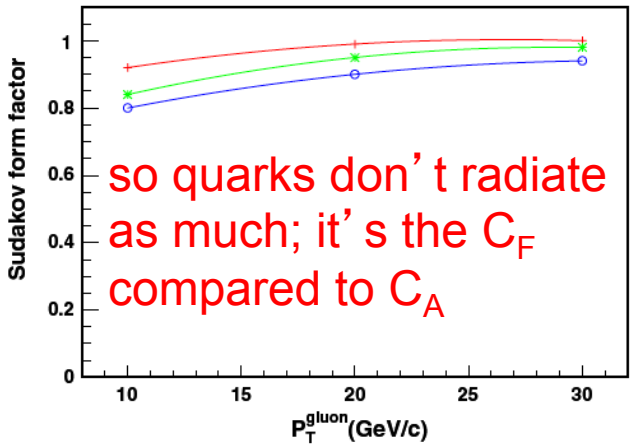

so quarks don't radiate as much; it's the C_F compared to C_A

Figure 23. The Sudakov form factors for initial-state quarks at a hard scale of 100 GeV as a function of the transverse momentum of the emitted gluon. The form factors are for (top to bottom) parton x values of 0.3, 0.1 and 0.03.

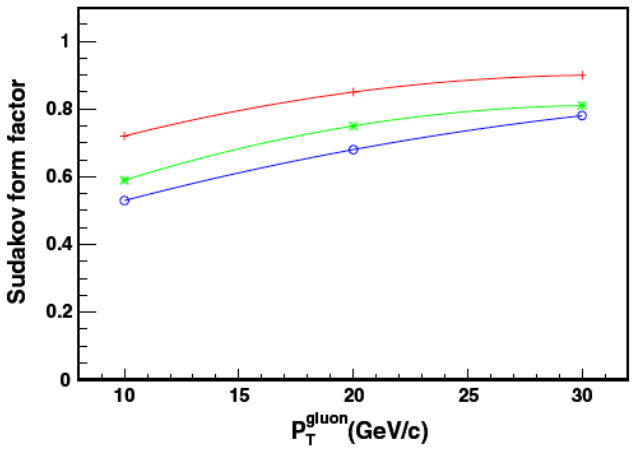

Figure 24. The Sudakov form factors for initial-state quarks at a hard scale of 500 GeV as a function of the transverse momentum of the emitted gluon. The form factors are for (top to bottom) parton x values of 0.3, 0.1 and 0.03.

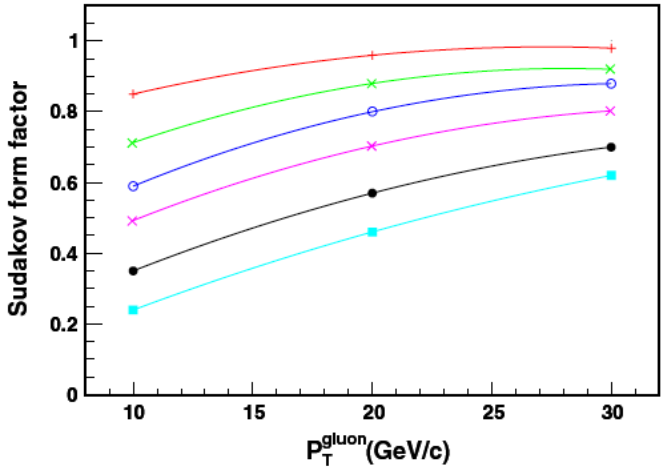

Figure 21. The Sudakov form factors for initial-state gluons at a hard scale of 100 GeV as a function of the transverse momentum of the emitted gluon. The form factors are for (top to bottom) parton x values of 0.3, 0.1, 0.03, 0.01, 0.001 and 0.0001.

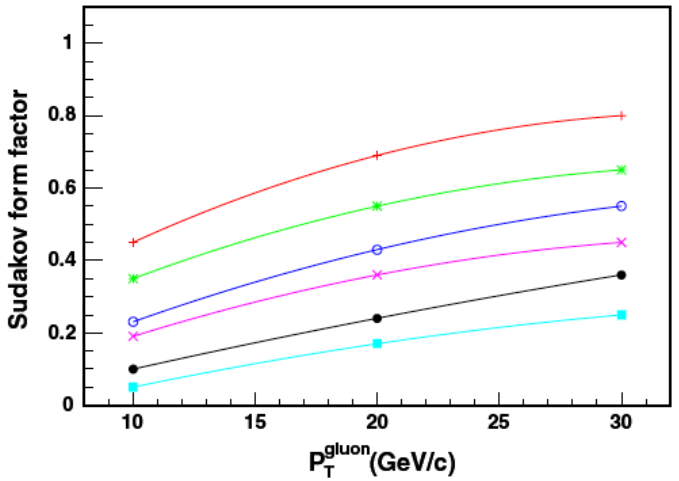

Figure 22. The Sudakov form factors for initial-state gluons at a hard scale of 500 GeV as a function of the transverse momentum of the emitted gluon. The form factors are for (top to bottom) parton x values of 0.3, 0.1, 0.03, 0.01, 0.001 and 0.0001.

Note

- We can only observe emissions above a certain resolution scale
- Below this resolution scale, singularities cancel, leaving a finite remnant
- (some of) the virtual corrections encountered in a full NLO calculation are included by the use of Sudakov suppression between vertices
- So a parton shower Monte Carlo is not purely a fixed order calculation, but has a higher order component as well
- This is a statement that you'll often hear

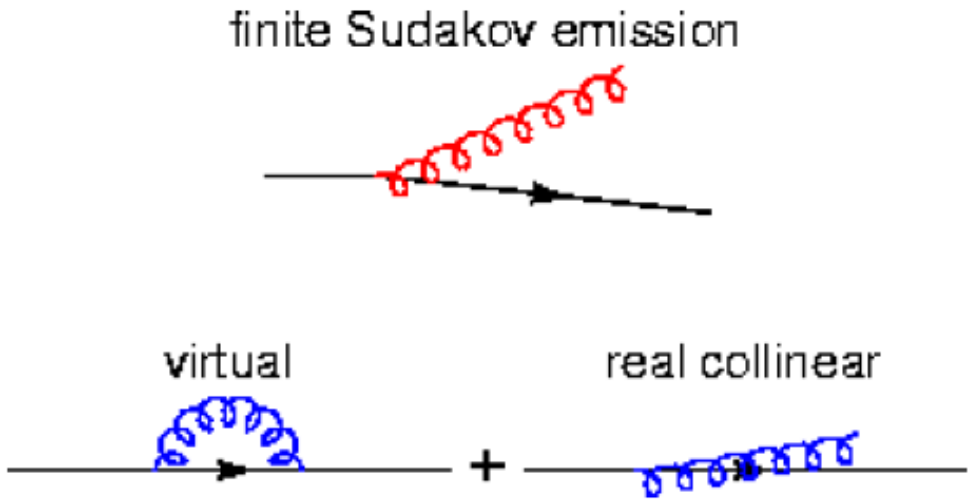

Merging ME and PS approaches

- Parton showers provide an excellent description in regions which are dominated by soft and collinear gluon emission
- Matrix element calculations provide a good description of processes where the partons are energetic and widely separated and also take into account interference effects between amplitudes
  - but do not take into account interference effects in soft and collinear emissions which cannot be resolved, and thus lead to Sudakov suppression of such emissions
- Hey, I know, let's put them together, but we have to be careful not to double-count
  - parton shower producing same event configuration already described by matrix element
  - Les Houches Accord (the first one) allows the ME program to talk to the PS program

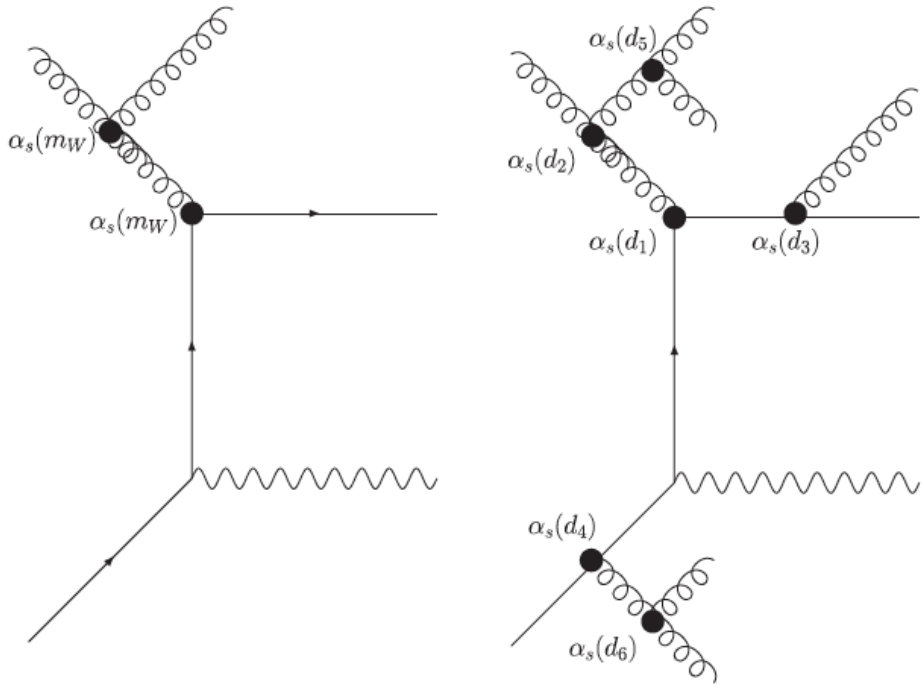

Figure 26. In the NLO formalism, the same scale, proportional to the hardness of the process, is used for each QCD vertex. For the case of the $W+$ 2 jet diagram shown above to the left, a scale related to the mass of the W boson, or to the average transverse momentum of the produced jets, is typically used. The figure to the right shows the results of a simulation using the CKKW formalism. Branchings occur at the vertices with resolution parameters d_i, where $d_1 > d_2 \gg d_{\rm ini} > d_3 > d_4 > d_5 > d_6$. Branchings at the vertices 1–2 are produced with matrix element information while the branchings at vertices 3–6 are produced by the parton shower.

Merging ME and PS approaches

- A number of techniques to combine, with most popular/correct being CKKW
  - matrix element description used to describe parton branchings at large angle and/or energy
  - parton shower description is used for smaller angle, lower energy emissions
- Division into two regions of phase space provided by a resolution parameter d_{ini}
- Argument of α_s at all of the vertices is taken to be equal to the resolution parameter d_i (showering variable) at which the branching has taken place
- Sudakov form factors are inserted on all of the quark and gluon lines to represent the lack of any emissions with a scale larger than d_{ini} between vertices
  - parton showering is used to produce additional emissions at scales less than d_i
- For typical matching scale, ~10% of the n-jet cross section is produced by parton showering from n-1 parton ME

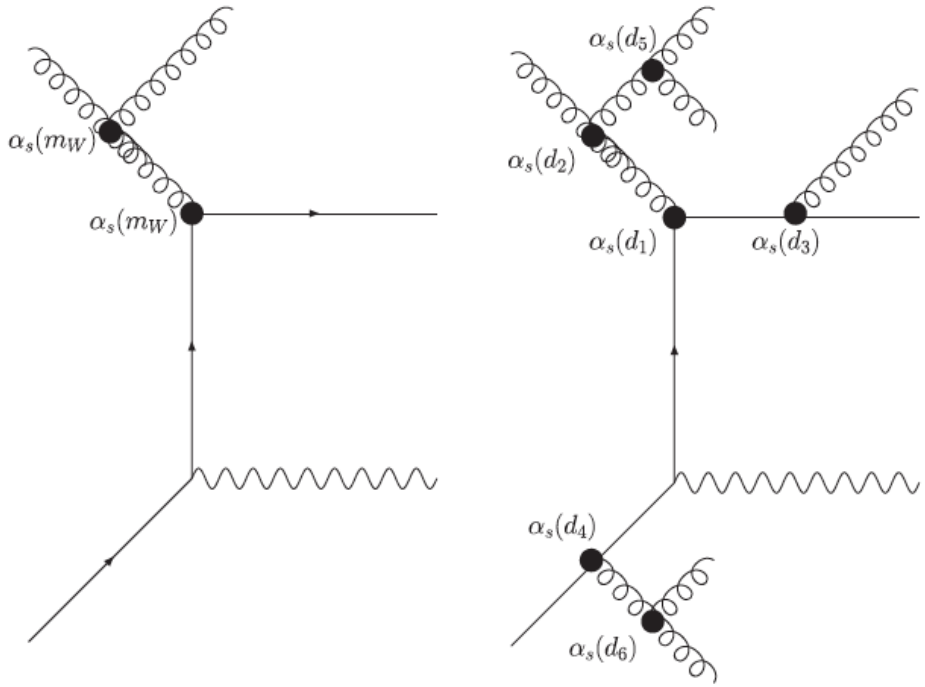

Figure 26. In the NLO formalism, the same scale, proportional to the hardness of the process, is used for each QCD vertex. For the case of the W+ 2 jet diagram shown above to the left, a scale related to the mass of the W boson, or to the average transverse momentum of the produced jets, is typically used. The figure to the right shows the results of a simulation using the CKKW formalism. Branchings occur at the vertices with resolution parameters d_i, where $d_1 > d_2 \gg d_{\rm ini} > d_3 > d_4 > d_5 > d_6$. Branchings at the vertices 1–2 are produced with matrix element information while the branchings at vertices 3–6 are produced by the parton shower.

see Alpgen, Madgraph, Sherpa,…
MLM approach (which I also named) is an approximation to the full CKKW procedure

Why does mlm matching/CKKW help stabilize the cross section?

- mlm
  - generate parton-level configurations for a given hard parton multiplicity N_{part}, with partons constrained by $p_T > p_{Tmin}$, $\Delta R_{jj} > R_{min}$
  - perform the parton showering
  - process the showered event with a cone jet algorithm defined by p_T^{jet} and R_{jet}
  - match partons and jet
    - for each hard parton, select the jet with min $\Delta R_{j\text{-parton}}$
    - if $\Delta R_{j\text{-parton}} < R_{jet}$, the parton is matched
    - a jet can only be matched to a single parton
    - if all partons are matched, keep the event; otherwise throw it away
    - for exclusive, require $N_{jets} = N_{part}$

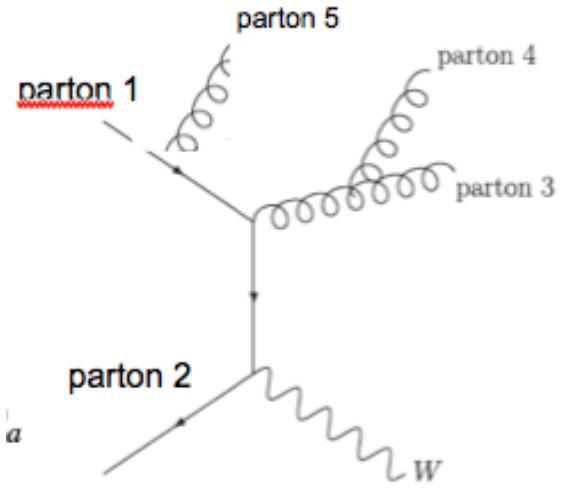

$$d\sigma = \sigma_0(W + 1\ \text{jet})\left[1 + \alpha_S(c_{12}L^2 + c_{11}L + c_{10}) + \alpha_S{}^2(c_{24}L^4 + c_{23}L^3 + c_{22}L^2 + c_{21}L + c_{20}) + \cdots\right]$$

- if partons 1 and 5 and/or partons 3 and 4 become collinear, then large logs and larger parton level cross section
- however, the requirement that $N_{jets} = N_{part}$ tends to equalize the cross sections regardless of R_{min} cut (for given R_{jet})

Next-to-leading best of all possible worlds

- Add NLO matrix element corrections to parton-shower Monte Carlo; be careful to take care of double-counting (real corrections and parton shower are trying to create basically the same cross section)
  - MC@NLO: automated procedure for carrying out NLO calculations is also applied to putting them through parton shower Monte Carlo; state of the art is W+2 jets at NLO
  - Powheg: positive weights for all (or at least most) events
  - Sherpa: using MC@NLO approach; state of the art is W+3 jets at NLO

Really the best of all possible worlds

- Be able to include NLO matrix elements where available, with CKKW LO matrix elements added for additional jet multiplicities
  - for example, W+1-5 jets at NLO, with 6,7…jets provided using CKKW formalism
  - so contributions to W p_T could come from all of these final states
- This is really a very tricky problem; there are approaches that are being developed but no final product
- Later I will show you something I have been working on at the purely partonic level

t-tbar in MC@NLO

- At low p_T for the t-tbar system, the cross section is described (correctly) by the parton shower, which resums the large logs near p_T~0
- At high p_T, the cross section is described (correctly) by the NLO matrix element

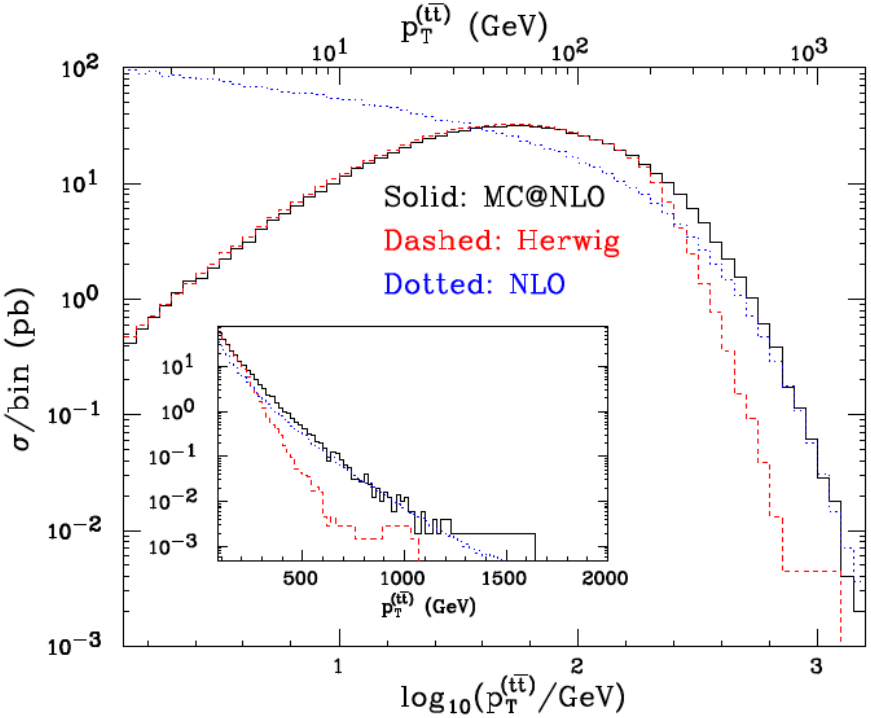

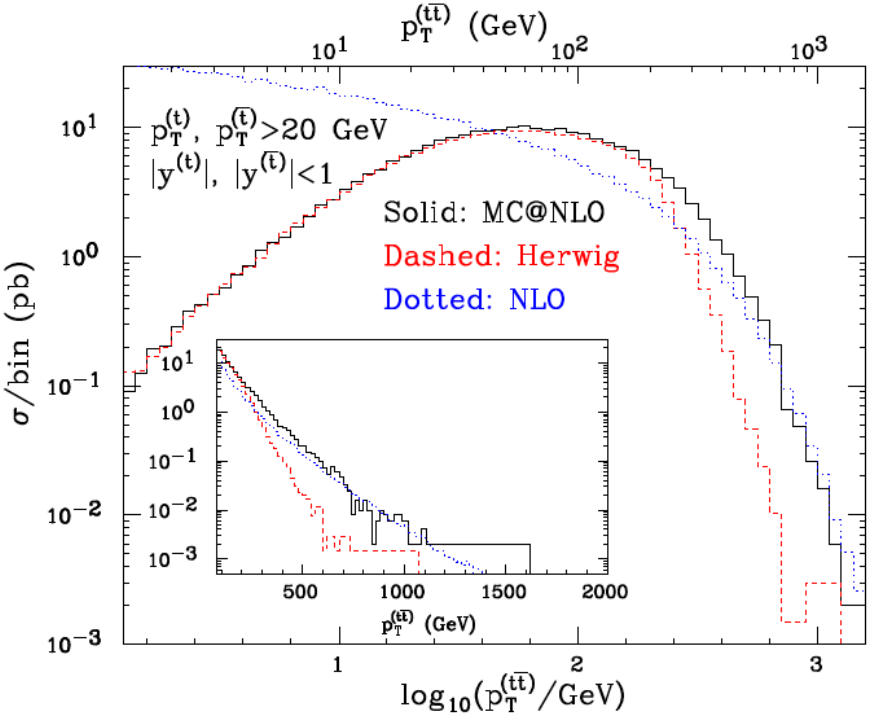

Hadrons and PDFs

- The proton is a dynamical object; the structure observed depends on the time-scale (Q^2) of the observation
- But we know how to calculate this variation (DGLAP)
- We just have to determine the starting points from fits to data

the higher the value of Q^2, the more detail we examine

from this picture, you can imagine that as Q^2 increases, there will be fewer valence quarks at high momentum fraction and more gluons and sea quarks at lower momentum

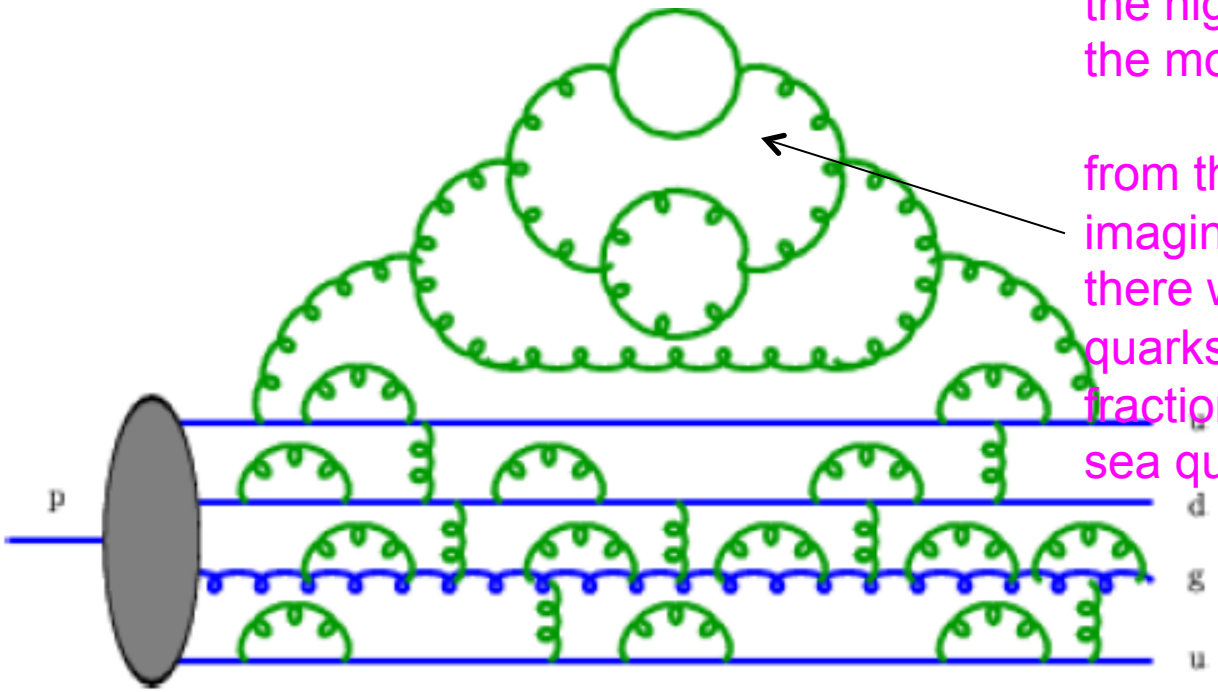

$f_i(x, Q^2) =$ number density of partons i
at momentum fraction x and probing scale Q^2

Hadrons and PDFs

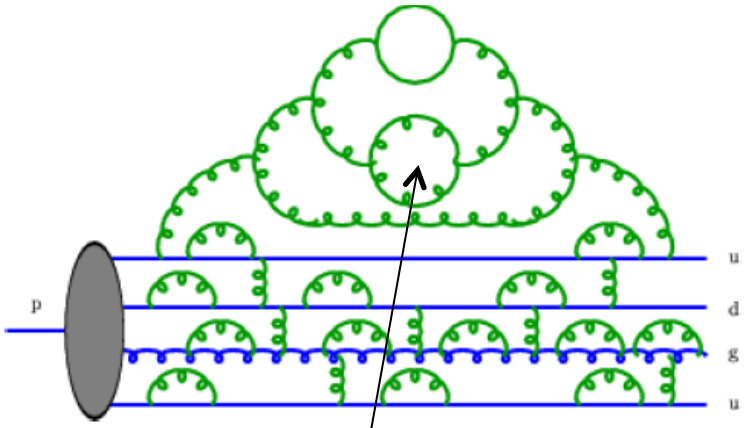

$f_i(x, Q^2)$ = number density of partons i
at momentum fraction x and probing scale Q^2

the higher the value of Q^2,
the more detail we examine

from this picture, you can
imagine that as Q^2 increases,
there will be fewer valence
quarks at high momentum
fraction and more gluons and
sea quarks at lower momentum

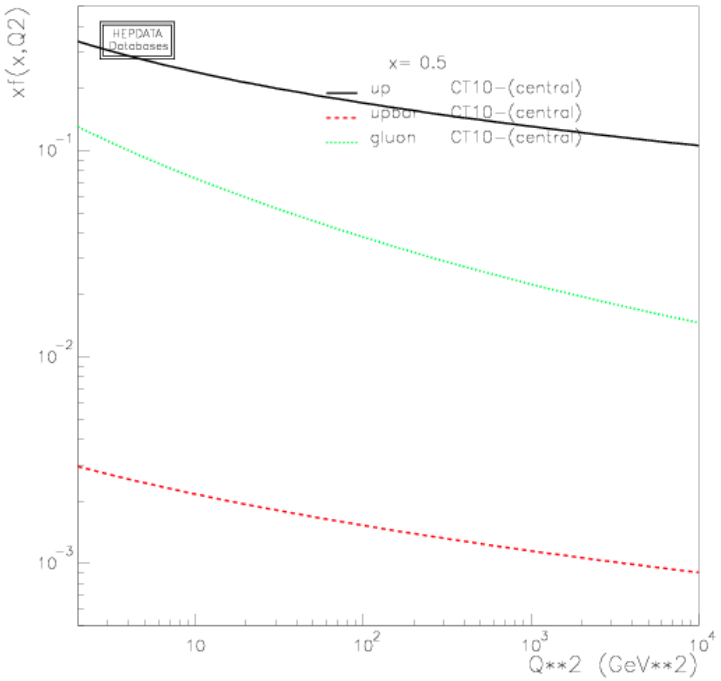

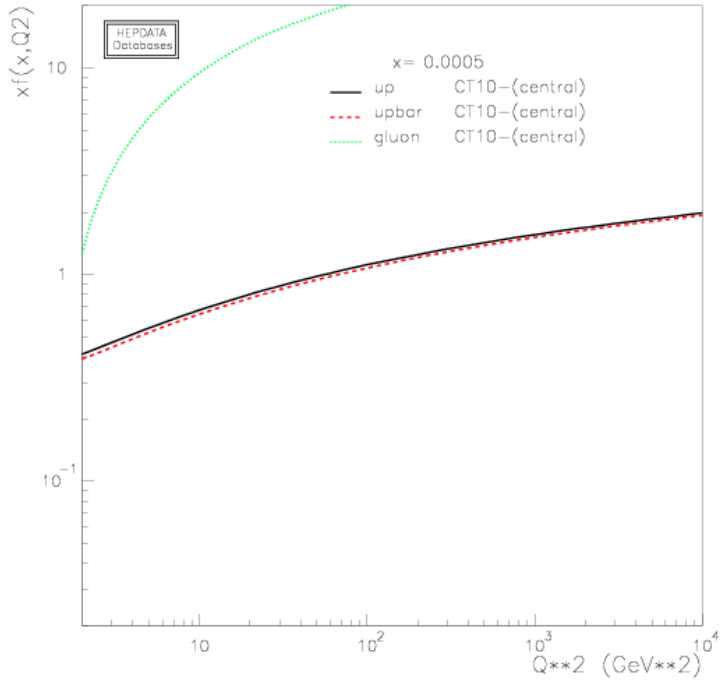

Hadrons and PDFs

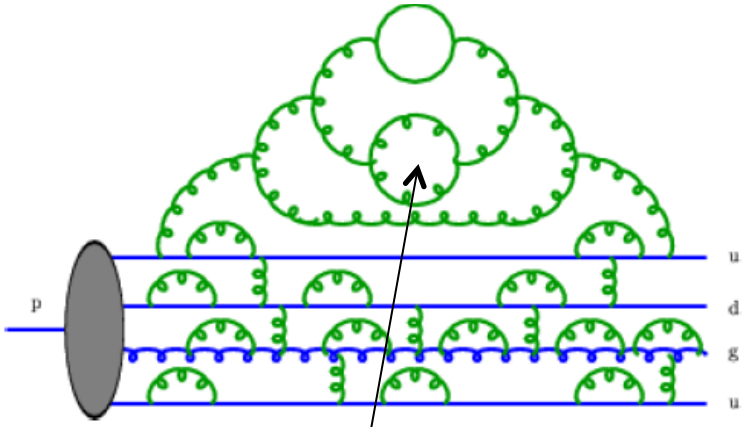

$f_i(x, Q^2)$ = number density of partons i
at momentum fraction x and probing scale Q^2

the higher the value of Q^2,
the more detail we examine

from this picture, you can imagine that as Q^2 increases, there will be fewer valence quarks at high momentum fraction and more gluons and sea quarks at lower momentum

consider x=0.1; not easy to see scaling violations here.

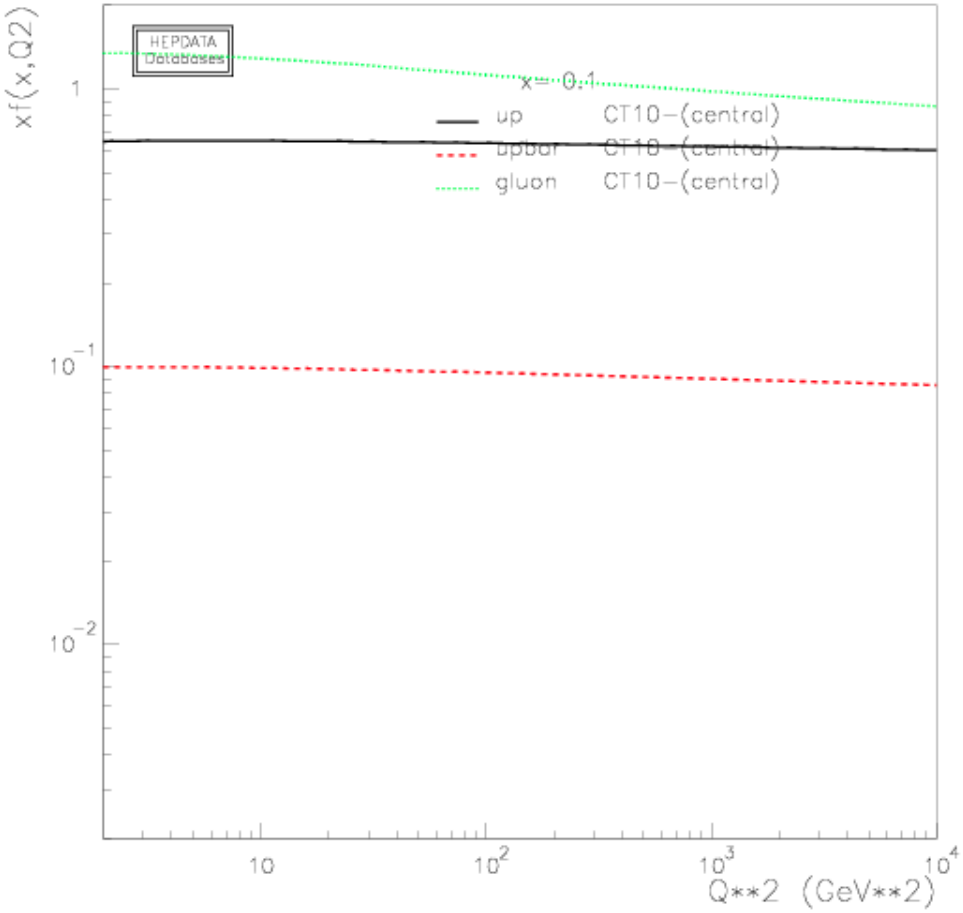

Parton distribution functions and global fits

- Calculation of production cross sections at the LHC relies upon knowledge of pdf's in the relevant kinematic region
- Pdf's are determined by global analyses of data from DIS, DY and jet production
- Three major groups that provide semi-regular updates to parton distributions when new data/ theory becomes available
  - MRS->MRST98->MRST99 ->MRST2001->MRST2002 ->MRST2003->MRST2004 ->MSTW2008
  - CTEQ->CTEQ5->CTEQ6 ->CTEQ6.1->CTEQ6.5 ->CTEQ6.6->CT09->CT10
  - NNPDF->NNPDF2.0- >NNPDF2.1->NNPDF2.2- >NNPDF2.3

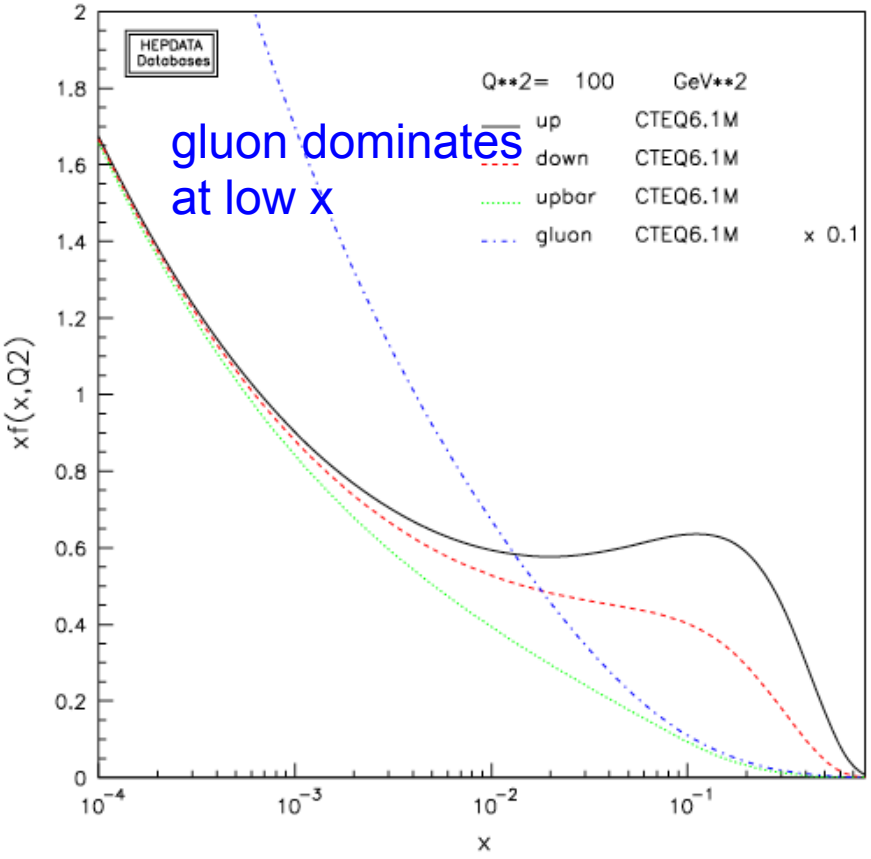

Figure 27. The CTEQ6.1 parton distribution functions evaluated at a Q of 10 GeV.

Global fits

- With the DGLAP equations, we know how to evolve pdf's from a starting scale Q_0 to any higher scale
  - remember the divergences from the initial state that we absorbed into the pdfs
- …but we can't calculate what the pdf's are ab initio
  - one of the goals of lattice QCD
- We have to determine them from a global fit to data
  - factorization theorem tells us that pdf's determined for one process are applicable to another
  - extremely important proof
- So what do we need
  - a value of Q_o (1.3 GeV for CTEQ, 1 GeV for MSTW) lower than the data used in the fit (or any prediction)
  - a parametrization for the pdf's
  - a scheme for the pdf's
  - hard-scattering calculations at the order being considered in the fit
  - pdf evolution at the order being considered in the fit
  - a world average value for α_s
  - a lot of data
    - with appropriate kinematic cuts
  - a treatment of the errors for the experimental data
  - MINUIT

Back to global fits

- Parametrization: initial form
  - $f(x) \sim x^{\alpha}(1-x)^{\beta}$
  - estimate β from quark counting rules
    - $\beta = 2n_s - 1$ with n_s being the minimum number of spectator quarks
    - so for valence quarks in a proton (qqq), $n_s=2$, $\beta=3$
    - for gluon in a proton (qqqg), $n_s=3$, $\beta=5$
    - for anti-quarks in a proton (qqqqqbar), $n_s=4$, $\beta=7$
  - estimate α from Regge arguments
    - gluons and anti-quarks have $\alpha \sim -1$ while valence quarks have $\alpha \sim = 1/2$
  - but at what Q value are these arguments valid?

- What do we know?

1. we know that the sum of the momentum of all partons in the proton is 1 (but not for modified LO fits)
2. we know the sum of valence quarks is 3
   - and 2 of them are up quarks and 1 of them is a down quark
   - we know that the net number of anti-quarks is 0, but what about dbar=ubar
3. we know that the net number of strange quarks (charm quarks/ bottom quarks) in the proton is 0
   - but we don't know if s=sbar locally

This already puts a lot of restrictions on the pdf's

Parametrizations

- That simple parametrization worked for early fits, where the data was not very precise (nor very abundant), but it does not work for modern global fits, where a more flexible form is needed
  - the simple ansatz can be dangerous in that it can (falsely) tie together low x and high x behavior (other than by momentum sum rule)
- In order to more finely tune parametrization,usually multiply simple form by a polynomial in x or some more complicated function

- CTEQ uses for the quark and gluon distributions (CTEQ6.6)

$$f(x) = x^{(a_1-1)}(1-x)^{a_2} e^{a_3 x}[1+e^{a_4} x]^{a_5}$$

- For the ratio of dbar/ubar

$$\frac{\bar{d}}{\bar{u}} = e^{a_1} x^{(a_2-1)}(1-x)^{a_3} + (1+a_4 x)(1-x)^{a_5}$$

- How do we know this is flexible enough?
  - data is well-described (χ^2/dof ~1 for a NLO fit)
  - adding more parameters just results in those parameters being unconstrained
  - but there is some remaining bias
  - note that with this form, the pdf's are positive definite (they don't have to be)

Orders and Schemes

- Fits are available at
  - LO
    - CTEQ6L or CTEQ6L1
      - 1 loop or 2 loop α_s
    - in common use with parton shower Monte Carlos
    - poor fit to data due to deficiencies of LO ME's
  - LO*
    - (perhaps) better for parton shower Monte Carlos (CT09MC1,CT09MC2, CT09MCS)
  - NLO
    - CTEQ6.1,CTEQ6.6,CT09, CT10
    - precision level: error pdf's defined at this order
  - NNLO
    - more accurate but not all processes known

- At NLO and NNLO, one needs to specify a scheme or convention for subtracting the divergent terms
- Basically the scheme specifies how much of the finite corrections to subtract along with the divergent pieces
  - most widely used is the modified minimal subtraction scheme (or MSbar)
  - used with dimensional regularization: subtract the pole terms and accompanying log 4π and Euler constant terms

$$\sigma_{real+virt} = \frac{\alpha_s}{2\pi} C_F \left(\frac{\mu^2}{Q^2}\right)^{\varepsilon} c_\Gamma \left[\left(\frac{2\pi^2}{3} - 6\right)\delta(1-z) - \frac{2}{\varepsilon} P_{qq}(z) - 2(1-z) + 4(1+z^2)\left[\frac{\ln(1-z)}{1-z}\right]_+ - 2\frac{1+z^2}{1-z}\ln z\right]$$

  - also may find pdf's in DIS scheme, where full order α_s correction for F_2 in DIS absorbed into quark pdf's

Scales and Masses

- Processes used in global fits are characterized by a single large scale
  - DIS-Q^2
  - lepton pair production-M^2
  - vector boson production-M_V^2
  - jet production-p_T^{jet}
- By choosing the factorization and renormalization scales to be of the same order as the characteristic scale
  - can avoid some large logarithms in the hard scattering cross section
  - some large logarithms in running coupling and pdf's are resummed
- Different treatment of quark masses and thresholds
  - fixed flavor number scheme (FFNS)
  - variable flavor number scheme (VFNS)
    - zero mass variable flavor number scheme (ZM-VFNS)
    - general mass variable flavor number scheme (GM-VFNS)

Data sets used in global fits (CTEQ6.6)

1. BCDMS F_2^{proton} (339 data points)
2. BCDMS $F_2^{deuteron}$ (251 data points)
3. NMC F_2 (201 data points)
4. NMC F_2^d/F_2^p (123 data points)
5. F_2(CDHSW) (85 data points)
6. F_3(CDHSW) (96 data points)
7. CCFR F_2 (69 data points)
8. CCFR F_3 (86 data points)
9. H1 NC e^-p (126 data points; 1998-98 reduced cross section)
10. H1 NC e^-p (13 data points; high y analysis)
11. H1 NC e^+p (115 data points; reduced cross section 1996-97)
12. H1 NC e^+p (147 data points; reduced cross section; 1999-00)
13. ZEUS NC e^-p (92 data points; 1998-99)
14. ZEUS NC e^+p (227 data points; 1996-97)
15. ZEUS NC e^+p (90 data points; 1999-00)
16. H1 F_2^c e^+p (8 data points;1996-97)
17. H1 $R\sigma^c$ for ccbar e^+p (10 data points;1996-97)
18. H1 R_σ^b for bbbar e^+p (10 data points; 1999-00)
19. ZEUS F_2^c e^+p (18 data points; 1996/97)
20. ZEUS F_2^C e+p (27 data points; 1998/00)
21. H1 CC e^-p (28 data points; 1998-99)
22. H1 CC e^+p (25 data points; 1994-97)
23. H1 CC e^+p (28 data points; 1999-00)
24. ZEUS CC e^-p (26 data points; 1998-99)
25. ZEUS CC e^+p (29 data points; 1994-97)
26. ZEUS CC e^+p (30 data points; 1999-00)
27. NuTev neutrino dimuon cross section (38 data points)
28. NuTev anti-neutrino dimuon cross section (33 data points)
29. CCFR neutrino dimuon cross section (40 data points)
30. CCFR anti-neutrino cross section (38 data points)
31. E605 dimuon (199 data points)
32. E866 dimuon (13 data points)
33. Lepton asymmetry from CDF (11 data points)
34. CDF Run 1B jet cross section (33 data points)
35. D0 Run 1B jet cross section (90 data points)

- 2794 data points from DIS, DY, jet production
  - actually fewer in CT10 because of the combined HERA data sets
- All with (correlated) systematic errors that must be treated correctly in the fit
- Note that DIS is the 800 pound gorilla of the global fit with many data points and small statistical and systematic errors
  - and fixed target DIS data still have a significant impact on the global fitting, even with an abundance of HERA data
- To avoid non-perturbative effects, kinematic cuts on placed on the DIS data
  - $Q^2>5$ GeV^2
  - $W^2(=m^2+Q^2(1-x)/x)>12.25$ GeV^2

Influence of data in global fit

- Charged lepton DIS

$$F_2(x,Q^2) = x\sum_i e_i^2[q_i(x,Q^2) + \bar{q}_i(x,Q^2)]$$

  - each flavor weighted by its squared charge
  - quarks and anti-quarks enter together
  - gluon doesn't enter, in lowest order, but does enter into the structure functions at NLO
  - also enters through mixing in evolution equations so gluon contributes to the change of the structure functions as Q^2 increases
  - at low values of x

$$Q^2\frac{dF_2}{dQ^2} \approx \frac{\alpha_s}{2\pi}\sum e_i^2 \int_x^1 \frac{dy}{y} P_{qg}(y) G(\frac{x}{y}, Q^2)$$

  - Q^2 dependence at small x is driven directly by gluon pdf

- At low x, structure functions increase with Q^2; at high x decrease

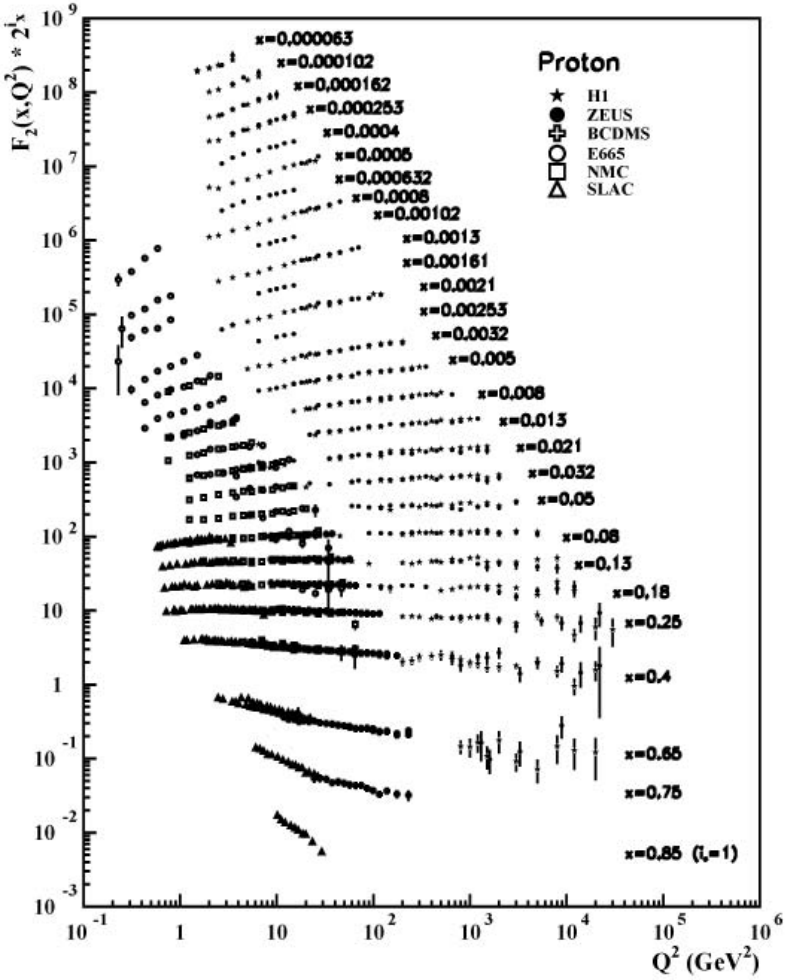

Influence of data in global fit

- Neutrino DIS

$$F_2(x,Q^2) = x\sum_i [q_i(x,Q^2) + \bar{q}_i(x,Q^2)]$$

$$xF_3(x,Q^2) = x\sum_i [q_i(x,Q^2) - \bar{q}_i(x,Q^2)]$$

  - additional (parity-violating) structure function allows the separation of quarks and antiquarks but not a complete flavor separation
  - caveat: neutrino observables usually obtained using nuclear targets so there is added question of nuclear corrections

Some observations from DIS

- DIS data provide strong constraints on the u and d distributions over the full range of x covered by the data
- The combination 4*ubar + dbar is well-constrained at small x
- The gluon is constrained at low values of x by the slope of the Q^2 dependence of F_2
  - momentum sum rule connects low x and high x behavior, but loosely

Inclusive jets and global fits

- We don't have many handles on the high x gluon distribution in the global pdf fits
- Best handle is provided by the inclusive jet cross section from the Tevatron

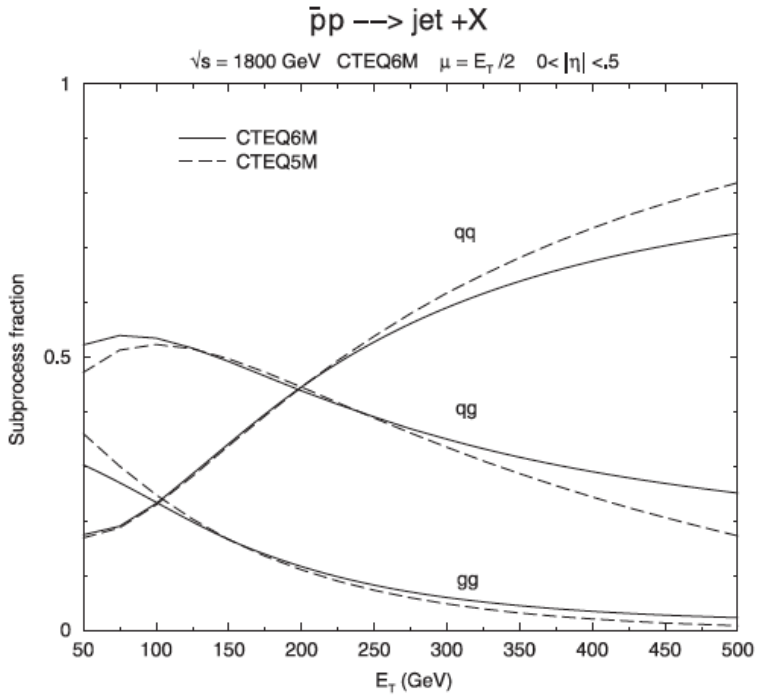

Figure 56. The subprocess contributions to inclusive jet production at the Tevatron for the CTEQ5M and CTEQ6M pdfs. The impact of the larger larger gluon at high x for CTEQ6 is evident.

- At high E_T (high x), gq is subdominant, but there's a great deal of freedom/uncertainty on the high x gluon distribution
  - about 42% of the proton's momentum is carried by gluons, and most of that momentum is at low x

X Bin	Momentum fraction
10^{-4} to 10^{-3}	0.6%
10^{-3} to 0.01	3%
0.01 to 0.1	16%
0.1 to 0.2	10%
0.2 to 0.3	6%
0.3 to 0.5	5%
0.5 to 1.0	1%

TABLE I. The momentum fraction carried by gluons in a a given x bin at a Q value of 5 GeV.

- The inclusion of the CDF/D0 inclusive jet cross sections from Run 1 boosted the high x gluon distribution and thus the predictions for the high E_T jet cross sections
  - The high x gluon has decreased due to influence of the Run 2 D0 jet data

ABKM exercise: S. Alekhin Trento 2010

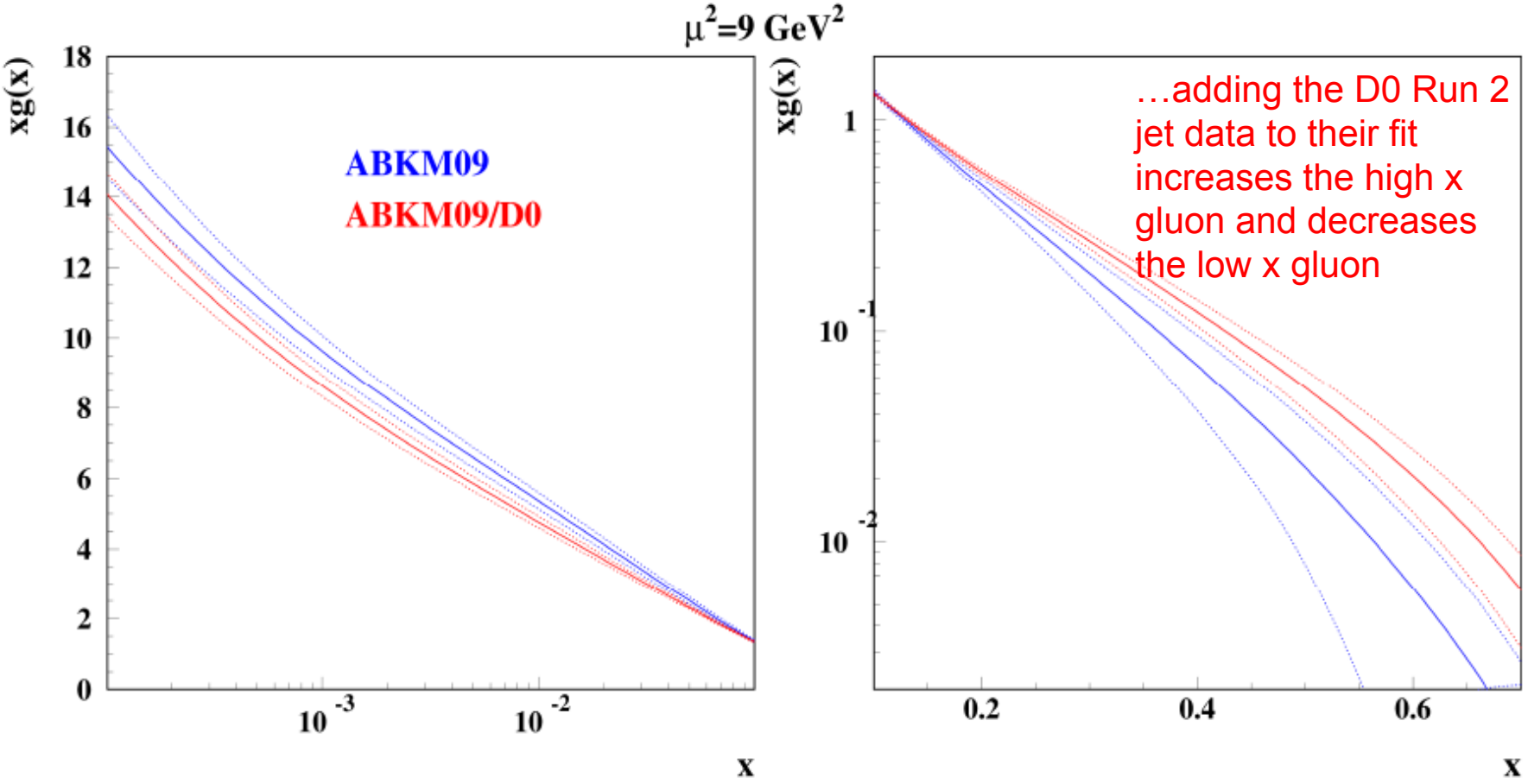

- Impact of the DO data is somewhat bigger than for the case of MSTW,
- Variation of the scales reduces significance of the data (work in progress)

Global fitting: best fit

- Using our 2794 data points, we do our global fit by performing a χ^2 minimization
  - where D_i are the data points and T_i are the theoretical predictions; we allow for a normalization shift f_N for each experimental data set
    - but we provide a quadratic penalty for any normalization shift
  - where there are k systematic errors β for each data point in a particular data set
    - and where we allow the data points to be shifted by the systematic errors with the shifts given by the s_j parameters
    - but we give a quadratic penalty for non-zero values of the shifts s_j
  - where σ_i is the statistical error for data point i

- For each data set, we calculate

$$\chi^2 = \sum_i \frac{\left[\left(f_N D_i - \sum_{j=1}^{k} \beta_{ij} s_j\right) - T_i\right]^2}{\sigma_i^2} + \sum_{j=1}^{k} s_j^2$$

- For a set of theory parameters it is possible to analytically solve for the shifts s_j,and therefore, continually update them as the fit proceeds
- To make matters more complicated, we may give additional weights to some experiments due to the utility of the data in those experiments (i.e. NA-51), so we adjust the χ^2 to be

$$\chi^2 = \sum_k w_k \chi_k^2 + \sum_k w_{N,k} \left[\frac{1 - f_N}{\sigma_N^{norm}}\right]^2$$

- where w_k is a weight given to the experimental data and $w_{N,k}$ is a weight given to the normalization

Minimization and errors

- Free parameters in the fit are parameters for quark and gluon distributions

$$f(x) = x^{(a_1 - 1)}(1 - x)^{a_2} e^{a_3 x}[1 + e^{a_4} x]^{a_5}$$

- Too many parameters to allow all to remain free
  - some are fixed at reasonable values or determined by sum rules
- 20 free parameters for CTEQ6.1, 22 for CTEQ6.6,24 for CT09, 26 for CT10
- update: in CT10, all data sets have weight 1, normalizations treated as other fit parameters

- Result is a global χ^2/dof on the order of 1
  - for a NLO fit
  - worse for a LO fit, since the LO pdf's can not make up for the deficiencies in the LO matrix elements

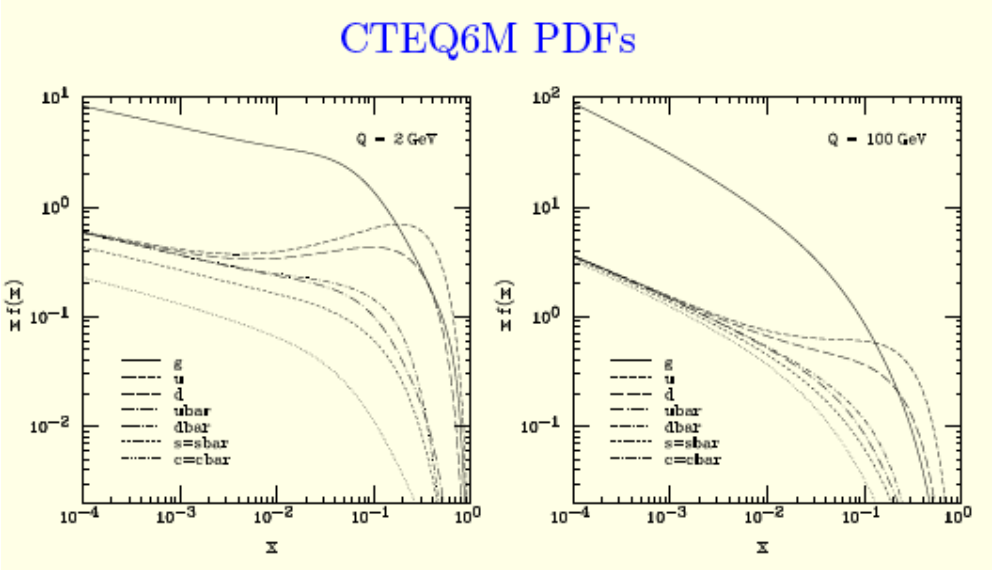

PDF Errors: old way

- Make plots of lots of pdf's (no matter how old) and take spread as a measure of the error
- Can either underestimate or overestimate the error
- Review sources of uncertainty on pdf's
  - data set choice
  - kinematic cuts
  - parametrization choices
  - treatment of heavy quarks
  - order of perturbation theory
  - errors on the data
- There are now more sophisticated techniques to deal with at least the errors due to the experimental data uncertainties

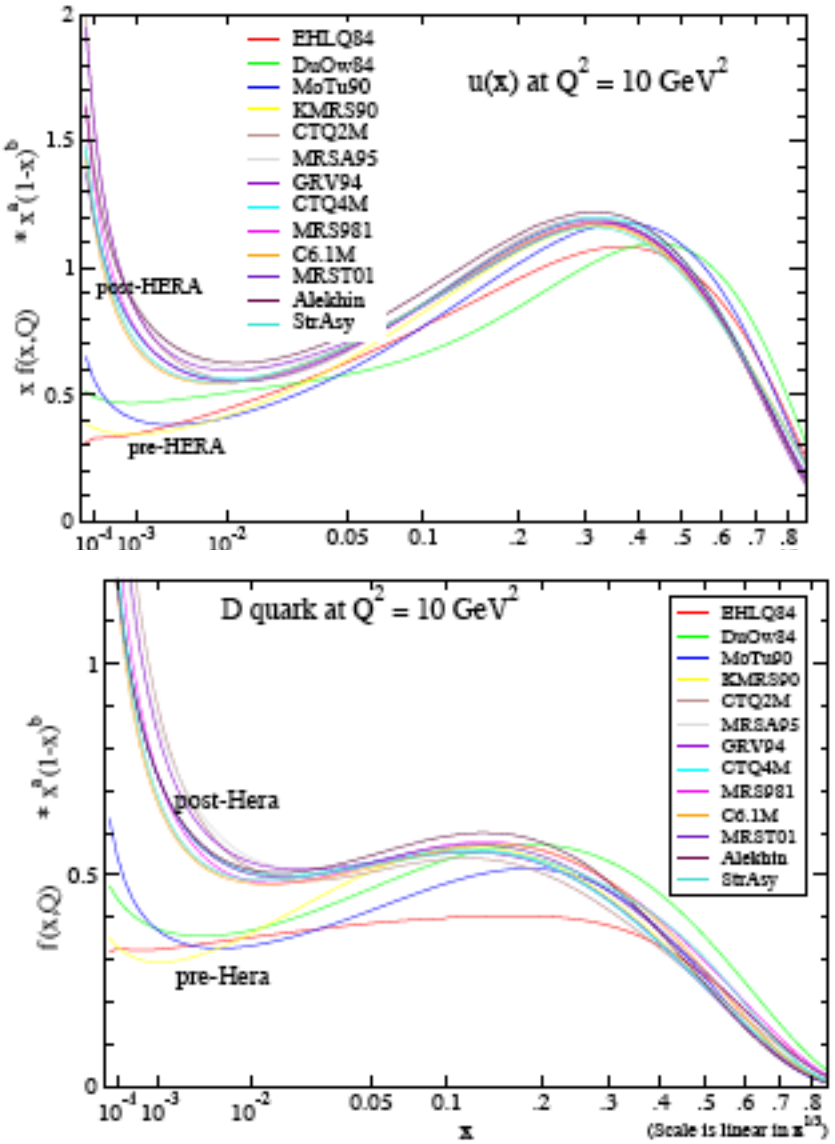

PDF Errors: new way

- So we have optimal values (minimum χ^2) for the d=20 (22 for CTEQ6.6, 26 for CT10) free pdf parameters in the global fit
  - $\{a_\mu\}, \mu=1,\ldots d$
- Varying any of the free parameters from its optimal value will increase the χ^2
- It's much easier to work in an orthonormal eigenvector space determined by diagonalizing the Hessian matrix, determined in the fitting process

$$H_{uv} = \frac{1}{2}\frac{\partial \chi^2}{\partial a_\mu \partial a_\nu}$$

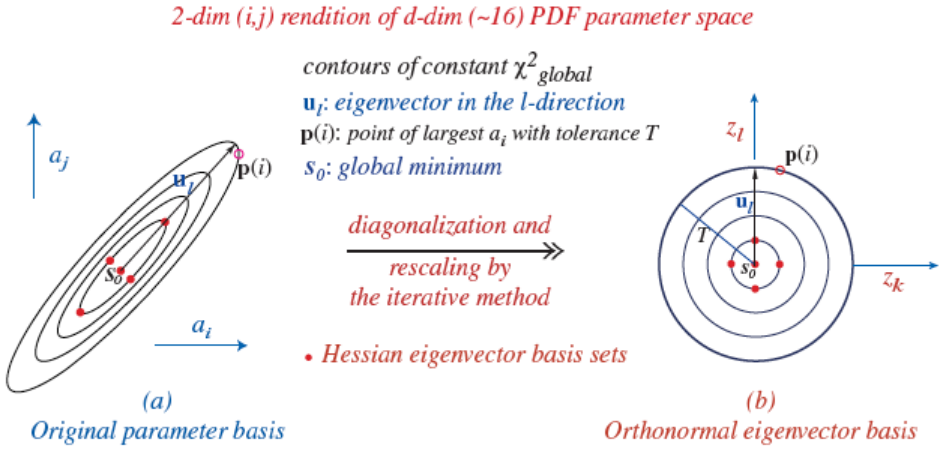

Figure 28. A schematic representation of the transformation from the pdf parameter basis to the orthonormal eigenvector basis.

To estimate the error on an observable X(a), due to the experimental uncertainties of the data used in the fit, we use the *Master Formula*

$$(\Delta X)^2 = \Delta\chi^2 \sum_{\mu,\nu} \frac{\partial X}{\partial a_\mu} \left(H^{-1}\right)_{\mu\nu} \frac{\partial X}{\partial a_\nu}$$

PDF Errors: new way

- Recap: 20 (22,26) eigenvectors with the eigenvalues having a range of >1E6
- Largest eigenvalues (low number eigenvectors) correspond to best determined directions; smallest eigenvalues (high number eigenvectors) correspond to worst determined directions
- Easiest to use Master Formula in eigenvector basis

$$\Delta X^{+}_{\max} = \sqrt{\sum_{i=1}^{N} [\max(X_i^{+} - X_0, X_i^{-} - X_0, 0)]^2},$$

$$\Delta X^{-}_{\max} = \sqrt{\sum_{i=1}^{N} [\max(X_0 - X_i^{+}, X_0 - X_i^{-}, 0)]^2}.$$

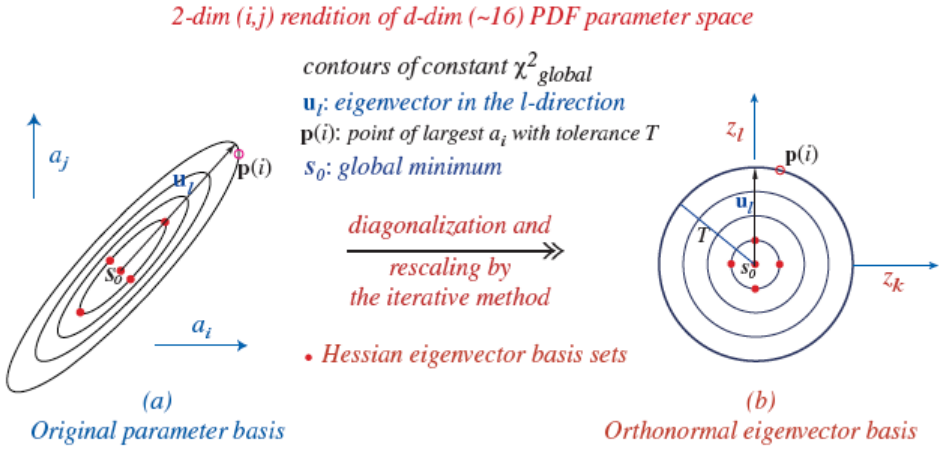

Figure 28. A schematic representation of the transformation from the pdf parameter basis to the orthonormal eigenvector basis.

To estimate the error on an observable X(a), from the experimental errors, we use the *Master Formula*

$$(\Delta X)^2 = \Delta\chi^2 \sum_{\mu,\nu} \frac{\partial X}{\partial a_\mu} \left(H^{-1}\right)_{\mu\nu} \frac{\partial X}{\partial a_\nu}$$

where X_i^+ and X_i^- are the values for the observable X when traversing a distance corresponding to the tolerance T(=sqrt($\Delta\chi^2$)) along the i^{th} direction

PDF Errors: new way

- Recap: 20 (22,26) eigenvectors with the eigenvalues having a range of >1E6

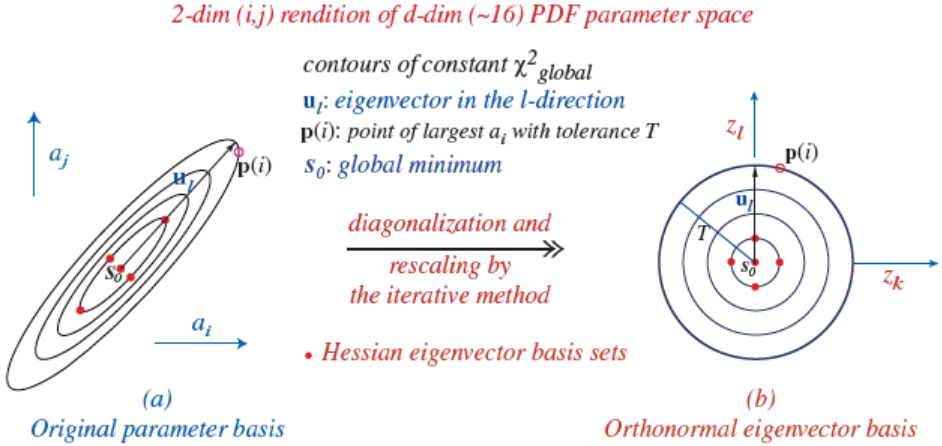

Figure 28. A schematic representation of the transformation from the pdf parameter basis to the orthonormal eigenvector basis.

- Largest eigenvalues (low number eigenvectors) correspond to best determined directions; smallest eigenvalues (high number eigenvectors) correspond to worst determined directions

These are the directions in which the χ^2 function increases most steeply if you vary the parameters from the their central fit values

These are the directions in which the χ^2 function increases the least if you vary the parameters from the their central fit values

PDF Errors: new way

- What is the tolerance T?
- This is one of the most controversial questions in global pdf fitting?
- We have 2794 data points in the CTEQ6.6 data set (on order of 2000 for CTEQ6.1)
- Technically speaking, a 1-sigma error corresponds to a tolerance T(=sqrt($\Delta\chi^2$))=1
- This results in far too small an uncertainty from the global fit
  - with data from a variety of processes from a variety of experiments from a variety of accelerators
- For CTEQ6.1/6.6, we chose a $\Delta\chi^2$ of 100 to correspond to a 90% CL limit
  - with an appropriate scaling for the larger data set for CTEQ6.6
- In the past, MSTW has chosen a $\Delta\chi^2$ of 50 for the same limit so CTEQ errors were larger than MSTW errors

$$\Delta X^{+}_{\max} = \sqrt{\sum_{i=1}^{N} [\max(X_i^{+} - X_0, X_i^{-} - X_0, 0)]^2},$$

$$\Delta X^{-}_{\max} = \sqrt{\sum_{i=1}^{N} [\max(X_0 - X_i^{+}, X_0 - X_i^{-}, 0)]^2}.$$

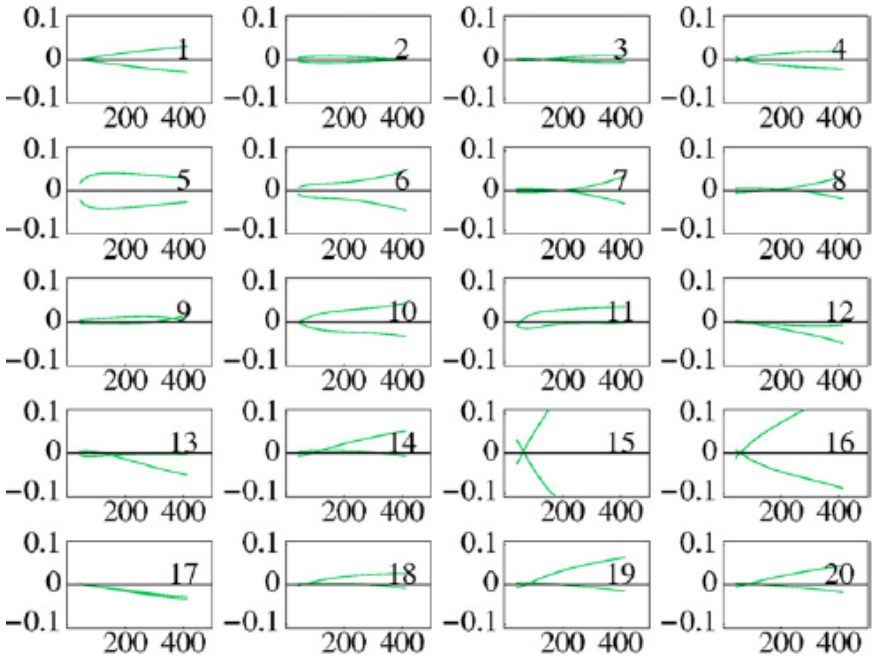

Figure 29. The pdf errors for the CDF inclusive jet cross section in Run 1 for the 20 different eigenvector directions. The vertical axes show the fractional deviation from the central prediction and the horizontal axes the jet transverse momentum in GeV.

Parametrization bias

- It's been shown by Jon Pumplin (**arXiv: 0909.5176)** that a large part of the need for a large value of $\Delta\chi^2$ is because of remaining parameterization biases present even with a very flexible parameterization
- Comparisons with NNPDF (which has less bias) even more important

What do the eigenvectors *mean*?

- Each eigenvector corresponds to a linear combination of all 20 (22,24) pdf parameters, so in general each eigenvector doesn't mean anything?
- However, with 20 (22,24,26) dimensions, often eigenvectors will have a large component from a particular direction
- Take eigenvector 1 (for CTEQ6.1); error pdf's 1 and 2
- It has a large component sensitive to the small x behavior of the u quark valence distribution
- Not surprising since this is the best determined direction

Sets	Shape Parameter	Component
1, 2	BP(2, 1)	0.057911
1, 2	BP(2, 2)	-0.022688
1, 2	BP(2, 3)	0.015496
1, 2	BP(2, 4)	0.035277
1, 2	BP(2, 5)	frozen
1, 2	BP(1, 1)	0.888833
1, 2	BP(1, 2)	-0.161942
1, 2	BP(1, 3)	0.118204
1, 2	BP(1, 4)	0.268405
1, 2	BP(1, 5)	0.276392
1, 2	BP(0, 1)	0.038555
1, 2	BP(0, 2)	-0.006610
1, 2	BP(0, 3)	frozen
1, 2	BP(0, 4)	-0.017717
1, 2	BP(0, 5)	frozen
1, 2	BP(-1, 1)	-0.007668
1, 2	BP(-1, 2)	0.012745
1, 2	BP(-1, 3)	0.001851
1, 2	BP(-1, 4)	frozen
1, 2	BP(-1, 5)	0.001004
1, 2	BP(-2, 1)	0.117517
1, 2	BP(-2, 2)	-0.008357
1, 2	BP(-2, 3)	0.006504
1, 2	BP(-2, 4)	frozen
1, 2	BP(-2, 5)	frozen

What do the eigenvectors *mean*?

- Take eigenvector 8 (for CTEQ6.1); error pdf's 15 and 16
- No particular direction stands out

Sets	Shape Parameter	Component
15, 16	BP(2, 1)	0.196388
15, 16	BP(2, 2)	0.387704
15, 16	BP(2, 3)	-0.226202
15, 16	BP(2, 4)	-0.411440
15, 16	BP(2, 5)	frozen
15, 16	BP(1, 1)	-0.193195
15, 16	BP(1, 2)	0.356604
15, 16	BP(1, 3)	0.018064
15, 16	BP(1, 4)	0.468888
15, 16	BP(1, 5)	0.376180
15, 16	BP(0, 1)	0.016734
15, 16	BP(0, 2)	-0.026136
15, 16	BP(0, 3)	frozen
15, 16	BP(0, 4)	-0.016537
15, 16	BP(0, 5)	frozen
15, 16	BP(-1, 1)	-0.176169
15, 16	BP(-1, 2)	0.136337
15, 16	BP(-1, 3)	0.074431
15, 16	BP(-1, 4)	frozen
15, 16	BP(-1, 5)	-0.030040
15, 16	BP(-2, 1)	-0.014533
15, 16	BP(-2, 2)	-0.067391
15, 16	BP(-2, 3)	0.049273
15, 16	BP(-2, 4)	frozen
15, 16	BP(-2, 5)	frozen

What do the eigenvectors *mean*?

- Take eigenvector 15 (for CTEQ6.1); error pdf's 29 and 30
- Probes high x gluon distribution

creates largest uncertainty for high p_T jet cross sections at both the Tevatron and LHC

29, 30	BP(2, 1)	0.012701
29, 30	BP(2, 2)	-0.162018
29, 30	BP(2, 3)	0.018666
29, 30	BP(2, 4)	-0.111238
29, 30	BP(2, 5)	frozen
29, 30	BP(1, 1)	-0.003049
29, 30	BP(1, 2)	-0.001074
29, 30	BP(1, 3)	-0.034151
29, 30	BP(1, 4)	-0.005735
29, 30	BP(1, 5)	0.032812
29, 30	BP(0, 1)	-0.045923
29, 30	BP(0, 2)	0.873418
29, 30	BP(0, 3)	frozen
29, 30	BP(0, 4)	-0.241822
29, 30	BP(0, 5)	frozen
29, 30	BP(-1, 1)	-0.071419
29, 30	BP(-1, 2)	-0.067488
29, 30	BP(-1, 3)	0.100283
29, 30	BP(-1, 4)	frozen
29, 30	BP(-1, 5)	0.179551
29, 30	BP(-2, 1)	-0.009441
29, 30	BP(-2, 2)	-0.196100
29, 30	BP(-2, 3)	0.211281
29, 30	BP(-2, 4)	frozen
29, 30	BP(-2, 5)	frozen

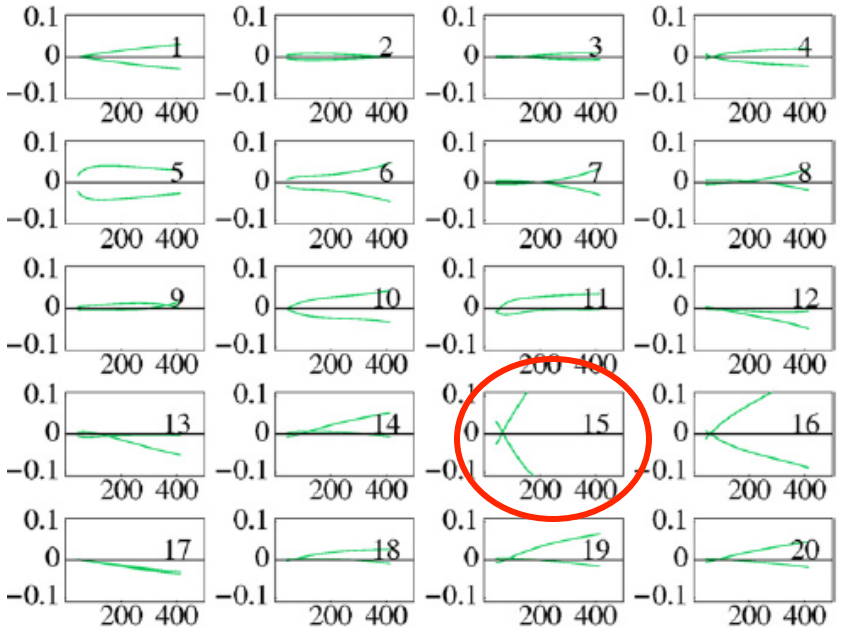

Figure 29. The pdf errors for the CDF inclusive jet cross section in Run 1 for the 20 different eigenvector directions. The vertical axes show the fractional deviation from the central prediction and the horizontal axes the jet transverse momentum in GeV.

Aside: PDF re-weighting

- Any physical cross section at a hadron-hadron collider depends on the product of the two pdf's for the partons participating in the collision convoluted with the hard partonic cross section
- Nominally, if one wants to evaluate the pdf uncertainty for a cross section, this convolution should be carried out 41 times (for CTEQ6.1); once for the central pdf and 40 times for the error pdf's
- However, the partonic cross section is not changing, only the product of the pdf's
- So one can evaluate the full cross section for one pdf (the central pdf) and then evaluate the pdf uncertainty for a particular cross section by taking the ratio of the product of the pdf's (the pdf luminosity) for each of the error pdf's compared to the central pdf's

$$\sigma_{AB} = \int \mathrm{d}x_a \mathrm{d}x_b \; f_{a/A}(x_a, Q^2)\, f_{b/B}(x_b, Q^2)\; \hat{\sigma}_{ab\to X}$$

f^i is the error pdf and f^0 the central pdf

$$\frac{f^{i}{}_{a/A}(x_a,Q^2) f^{i}{}_{b/B}(x_b,Q^2)}{f^{0}{}_{a/A}(x_a,Q^2) f^{0}{}_{b/B}(x_b,Q^2)}$$

This works exactly for fixed order calculations and works well enough (see later) for parton shower Monte carlo calculations.

Most experiments now have code to easily do this…
and many programs will do it for you (MCFM)

A very useful tool

Allows easy calculation and comparison of pdf's

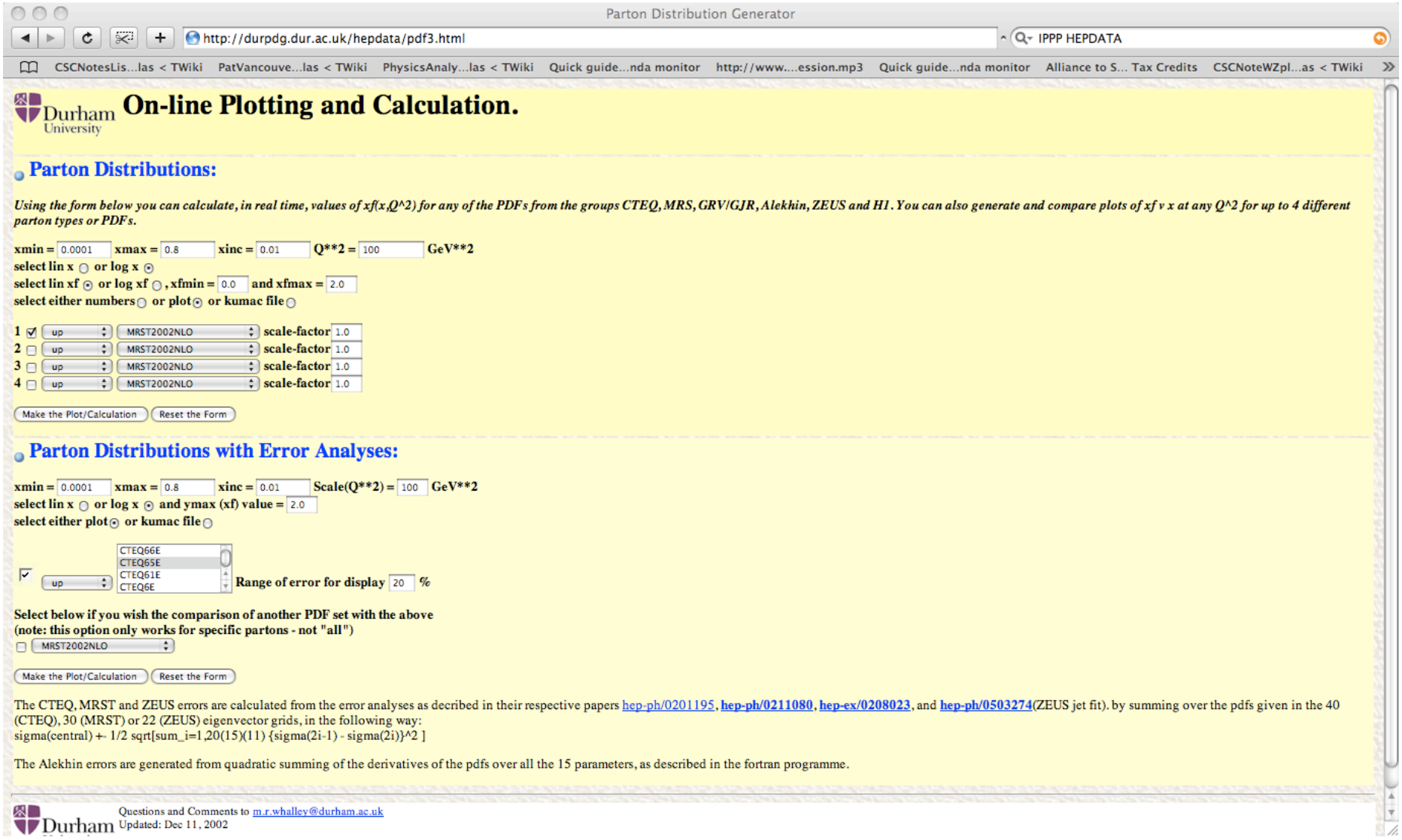

Let's try it out

Up and down quarks dominate at high x, gluon at low x.
As Q^2 increases, note the growth of the gluon distribution, and to a lesser extent the sea quark distributions.

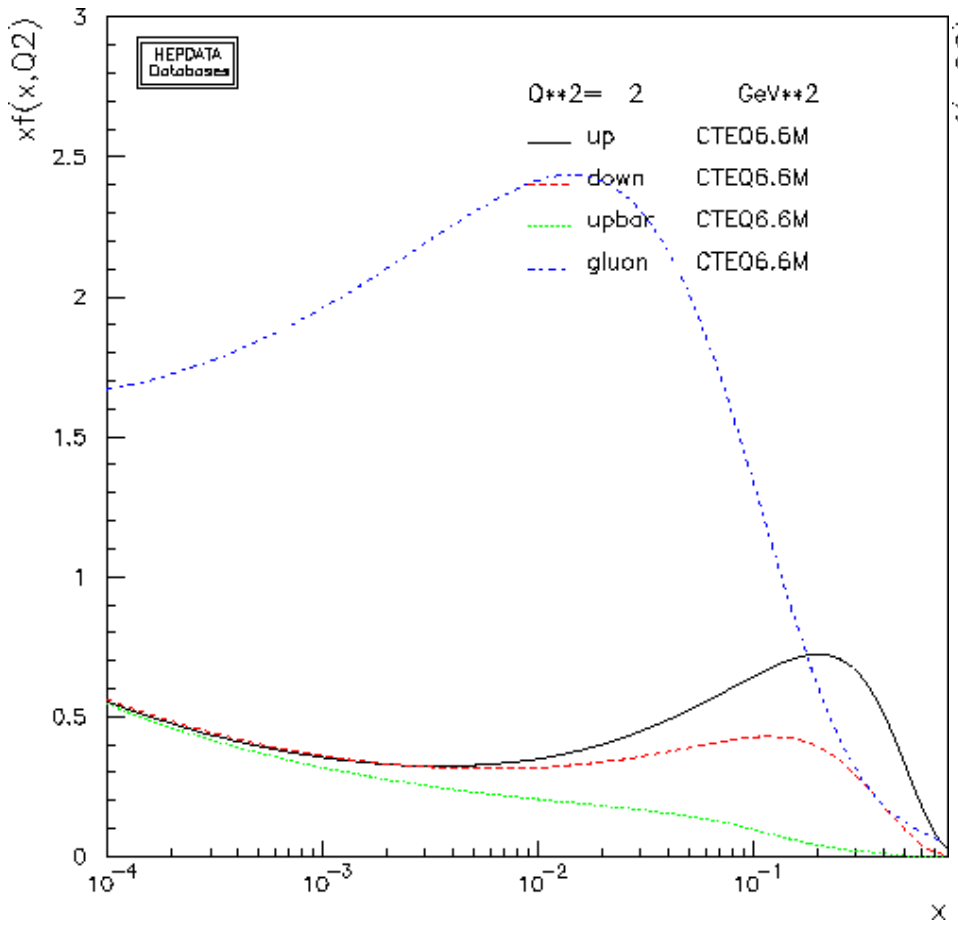

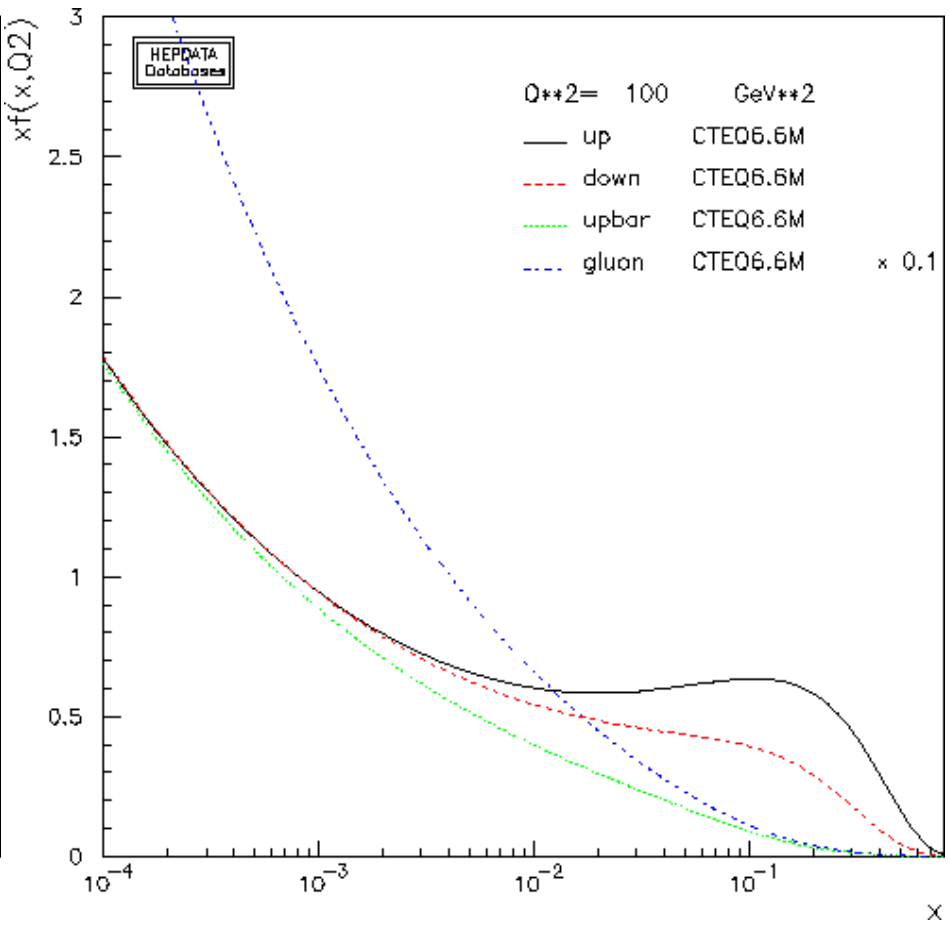

Uncertainties

uncertainties get large at high x

uncertainty for gluon larger than that for quarks

pdf's from one group don't necessarily fall into uncertainty band of another …would be nice if they did

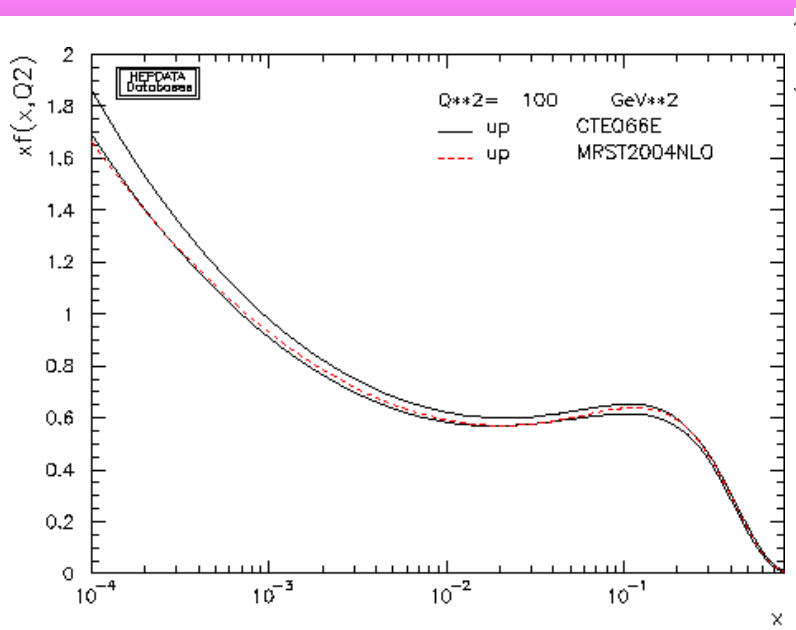

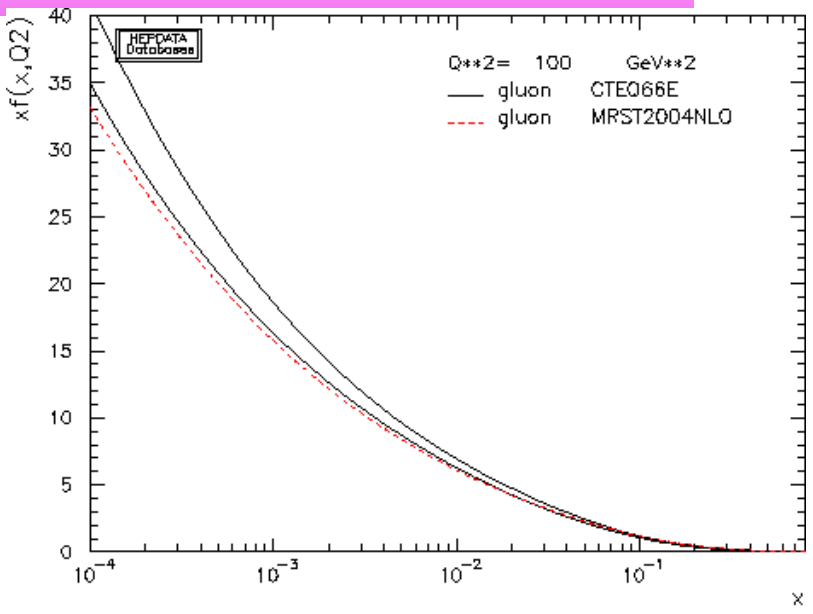

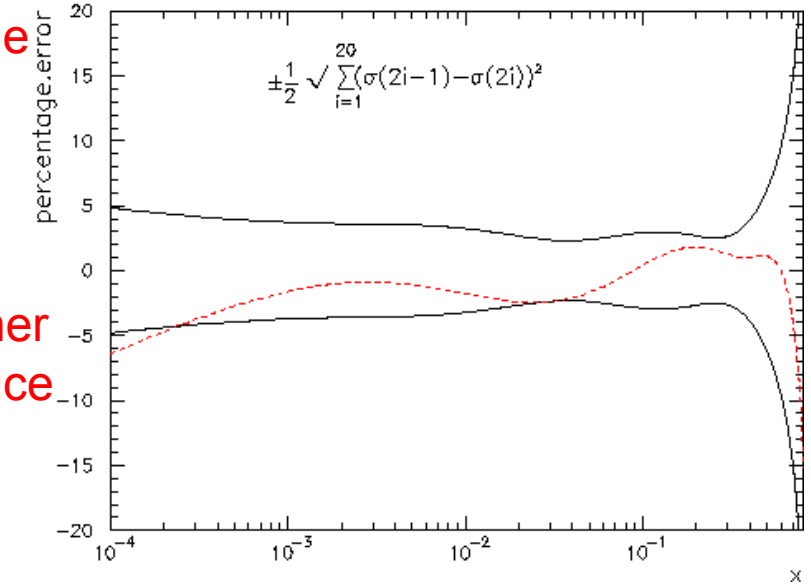

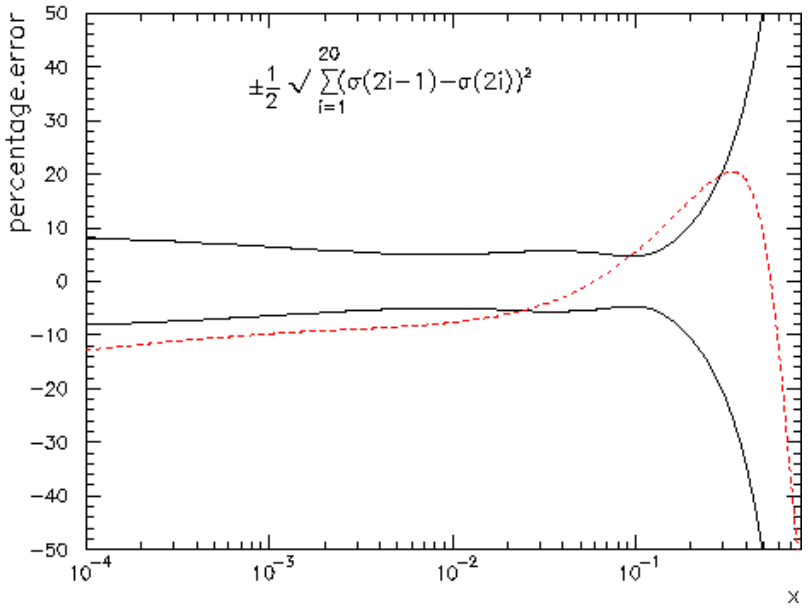

Uncertainties and parametrizations

- Beware of extrapolations to x values smaller than data available in the fits, especially at low Q^2
- Parameterization may artificially reduce the apparent size of the uncertainties
- Compare for example uncertainty for the gluon at low x from the recent neural net global fit to global fits using a parametrization

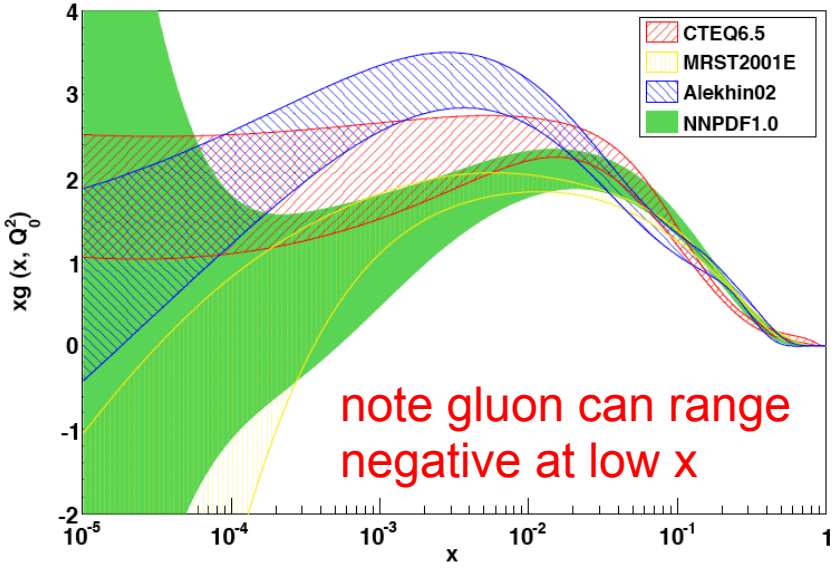

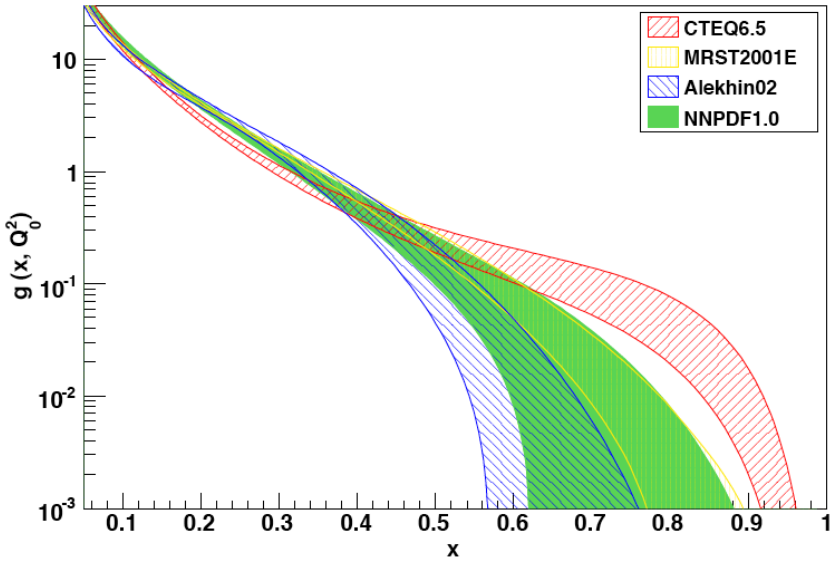

$Q^2=2\ GeV^2$

Correlations

- Consider a cross section X(a)
- i^{th} component of gradient of X is

$$\frac{\partial X}{\partial a_i} \equiv \partial_i X = \frac{1}{2}(X_i^{(+)} - X_i^{(-)})$$

- Now take 2 cross sections X and Y
  - or one or both can be pdf's
- Consider the projection of gradients of X and Y onto a circle of radius 1 in the plane of the gradients in the parton parameter space
- The circle maps onto an ellipse in the XY plane
- The angle ϕ between the gradients of X and Y is given by

$$\cos\varphi = \frac{\vec{\nabla}X \cdot \vec{\nabla}Y}{\Delta X \Delta Y} = \frac{1}{4\Delta X\,\Delta Y}\sum_{i=1}^{N}\left(X_i^{(+)} - X_i^{(-)}\right)\left(Y_i^{(+)} - Y_i^{(-)}\right)$$

- The ellipse itself is given by

$$\left(\frac{\delta X}{\Delta X}\right)^2 + \left(\frac{\delta Y}{\Delta Y}\right)^2 - 2\left(\frac{\delta X}{\Delta X}\right)\left(\frac{\delta Y}{\Delta Y}\right)\cos\varphi = \sin^2\varphi$$

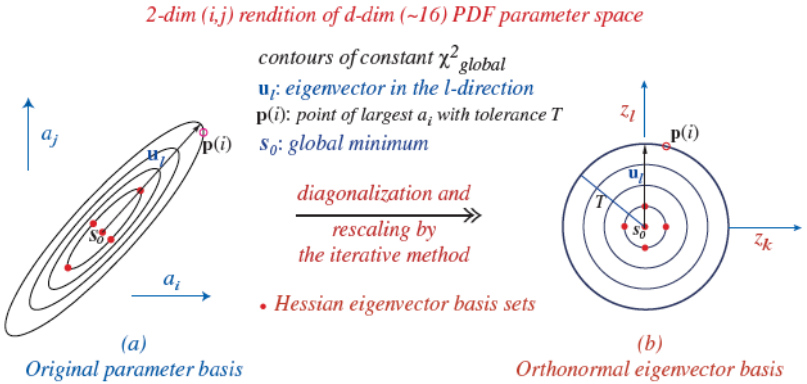

Figure 28. A schematic representation of the transformation from the pdf parameter basis to the orthonormal eigenvector basis.

- If two cross sections/pdf's are very correlated, then cosϕ~1
- …uncorrelated, then cosϕ~0
- …anti-correlated, then cosϕ~-1

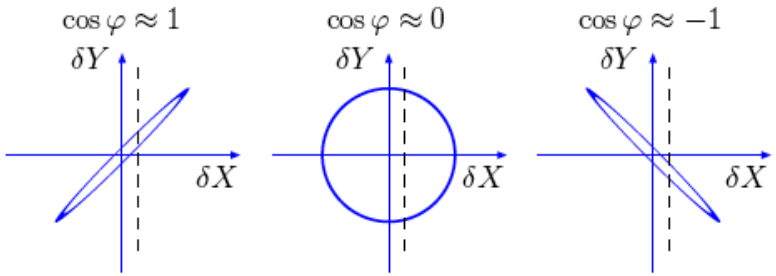

Figure 1: Dependence on the correlation ellipse formed in the $\Delta X - \Delta Y$ plane on the value of the correlation cosine $\cos\varphi$.

Correlations

- Consider a cross section X(a)
- i^{th} component of gradient of X is

$$\frac{\partial X}{\partial a_i} \equiv \partial_i X = \frac{1}{2}(X_i^{(+)} - X_i^{(-)})$$

- Now take 2 cross sections X and Y
  - or one or both can be pdf's
- Consider the projection of gradients of X and Y onto a circle of radius 1 in the plane of the gradients in the parton parameter space
- The circle maps onto an ellipse in the XY plane
- The angle ϕ between the gradients of X and Y is given by

$$\cos\varphi = \frac{\vec{\nabla}X \cdot \vec{\nabla}Y}{\Delta X \Delta Y} = \frac{1}{4\Delta X\,\Delta Y}\sum_{i=1}^{N}\left(X_i^{(+)} - X_i^{(-)}\right)\left(Y_i^{(+)} - Y_i^{(-)}\right)$$

- The ellipse itself is given by

$$\left(\frac{\delta X}{\Delta X}\right)^2 + \left(\frac{\delta Y}{\Delta Y}\right)^2 - 2\left(\frac{\delta X}{\Delta X}\right)\left(\frac{\delta Y}{\Delta Y}\right)\cos\varphi = \sin^2\varphi$$

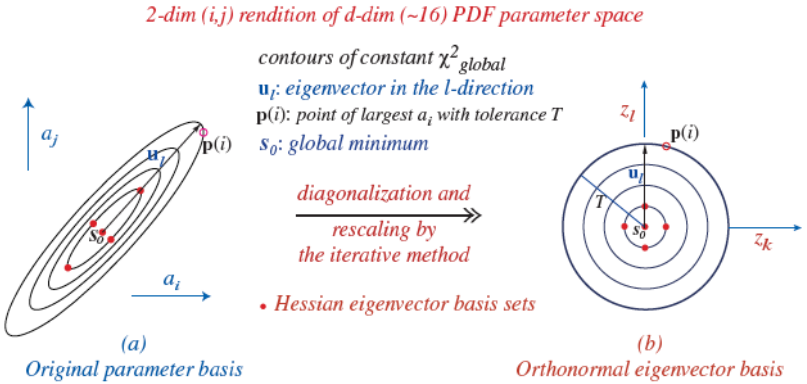

Figure 28. A schematic representation of the transformation from the pdf parameter basis to the orthonormal eigenvector basis.

- If two cross sections/pdf's are very correlated, then cosϕ~1
- …uncorrelated, then cosϕ~0
- …anti-correlated, then cosϕ~-1

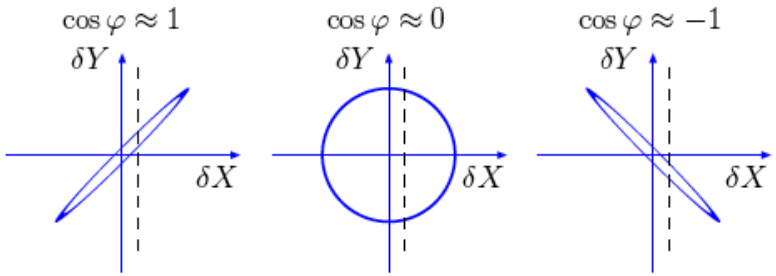

Figure 1: Dependence on the correlation ellipse formed in the $\Delta X - \Delta Y$ plane on the value of the correlation cosine $\cos\varphi$.

Correlations between pdf's

Correlations between $f(x_1, Q)$ and $f(x_2, Q)$ at $Q = 85$ GeV

$f_1(x_1, Q)$ vs. $f_1(x_2, Q)$

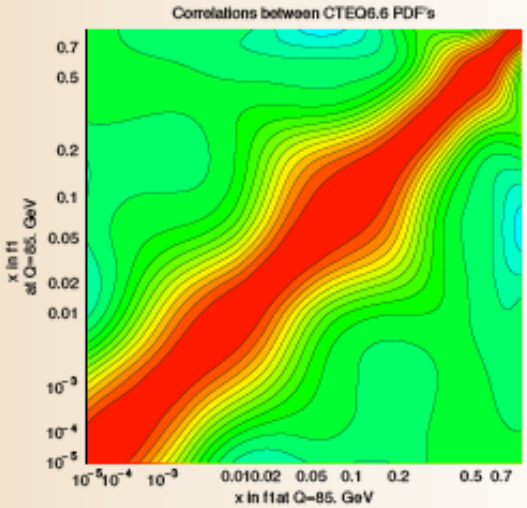

$f_2(x_1, Q)$ vs. $f_2(x_2, Q)$

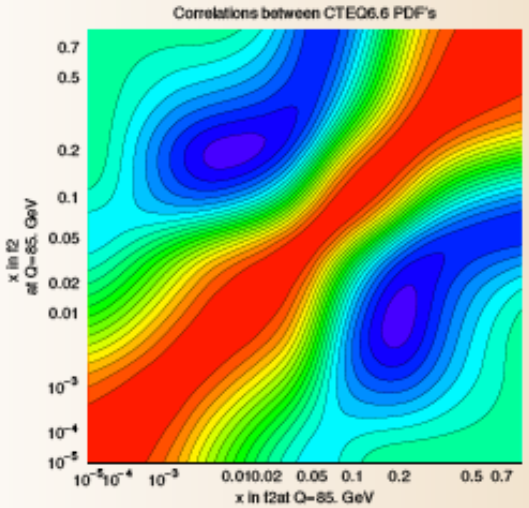

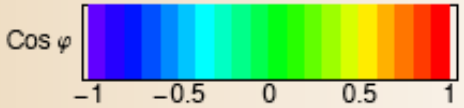

Pavel Nadolsky

Can you guess which PDF's these are?

Homework assignment: which pdf's and why?

Correlations between $f_1(x_1, Q)$ and $f_2(x_2, Q)$ at $Q = 85$ GeV

d vs u

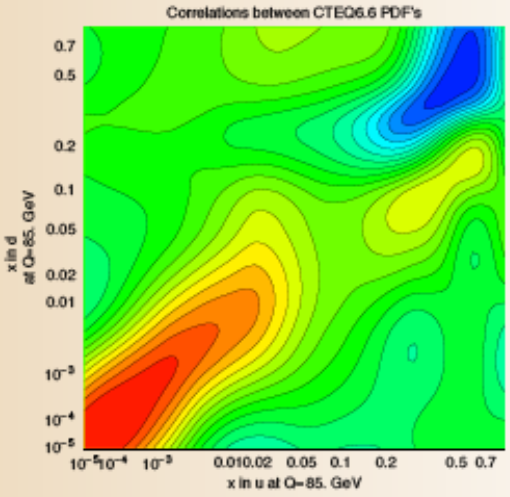

s vs $\bar{u}$ at Q=2

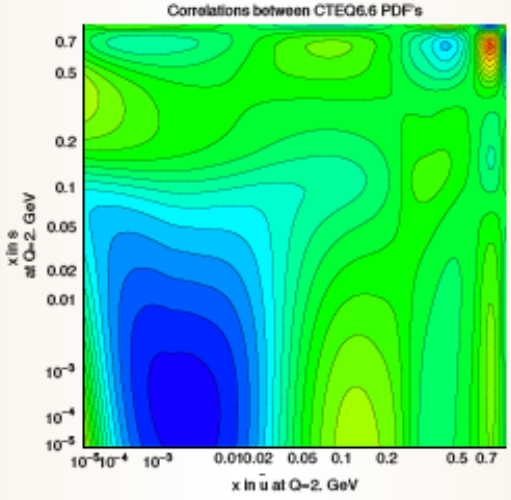

s vs. g

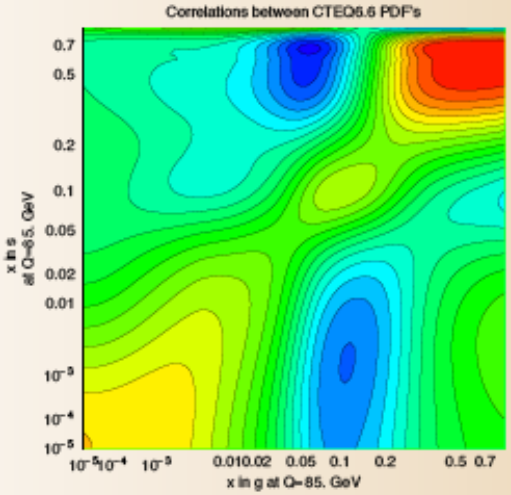

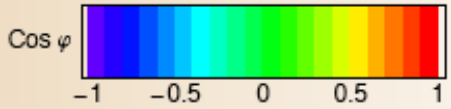

Sometimes there is a clear physics reason behind the correlation (e.g., sum rules or assumed Regge-like behavior); sometimes not

α_s series

- Take CTEQ6.6 as base, and vary $\alpha_s(m_Z)$ +/-0.002 (in 0.001 steps) around central value of 0.118
- Blue is the PDF uncertainty from eigenvectors; green is the uncertainty in the gluon from varying α_s
- We have found that change in gluon due to α_s error (+/-0.002 range) is typically smaller than PDF uncertainty with a small correlation with PDF uncertainty over this range
  - as shown for gluon distribution on right
- **PDF error and α_s error can be added in quadrature**
  - expected because of small correlation
  - in recent CTEQ paper, it has been proven this is correct regardless of correlation, within quadratic approximation to χ^2 distribution

arXiv:1004.4624; PDFs available from LHAPDF

So the CTEQ prescription for calculating the total uncertainty (PDF+α_s) involves the use of the 45 CTEQ6.6 PDFs and the two extreme α_s error PDF's (0.116 and 0.120)

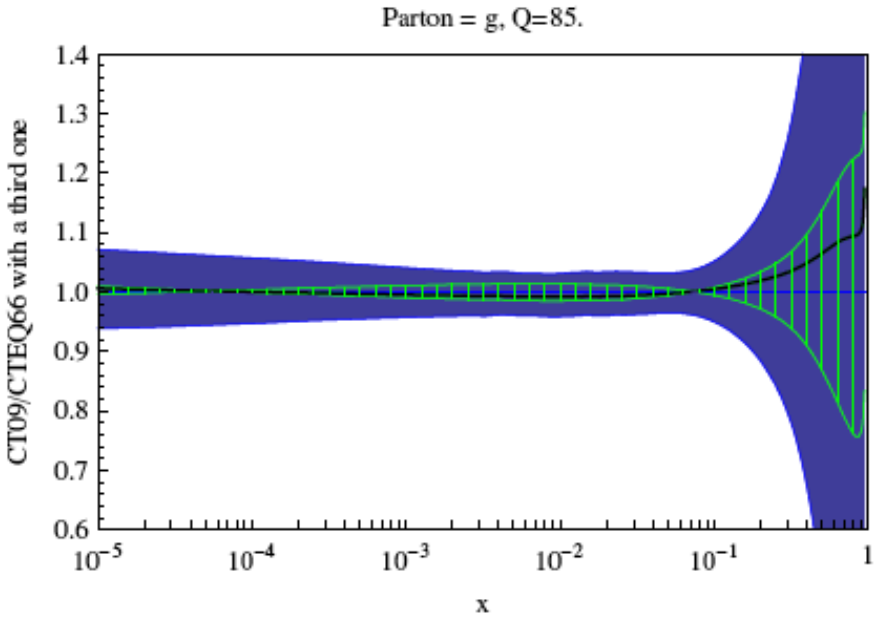

This also means that one can naively scale between 68% and 90% CL.

New from CTEQ-TEA (Tung et al)->CT10 PDFs

- Combined HERA-1 data
- CDF and D0 Run-2 inclusive jet data
- Tevatron Run 2 Z rapidity from CDF and D0
- W electron asymmetry from CDFII and D0II (D0 muon asymmetry) (in CT10W)
- Other data sets same as CTEQ6.6
- All data weights set to unity (except for CT10W)
- Tension observed between D0 II electron asymmetry data and NMC/BCDMS data
- Tension between D0 II electron and muon asymmetry data
- Experimental normalizations are treated on same footing as other correlated systematic errors
- More flexible parametrizations: 26 free parameters (26 eigenvector directions)
- Dynamic tolerance: look for 90% CL along each eigenvector direction
  - within the limits of the quadratic approximation, can scale between 68% and 90% CL with naïve scaling factor
- Two series of PDF's are introduced
  - CT10: no Run 2 W asymmetry
  - CT10W: Run 2 W asymmetry with an extra weight

Modified LO PDFs: motivation

- There is a big change in general for PDFs in going from LO to NLO; from NLO to NNLO->not so much

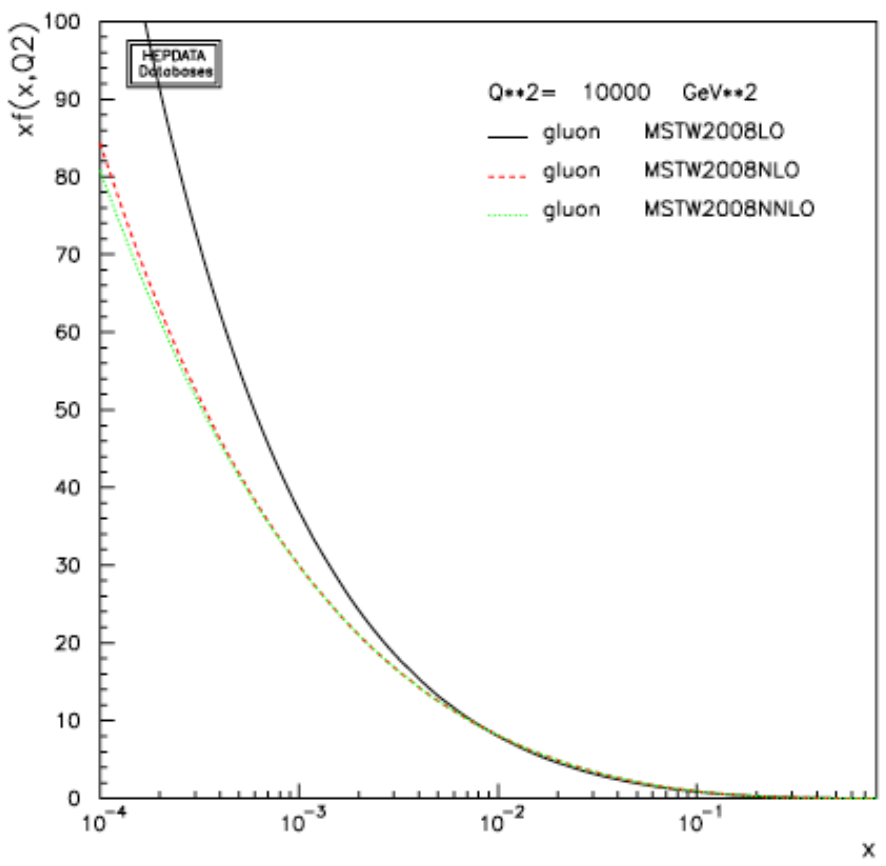

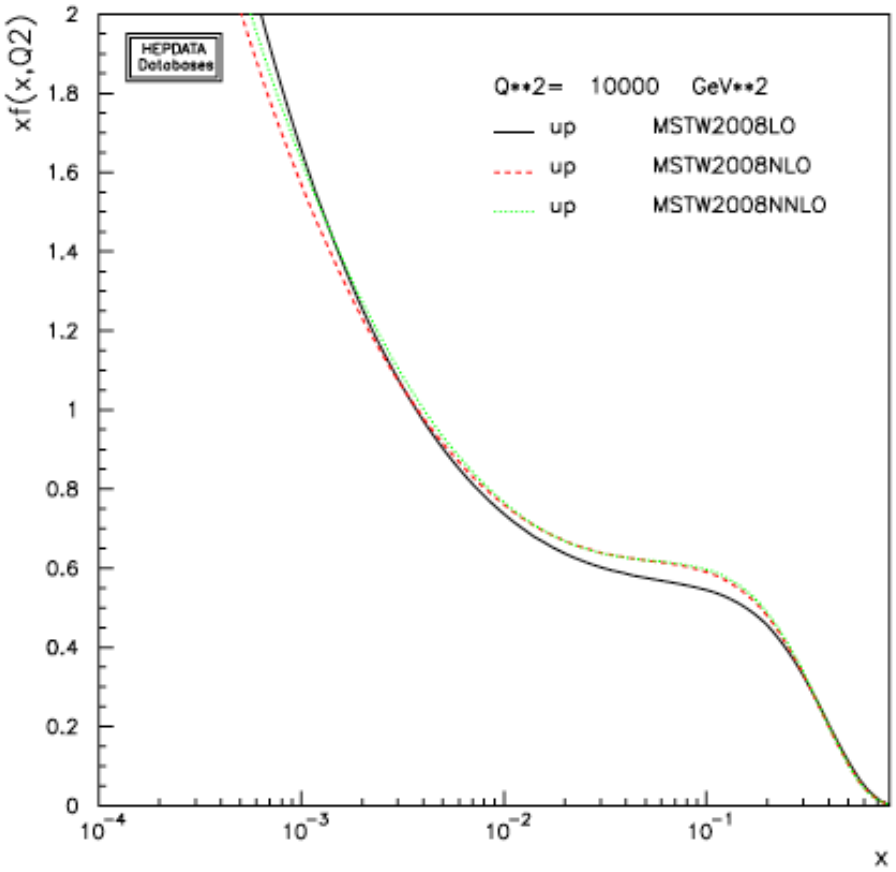

LO PDFs

- Workhorse for many predictions at the LHC are still LO PDFs
- Many LO predictions at the LHC differ significantly from NLO predictions, not because of the matrix elements but because of the PDFs
- W^+ rapidity distribution is the poster child
  - the forward-backward peaking obtained at LO is an artifact
  - large x u quark distribution is higher at LO than NLO due to deficiencies in the LO matrix elements for DIS

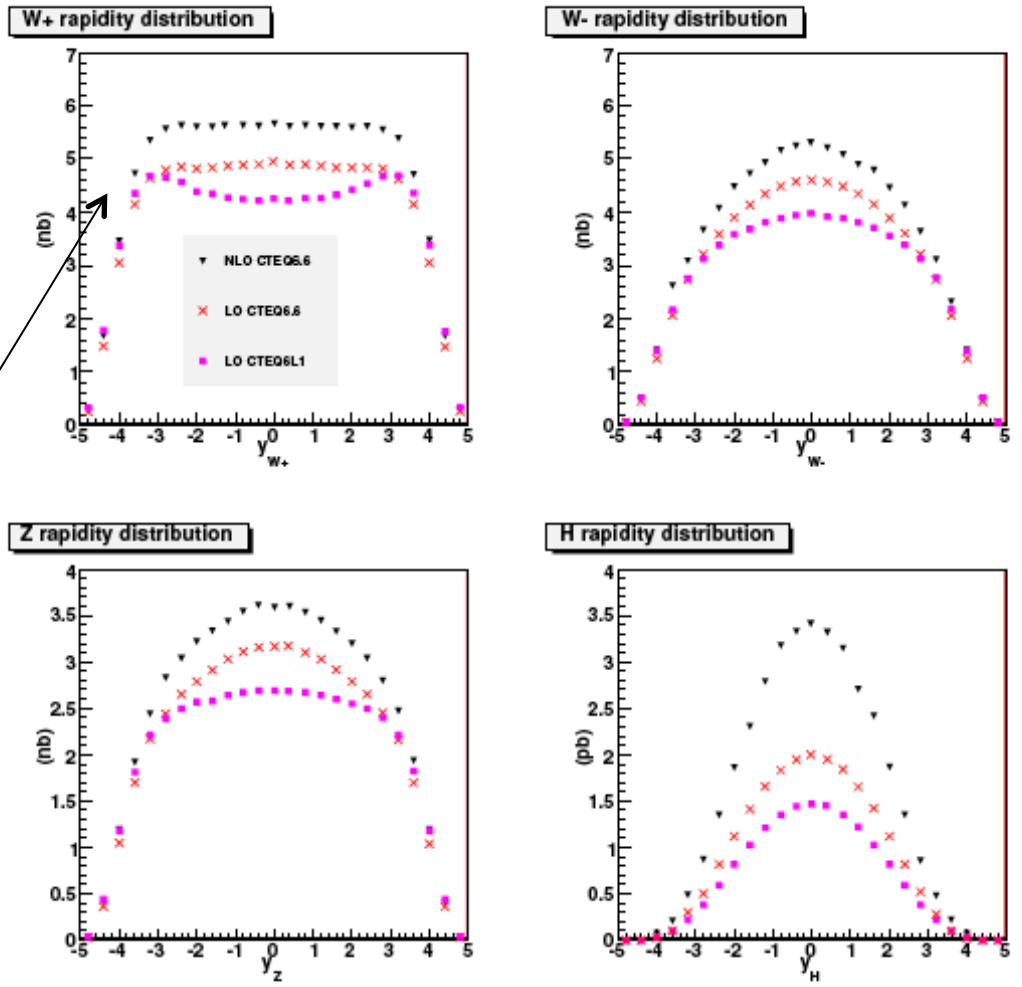

Figure 1. A comparison of the NLO pseudodata for SM boson rapidity distributions (in Δy=0.4 bins) predicted at the LHC (14 TeV) to the respective LO predictions based on CTEQ6.6M and CTEQ6L1 PDFs.

Where are the differences between LO and NLO partons?

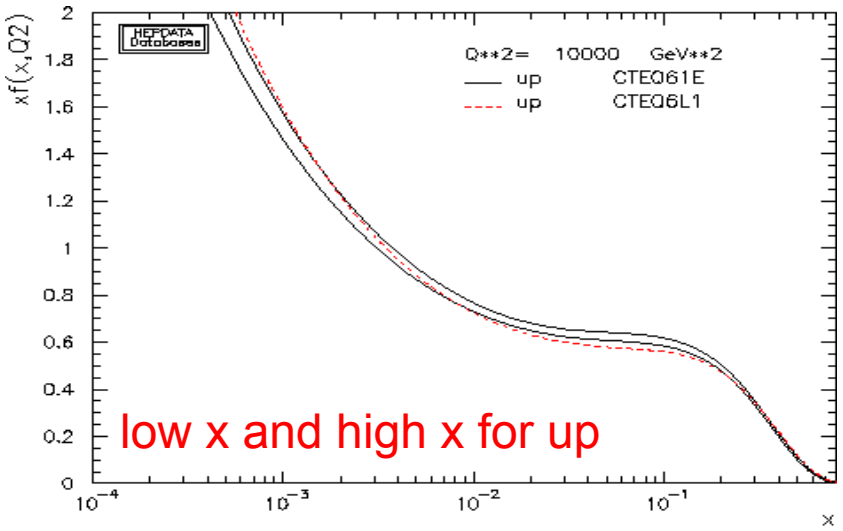

low x and high x for up

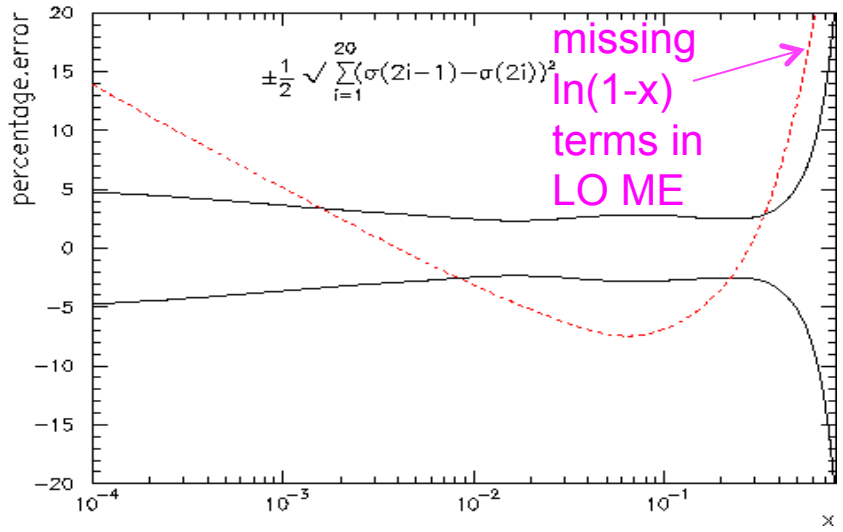

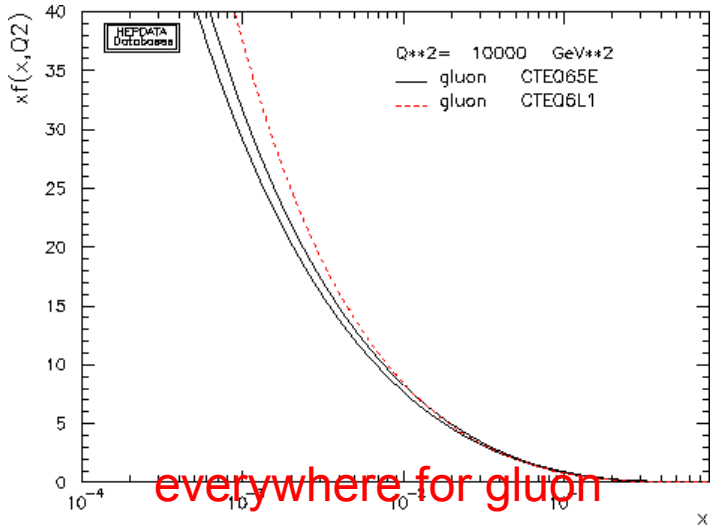

everywhere for gluon

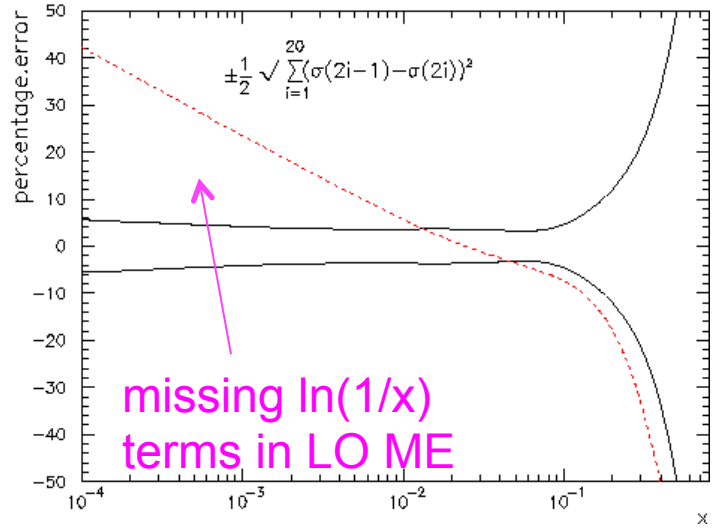

Modified LO pdf's (LO*)

- What about pdf's for parton shower Monte Carlos?
  - standard has been to use LO pdf's, most commonly CTEQ5L/ CTEQ6L, in Pythia, Herwig, Sherpa, ALPGEN/Madgraph+…
- …but
  - LO pdf's can create LHC cross sections/acceptances that differ in both shape and normalization from NLO
    - due to influence of HERA data
    - and lack of ln(1/x) and ln(1-x) terms in leading order pdf's and evolution
  - …and are often outside NLO error bands
  - experimenters use the NLO error pdf's in combination with the central LO pdf even with this mis-match
    - causes an error in pdf re-weighting due to non-matching of Sudakov form factors
  - predictions for inclusive observables from LO matrix elements for many of the collider processes that we want to calculate are not so different from those from NLO matrix elements (aside from a reasonably constant K-factor)

Modified LO pdf's (LO*)

- …but
  - we (and in particular Torbjorn Sjostrand) *like* the low x behavior of LO pdf's and rely upon them for our models of the underlying event at the Tevatron and its extrapolation to the LHC
  - as well as calculating low x cross sections at the LHC
  - and no one listened to me when I urged the use of NLO pdf's
- thus, the need for modified LO pdf's

- Carry out a LO fit, but
  - relax the momentum sum rule (CTEQ, MRST), so extra glue goes where it's *needed*; other sum rules still in effect
  - add NLO pseudo-data into fit to force desired behavior (CTEQ)
  - use 1-loop $\alpha_s(m_Z)$ (CTEQ, MRST) or 2-loop $\alpha_s(m_Z)$ (CTEQ, MRST)

Aside: Parton showers and PDFs

- There's a difference between tree level fixed order predictions and those from parton shower Monte Carlos
- The incoming partons can radiate hard gluons pushing the incoming partons off-mass shell

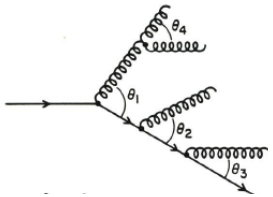

- We expect that there will be a kinematic suppression of distributions formed by parton showers compared to those generated by tree level calculations
- Although this is a sizeable effect for low Q^2 processes, the effect is diminished for most processes we want to calculate at the LHC

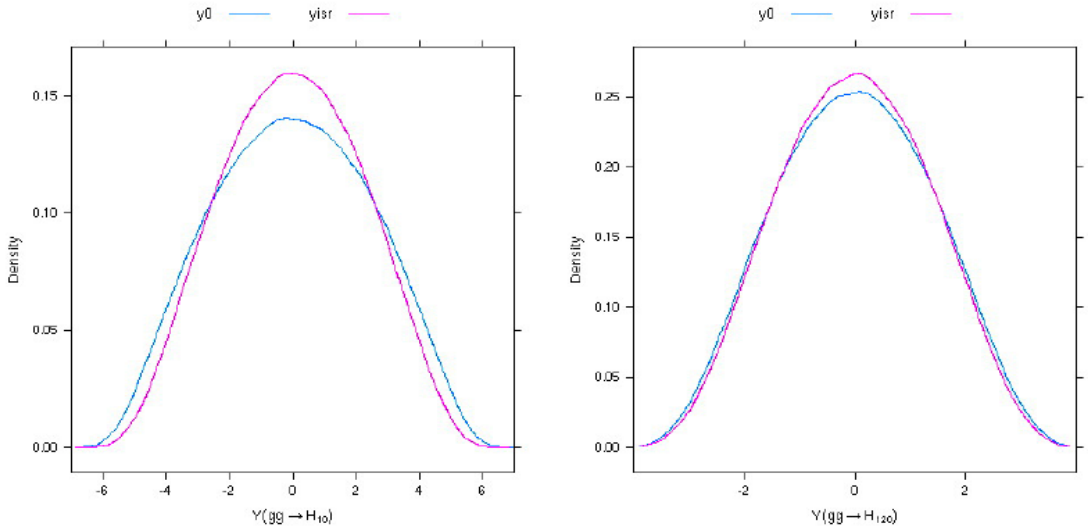

Figure 2: Leading order predictions for the production of a 10 GeV Higgs boson (left) and a 120 GeV Higgs boson (right) at the LHC with and without the influence of parton showering. CTEQ6L1 PDFs are used for both predictions.

MRST2007lomod

- Momentum sum rule is relaxed (100%->114%)
- Better fit to benchmark LHC cross sections than with standard LO PDFs, but shapes often not fully described
- …but, mimics full NLO predictions for b p_T distributions
- Standard now for ATLAS LO Monte Carlo generation
- Described in
  - arXiv:0711.2473
  - arXiv:0807.2132

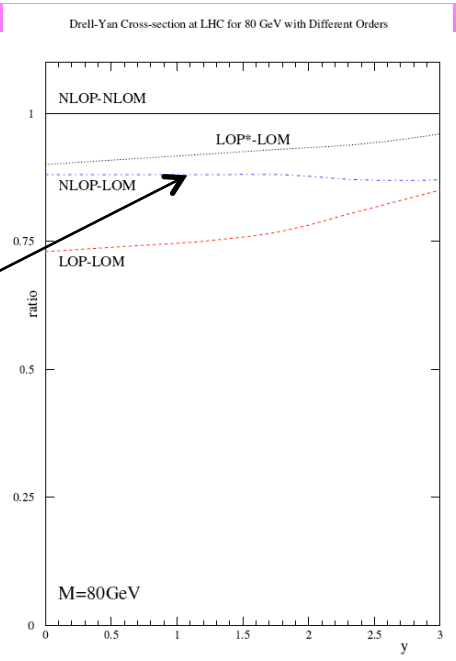

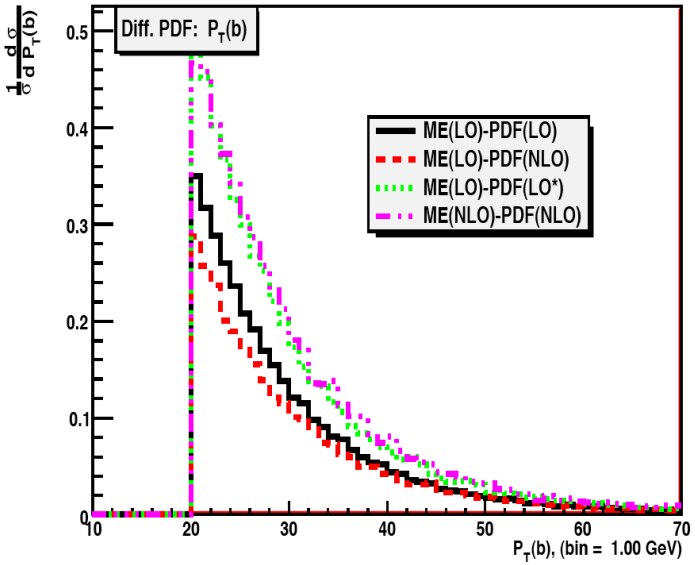

Modified LO PDFs

- Try to make up for the deficiencies of LO PDFs by
  - relaxing the momentum sum rule (MRST,CTEQ)
  - including NLO pseudo-data in the LO fit to guide the modified LO distributions (CTEQ)
- Results tend to be in better agreement with NLO predictions, both in magnitude and in shape
- Some might say that the PDFs then have no predictive power, but this is true for any LO PDFs

- See arXiv:0910.4183; PDFs available from LHAPDF
- See arXiv:0711.2473 for MRST2007lomod PDFs

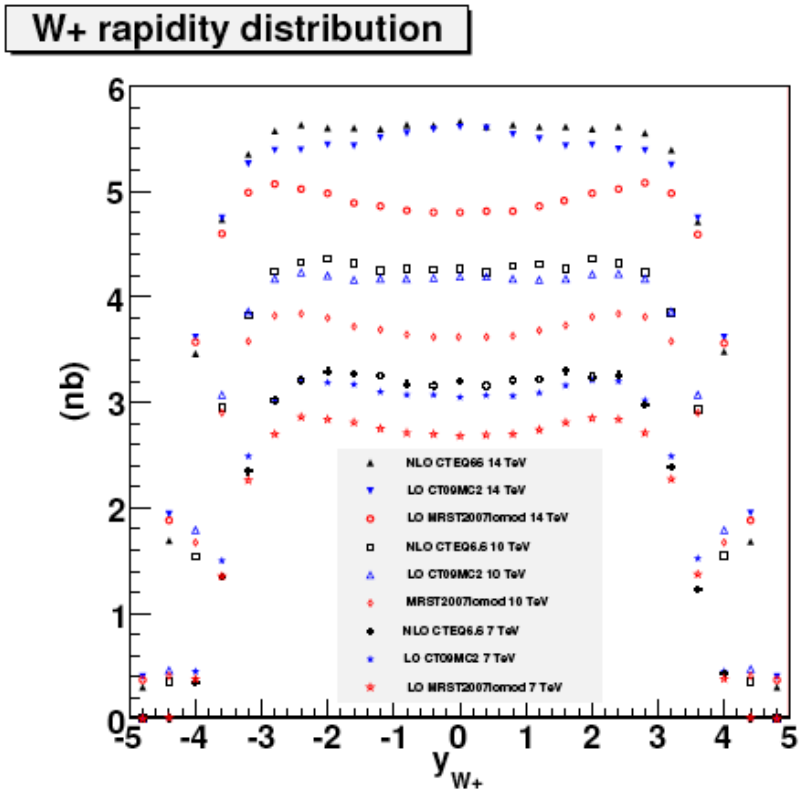

Figure 6. Predictions for the W^+ rapidity distribution at the LHC ($\sqrt{s}$ =7, 10 and 14 TeV) in Δy =0.4 bins, given at NLO using the CTEQ6.6M PDFs, and at LO using the CT09MC2 and MRST2007lomod PDFs. The actual cross sections (without normalization rescaling factors) are shown.

Also

W- rapidity distribution

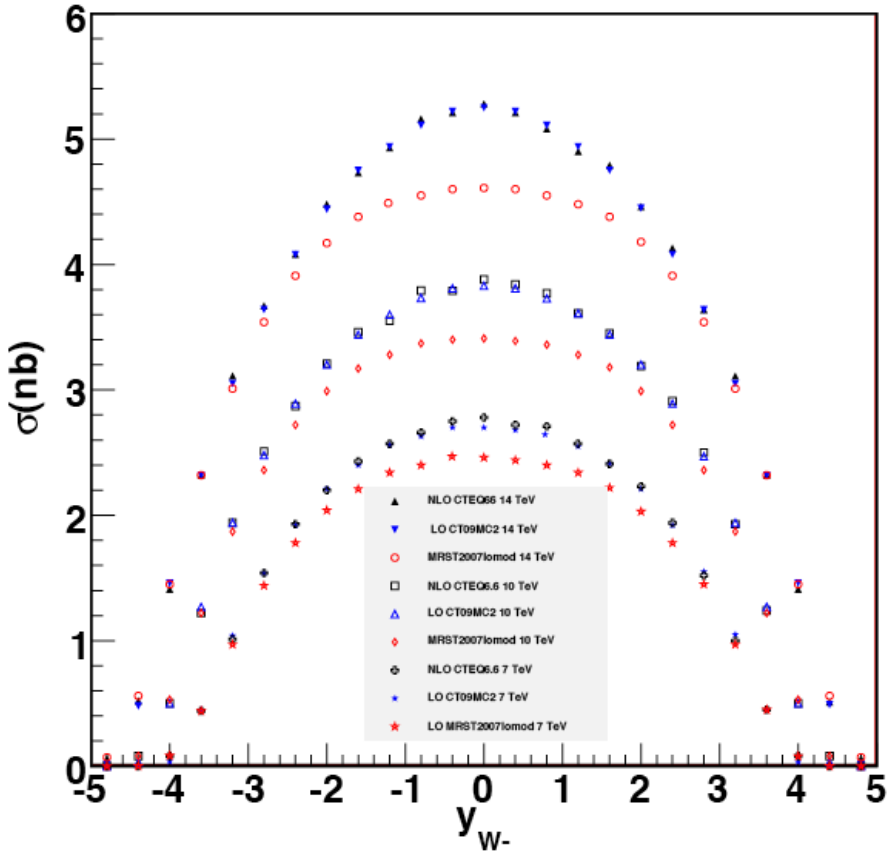

Z rapidity distribution

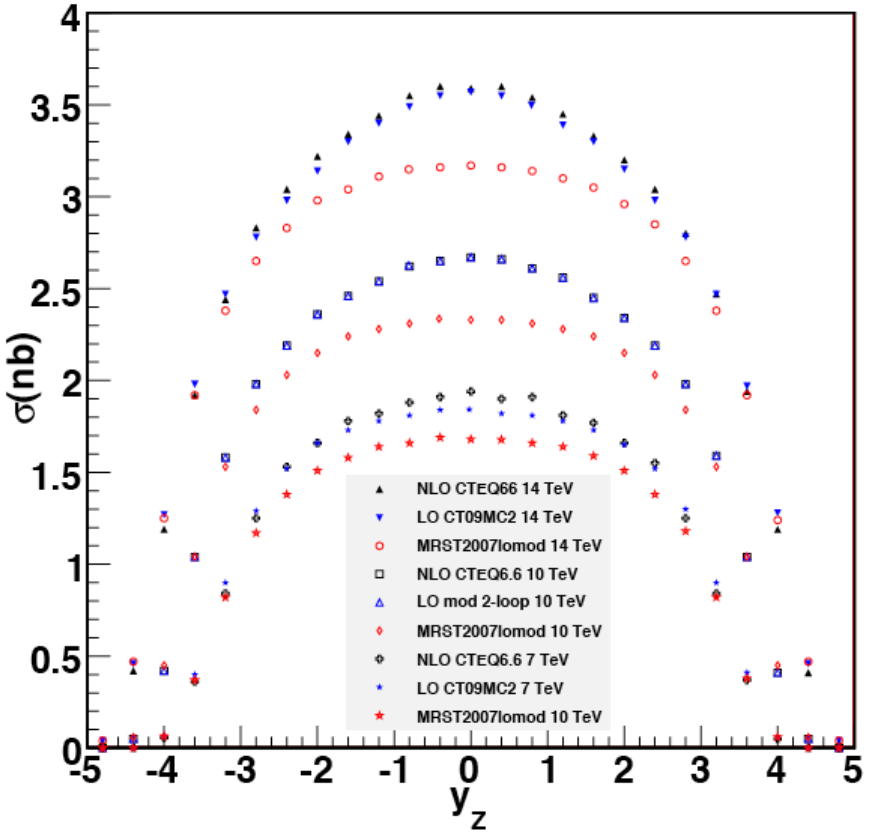

gg->Higgs

- Higgs K-factor is too large to absorb into PDFs (nor would you want to)
- Shape is ok with LO PDF's, improves a bit with the modified LO PDFs

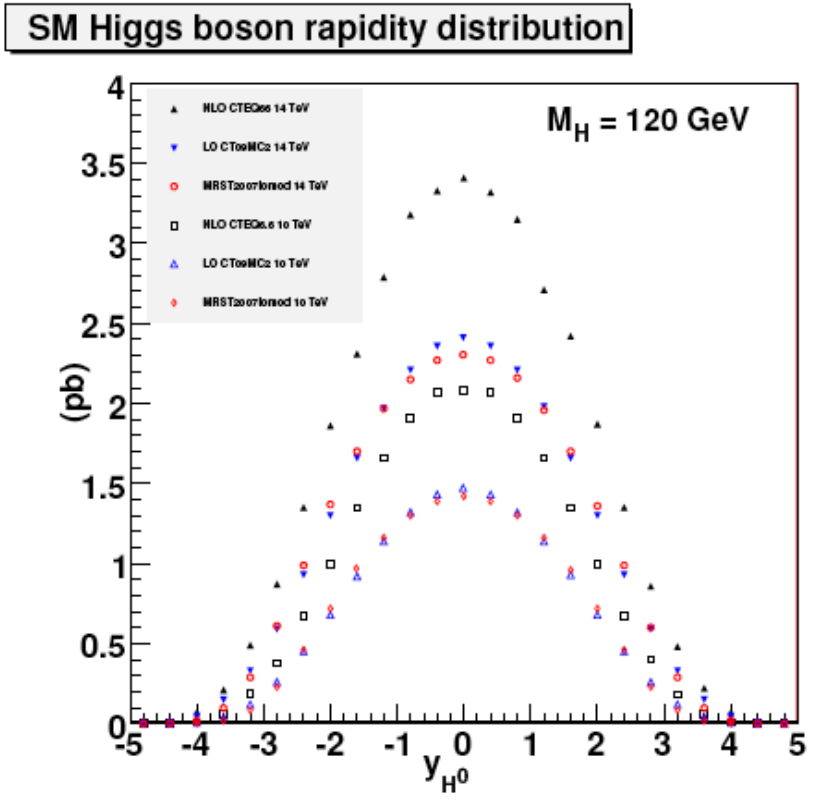

Figure 9. Same as figure 6, for the Higgs boson rapidity distribution at $\sqrt{s}$ =10 and 14 TeV. To maintain legibility, the distribution for $\sqrt{s}$ =7 TeV is not shown.

Some comparisons: low x gluon

- Low x behavior of modified LO PDFs similar to each other and to normal LO PDF
- But somewhat more glue at low x, so MC tunes have to take this into account

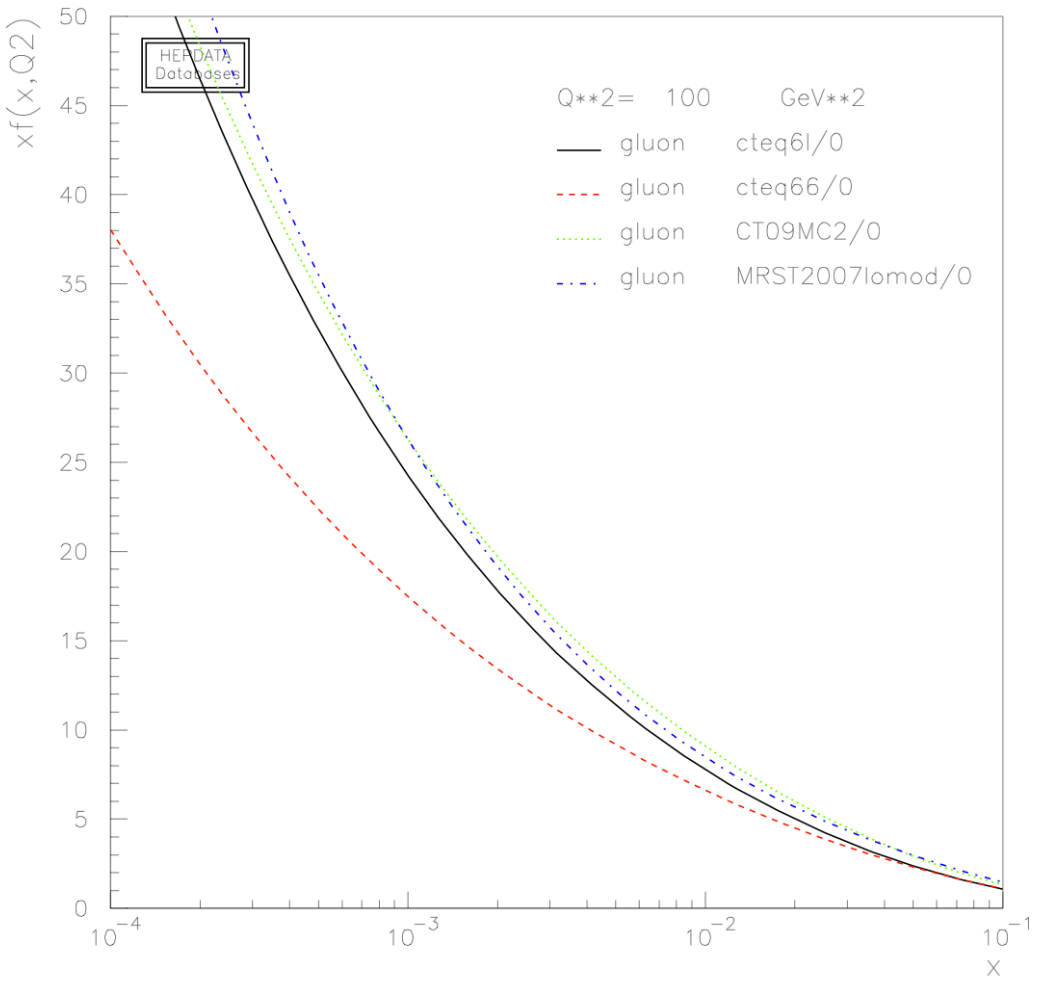

Some comparisons: u and ubar quark

- Up quark distributions for mod LO still larger than those for NLO
- Ubar distributions tend to be higher than either for LO or NLO

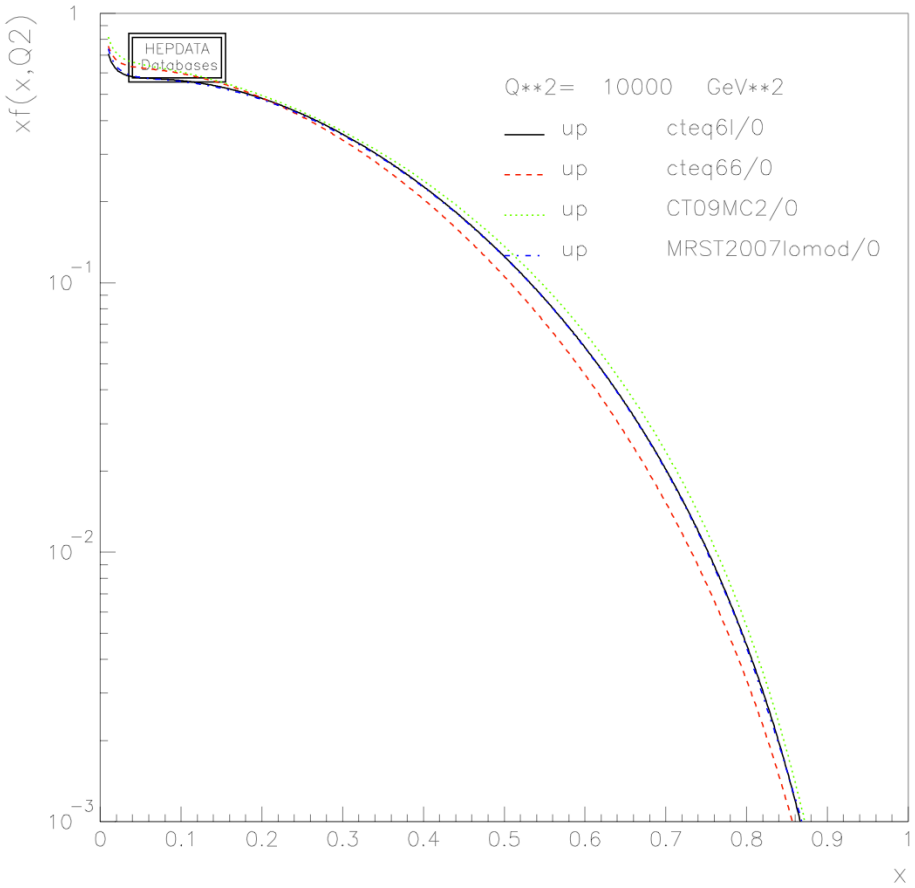

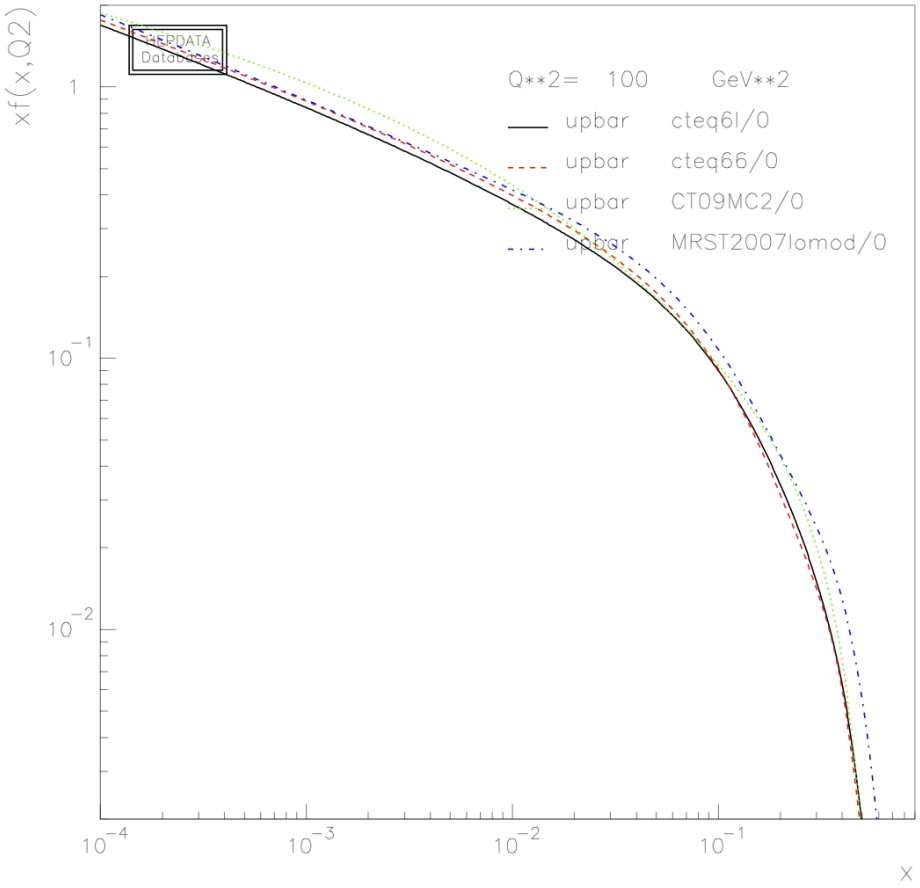

…so

- We have modified LO PDFs from CTEQ and MSTW (MRST)
  - all are available in LHAPDF
- MRST2007lomod PDFs have been used for ATLAS Monte Carlo generation, but are now being phased out…too many problems
- Note that modified LO PDFs were made to solve a problem
  - NLO high x behavior of LO PDFs wrong for LHC cross sections
  - NLO low x gluon behavior wrong for multiple parton scattering models
  - mod LO PDFs offer a way out, but are not perfect
- Another way out of this problem is to use a LO PDF for the underlying event generation and a NLO PDF for the matrix element evaluation
  - possible in modern Monte Carlos
- Or since so many of the needed processes are already in NLO Monte Carlos, just use those, and the preferred NLO PDF set
- So it seems that the time of modified LO PDFs may be over

K-factor table from CHS paper

K-factors for LHC slightly less K-factors at Tevatron

K-factors with NLO PDFs at LO are more often closer to unity

Process	Typical scales μ_0	Typical scales μ_1	Tevatron K-factor $\mathcal{K}(\mu_0)$	Tevatron K-factor $\mathcal{K}(\mu_1)$	Tevatron K-factor $\mathcal{K}'(\mu_0)$	LHC K-factor $\mathcal{K}(\mu_0)$	LHC K-factor $\mathcal{K}(\mu_1)$	LHC K-factor $\mathcal{K}'(\mu_0)$	LHC K-factor $\mathcal{K}''(\mu_0)$
W	m_W	$2m_W$	1.33	1.31	1.21	1.15	1.05	1.15	0.95
W+1jet	m_W	$p_T^{\rm jet}$	1.42	1.20	1.43	1.21	1.32	1.42	0.99
W+2jets	m_W	$p_T^{\rm jet}$	1.16	0.91	1.29	0.89	0.88	1.10	0.90
WW+jet	m_W	$2m_W$	1.19	1.37	1.26	1.33	1.40	1.42	1.10
$t\bar{t}$	m_t	$2m_t$	1.08	1.31	1.24	1.40	1.59	1.19	1.09
$t\bar{t}$+1jet	m_t	$2m_t$	1.13	1.43	1.37	0.97	1.29	1.10	0.85
$b\bar{b}$	m_b	$2m_b$	1.20	1.21	2.10	0.98	0.84	2.51	–
Higgs	m_H	$p_T^{\rm jet}$	2.33	–	2.33	1.72	–	2.32	1.43
Higgs via VBF	m_H	$p_T^{\rm jet}$	1.07	0.97	1.07	1.23	1.34	0.85	0.78
Higgs+1jet	m_H	$p_T^{\rm jet}$	2.02	–	2.13	1.47	–	1.90	1.33
Higgs+2jets	m_H	$p_T^{\rm jet}$	–	–	–	1.15	–	–	1.13

Table 3: K-factors for various processes at the LHC calculated using a selection of input parameters. Have to fix this table. In all cases, the CTEQ6M PDF set is used at NLO. $\mathcal{K}$ uses the CTEQ6L1 set at leading order, whilst $\mathcal{K}'$ uses the same set, CTEQ6M, as at NLO and $\mathcal{K}''$ uses the modified LO (2-loop) PDF set. For Higgs+1,2jets, a jet cut of 40 GeV/c and $|\eta| < 4.5$ has been applied. A cut of $p_T^{\rm jet} > 20\ GeV/c$ has been applied for the $t\bar{t}$+jet process, and a cut of $p_T^{\rm jet} > 50\ GeV/c$ for WW+jet. In the W(Higgs)+2jets process the jets are separated by $\Delta R > 0.52$, whilst the VBF calculations are performed for a Higgs boson of mass 120 GeV. In each case the value of the K-factor is compared at two often-used scale choices, where the scale indicated is used for both renormalization and factorization scales.

CT09MC2

Note K-factor for W < 1.0, since for this table the comparison is to CTEQ6.1 and not to CTEQ6.6, i.e. corrections to low x PDFs due to treatment of heavy quarks in CTEQ6.6 "built-in" to mod LO PDFs